Yuta Hamada

Higgs Potential and Naturalness After the Higgs Discovery

Springer

Springer Theses

Recognizing Outstanding Ph.D. Research

Aims and Scope

The series "Springer Theses" brings together a selection of the very best Ph.D. theses from around the world and across the physical sciences. Nominated and endorsed by two recognized specialists, each published volume has been selected for its scientific excellence and the high impact of its contents for the pertinent field of research. For greater accessibility to non-specialists, the published versions include an extended introduction, as well as a foreword by the student's supervisor explaining the special relevance of the work for the field. As a whole, the series will provide a valuable resource both for newcomers to the research fields described, and for other scientists seeking detailed background information on special questions. Finally, it provides an accredited documentation of the valuable contributions made by today's younger generation of scientists.

Theses are accepted into the series by invited nomination only and must fulfill all of the following criteria

- They must be written in good English.
- The topic should fall within the confines of Chemistry, Physics, Earth Sciences, Engineering and related interdisciplinary fields such as Materials, Nanoscience, Chemical Engineering, Complex Systems and Biophysics.
- The work reported in the thesis must represent a significant scientific advance.
- If the thesis includes previously published material, permission to reproduce this must be gained from the respective copyright holder.
- They must have been examined and passed during the 12 months prior to nomination.
- Each thesis should include a foreword by the supervisor outlining the significance of its content.
- The theses should have a clearly defined structure including an introduction accessible to scientists not expert in that particular field.

More information about this series at http://www.springer.com/series/8790

Yuta Hamada

Higgs Potential and Naturalness After the Higgs Discovery

Doctoral Thesis accepted by
Kyoto University, Kyoto, Japan

Springer

Author
Dr. Yuta Hamada
Theory Center
High Energy Accelerator Research
    Organization
Tsukuba, Ibaraki
Japan

Supervisor
Prof. Hikaru Kawai
Department of Physics
Kyoto University
Kyoto
Japan

Supervisor's Foreword

One of the most important problems of present particle theory is the naturalness of the Higgs mass and the cosmological constant. Before the results of the Large Hadron Collider (LHC), many physicists expected that at least the naturalness of the Higgs mass could be explained by supersymmetry. However, contrary to this expectation, the LHC has discovered the absence of low-energy supersymmetry, which suggests that the naturalness should be explained by some mechanism that is not in the conventional field theory. In this thesis, Yuta Hamada has examined the naturalness problem from two sides. One is so to speak a bottom-up approach, in which the behavior of the Higgs potential near the Planck scale is analyzed using the recent experimental data. The other is so to speak a top-down approach, in which the effects of quantum gravity, especially those of the topology change of space–time, are investigated. First, it is shown that the standard model (SM) is valid up to the Planck scale without introducing additional particles. In fact the bare parameters have been calculated as a function of the cutoff scale from the newest experimental data for the Higgs mass, top quark mass, and the gauge couplings. Here it is crucial to distinguish the physical top quark mass from the Monte Carlo parameter used in experimental analyses. Then the result of the calculation tells us that the vacuum is stable and that all the bare parameters are finite if the cutoff scale is smaller than the Planck scale. Furthermore, it is shown that the bare Higgs potential becomes zero if the cutoff scale is close to the Planck scale. In fact, three quantities, the bare Higgs mass, the bare Higgs self-coupling, and the beta function of the Higgs self-coupling, become zero simultaneously around the Planck scale. Surprisingly, this phenomenon was already predicted by Froggatt and Nielsen in the middle nineties. Their argument is based on a rather non-standard principle called the multiple-point criticality principle, whose real origin is not clear at present. However, we can show that it indeed arises in various theories that involve a slight modification of the ordinary field theory such as Coleman's wormhole mechanism. This phenomenon has a major significance not only in particle physics but also in cosmology. Yuta has picked up two interesting subjects in this direction. One is the so-called Higgs inflation. He discusses the fact that the realistic parameters of the

inflation of the early universe can be naturally explained by the SM because the Higgs potential is sufficiently flat around the Planck scale due to the phenomenon. The other is the mass of the dark matter. Interestingly, rather strong upper and lower bounds on it are obtained if one assumes that the stability and the flatness of the Higgs potential are not violated by the dark matter. Then Yuta discusses various mechanisms for solving the naturalness problem including the origin of the flatness of the Higgs potential. By refining Coleman's wormhole mechanism for space–time with the Minkowski signature, one obtains what may be called the maximum entropy principle, that is, the parameters of the theory are tuned by themselves to maximize the entropy of the universe. Yuta has applied this principle to various parameters in the SM. First of all, if one accepts the Higgs inflation, the flatness of the Higgs potential can be explained because a flat potential produces a large e-fold number of inflation and makes the entropy of the universe very large. He further has examined the validity of the principle for various parameters of the SM such as the Fermi constant and the strong CP phase. It has turned out that the couplings predicted by the principle qualitatively agree with the observed values, but there are significant discrepancies. In this thesis Yuta has examined various aspects of the naturalness problem. He has discovered the rather mysterious coincidences in the Higgs potential around the Planck scale. He also has tried to explain it by finding a new mechanism that arises naturally in quantum gravity. Although no complete theory has been found so far, he has obtained many interesting results that indicate the future direction of particle physics.

Kyoto, Japan   Prof. Hikaru Kawai
April 2016

Parts of this thesis have been published in the following journal articles:

1. Y. Hamada, H. Kawai, and K.-y. Oda, Bare Higgs mass at Planck scale, Phys. Rev. D87 (2013), no. 5, 053009; arXiv:1210.2538.
2. Y. Hamada, H. Kawai, and K.-y. Oda, Minimal Higgs inflation, PTEP 2014 (2014), 023B02; arXiv:1308.6651.
3. Y. Hamada, H. Kawai, K.-y. Oda, and S.C. Park, Higgs inflation still alive, Phys.Rev.Lett. 112 (2014), 241301; arXiv:1403.5043.
4. Y. Hamada, H. Kawai, K.-y. Oda, and S. C. Park, Higgs inflation from Standard Model criticality, Phys. Rev. D91 (2015), 053008; arXiv:1408.4864.
5. Y. Hamada, H. Kawai, and K. Kawana, Weak Scale From the Maximum Entropy Principle, PTEP 2015 (2015), 033B06; arXiv:1409.6508.
6. Y. Hamada, K. Kawana, and K. Tsumura, Landau pole in the Standard Model with weakly interacting scalar fields, Phys. Lett. B747 (2015), 238–244; arXiv:1505.01721.
7. Y. Hamada and K. Kawana, Vanishing Higgs Potential in Minimal Dark Matter Models, Phys. Lett. B751 (2015), 164–170; arXiv:1506.06553.

Acknowledgements

First of all, I would like to thank my supervisor, Hikaru Kawai. He drew my attention to the connection between Higgs physics and Planck scale physics. Discussion with him is always exciting, and I learned many things from him. His advice is always critical and instructive and makes the point clear. I also appreciate support from Tatsuo Kobayashi. He helped me throughout my master's and doctoral courses and taught me the basis of string phenomenology and cosmology. Through the collaboration with him, I could study many topics such as D-brane model building, topological defects, flavor physics, and so on.

I thank Kin-ya Oda and Koji Tsumura for productive collaboration and continuous encouragement. During the joint research with them, I could learn how to write scientific papers and improve my presentation skills.

My work at Kyoto University could not have been realized without the help of my collaborators in many topics to whom I am also grateful: Minoru Eto, Kohei Kamada, Kiyoharu Kawana, Atsushi Ogasahara, Keisuke Ohashi, Yuji Omura, Yutaka Ookouchi, Seong Chan Park, Fuminobu Takahashi, Fumihiro Takayama, Shohei Uemura, and Daiki Yasuhara.

This work was supported by a research fellowship of the Japan Society for the Promotion of Science (JSPS) for young scientists.

Finally, I would like to extend my indebtedness to my family for their understanding, support, and encouragement throughout my study.

Contents

Chapter 1
Introduction

1.1 Overview

The discovery of the Higgs boson in 2012 [1, 2] at the large hadron collider (LHC) makes a big impact on the standard model (SM), which determines the finial parameters of the SM. Now the existence of a fundamental scalar is established and the SM has been completed. The next step is to figure out the physics behind the SM.

To accomplish this purpose, another observation in the LHC would be important: there is no evidence of the beyond SM physics. In other words, no new particles are discovered. Before the running of the LHC, the beyond SM physics appears soon from the point of view of the hierarchy problem unless the mass of the Higgs boson is unnaturally small. Such candidates are, for example, supersymmetry, extra dimension and compositeness, which solve hierarchy thanks to new symmetry or dynamics. The fact that we do not find new physics up to 1 TeV scale may imply that our understanding about field theory is not complete, or we have to consider beyond the ordinary field theory in order to solve this problem. Moreover, the smallness of the cosmological constant requires more severe fine-tuning than that of the Higgs mass. We also do not know the solution to the strong CP problem. This is the problem that, in principle, the P and CP can be broken in the quantum chromodynamics (QCD) sector by $F\tilde{F}$ term, in addition to the usual CP violation in Yukawa sector, but nature does not choose absence of CP violation in QCD sector.

Taking above situations into account, we investigate the following two subjects in the thesis. First is to examine the theoretical consistency of the SM with arbitrary cutoff scale Λ, and to check whether the SM is valid up to the string/Planck scale, which is the scale of the quantum gravity. We perform this calculation at the two loop level. In particular, we perform the two loop calculation of the bare Higgs mass.

As a result of the analysis of the renormalization group, it is found that there is another vacuum around the string/Planck scale which is degenerate in energy with the electroweak one, depending on the value of the top quark mass. This would be related to the Planck scale physics. There are some mechanisms which may be behind this degeneracy. For example, multiple point criticality principle (MPP)

[3–5] proposed by Froggatt and Nielsen explains the degeneracy by starting from not the canonical ensemble, but the micro-canonical ensemble. The other arguments are the asymptotic safety [6, 7], the hidden duality and symmetry [8, 9], the classical conformality [10–20] and the eternal topological Higgs inflation [21, 22].

Second is to look for a new solution to the naturalness problem. The new solution should be consistent with non-observation of the new physics at the LHC. However, if we believe the argument of the ordinary local field theory, in order to solve the fine-tuning problem of the Higgs mass, we need new physics around the TeV scale. Therefore, we should be beyond the ordinary local field theory. In this thesis, we consider the baby universe theory originally proposed by Coleman. The integration of the wormhole configuration gives rise to non-local interaction from the view point of large universe, which makes the parameter in the theory dynamical variable. The resultant low energy effective action is not given by usual local action, but given by the multi-local action, multiplication of the local action. We consider the Lorentz version of this mechanism, and try to solve the naturalness problem of the Higgs mass as well as the cosmological constant problem and strong CP problem. Furthermore, we show that this mechanism can also explain the degeneracy of the Higgs potential.

Despite the triumph of the SM, there remains a few things which can not be explained within the SM, one of which is the existence of the dark matter of the universe. Taking into account the success of the minimal SM, it seems that the inclusion of the dark matter to the SM may be achieved not by radical modification of SM such as supersymmetry, but by the simple extension of the SM. As a simple model, we consider the singlet and weakly interacting dark matter, and investigate their impact on the Higgs potential.

1.2   Organization of the Thesis

This thesis is organized as follows. In Chap. 2, we calculate the bare parameters at the Planck scale, and show that there exists triple coincidence if the top quark mass is around 170 GeV: all the bare Higgs mass, Higgs quartic coupling and its beta function take zero around the string/Planck scale. In Chap. 3, we investigate a phenomenological implication of the Higgs flat potential around the Planck scale. The Higgs inflation with flat potential drastically changes the prediction of the conventional Higgs inflation. In Chap. 4, we revisit the notorious problem of the SM, the fine-tuning of the Higgs mass. It turns out that the topological changing fluctuation of the spacetime metric can affect the fine-tuning of the parameters in the SM. We show that the Fermi constant, θ parameter and Higgs quartic coupling are indeed fixed around the real value. In Chap. 5, we consider the possible dark matter in the desert picture, and examine the relation between the Higgs potential and the dark matter. In Chap. 6, we summarize our results. In Appendix A, we fix the notations we use in the thesis. In Appendix B, the renormalization group equations (RGE) of simple extensions of the SM are shown. In Appendix C, we briefly review the inflation paradigm. In Appendix D, we summarize the strong CP problem and its possible

solution. In Appendix E, the quantization of Majorana field is written. This is needed when we treat the neutrino or Majorana fermion dark matter. In Appendix F, the integration appeared in Chap. 4 is evaluated.

References

1. ATLAS Collaboration, G. Aad et al., Observation of a new particle in the search for the Standard Model Higgs boson with the ATLAS detector at the LHC. Phys. Lett. B **716**, 1–29 (2012). arXiv:1207.7214
2. CMS Collaboration, S. Chatrchyan et al., Observation of a new boson at a mass of 125 GeV with the CMS experiment at the LHC. Phys. Lett. B **716**, 30–61 (2012). arXiv:1207.7235
3. C. Froggatt, H.B. Nielsen, Standard model criticality prediction: top mass 173 +- 5-GeV and Higgs mass 135 +- 9-GeV. Phys. Lett. B **368**, 96–102 (1996). arXiv:hep-ph/9511371
4. C. Froggatt, H.B. Nielsen, Y. Takanishi, Standard model Higgs boson mass from borderline metastability of the vacuum. Phys. Rev. D **64**, 113014 (2001). arXiv:hep-ph/0104161
5. H.B. Nielsen, PREdicted the Higgs mass. 94–126 (2012). arXiv:1212.5716
6. M. Shaposhnikov, C. Wetterich, Asymptotic safety of gravity and the Higgs boson mass. Phys. Lett. B **683**, 196–200 (2010). arXiv:0912.0208
7. K.-Y. Oda, M. Yamada, Non-minimal coupling in Higgs Yukawa model with asymptotically safe gravity. Class. Quantum Gravity **33**(12), 125011 (2016). arXiv:1510.03734
8. Y. Kawamura, Naturalness, conformal symmetry and duality. PTEP **2013**(11), 113B04 (2013). arXiv:1308.5069
9. Y. Kawamura, Gauge hierarchy problem, supersymmetry and fermionic symmetry. Int. J. Mod. Phys. A **30**(25), 1550153 (2015). arXiv:1311.2365
10. K.A. Meissner, H. Nicolai, Conformal symmetry and the standard model. Phys. Lett. B **648**, 312–317 (2007). arXiv:hep-th/0612165
11. R. Foot, A. Kobakhidze, K.L. McDonald, R.R. Volkas, A solution to the hierarchy problem from an almost decoupled hidden sector within a classically scale invariant theory. Phys. Rev. D **77**, 035006 (2008). arXiv:0709.2750
12. K.A. Meissner, H. Nicolai, Effective action, conformal anomaly and the issue of quadratic divergences. Phys. Lett. B **660**, 260–266 (2008). arXiv:0710.2840
13. S. Iso, N. Okada, Y. Orikasa, Classically conformal $B - L$ extended standard model. Phys. Lett. B **676**, 81–87 (2009). arXiv:0902.4050
14. S. Iso, N. Okada, Y. Orikasa, The minimal $B - L$ model naturally realized at TeV scale. Phys. Rev. D **80**, 115007 (2009). arXiv:0909.0128
15. H. Aoki, S. Iso, Revisiting the naturalness problem—who is afraid of quadratic divergences?. Phys. Rev. D **86**, 013001 (2012). arXiv:1201.0857
16. S. Iso, Y. Orikasa, TeV Scale B-L model with a flat Higgs potential at the Planck scale—in view of the hierarchy problem. PTEP **2013**,023B08 (2013). arXiv:1210.2848
17. M. Hashimoto, S. Iso, Y. Orikasa, Radiative symmetry breaking at the Fermi scale and flat potential at the Planck scale. Phys. Rev. D **89**,016019 (2014). arXiv:1310.4304
18. M. Hashimoto, S. Iso, Y. Orikasa, Radiative symmetry breaking from flat potential in various U(1)' models. Phys. Rev. D **89**, 056010 (2014). arXiv:1401.5944
19. P.H. Chankowski, A. Lewandowski, K.A. Meissner, H. Nicolai, Softly broken conformal symmetry and the stability of the electroweak scale (2014). arXiv:1404.0548
20. A. Latosinski, A. Lewandowski, K.A. Meissner, H. Nicolai, Conformal standard model with an extended scalar sector. JHEP **10**, 170 (2015). arXiv:1507.01755
21. Y. Hamada, K.-Y. Oda, F. Takahashi, Topological Higgs inflation: origin of standard model criticality. Phys. Rev. D **90**(9), 097301 (2014). arXiv:1408.5556
22. Y. Hamada, H. Kawai, K.-Y. Oda, Eternal Higgs inflation and the cosmological constant problem. Phys. Rev. D **92**,045009 (2015). arXiv:1501.04455

Chapter 2
Bare Parameters at Cutoff Scale

Abstract The discovery of the Higgs boson determines the last parameter in the SM, the Higgs self coupling λ. This allows us to extrapolate the SM up to very high scale such as the string/Planck scale. In this chapter, we calculate the bare parameters as functions of the cutoff scale Λ, and check the theoretical consistency, instability and perturbatively. Especially, we focus on the structure of the Higgs potential. In Sect. 2.1, we present the effective potential of the SM. In Sect. 2.2, we calculate the quadratic divergent part of the bare Higgs mass at the two loop level. In Sect. 2.3, we give the numerical estimation of bare parameters as functions of the cutoff scale. In Sect. 2.4, we give the relation between bare couplings and $\overline{\text{MS}}$ ones. In Sect. 2.5, we discuss the effect of the graviton on bare parameters. In Sect. 2.6, we comment on the metastability issue of the electroweak vacuum.

2.1 The Standard Model Effective Potential

In order to discuss the Higgs potential precisely, we need to calculate the loop correction of the Higgs potential. The general one loop potential [1] in $\overline{\text{MS}}$ scheme is given by [2]

$$V = \sum_n (-1)^{2s_n}(2s_n + 1)\frac{1}{64\pi^2}m_n^4\left(\log\frac{m_n^2}{\mu^2} + a\right),\tag{2.1}$$

where $a = -3/2$ for spin $s_n = 0, 1/2$ and $a = -5/6$ for spin $s_n = 1$ with m_n being effective mass. The summation is taken over real scalars, two component fermions and vectors.

Then, in the Landau gauge, Coleman-Weinberg potential of the SM Higgs is calculated as

$$V_{\text{tree}} = e^{4\Gamma(\varphi)}\frac{\lambda(\mu)}{4}\varphi^4,\tag{2.2}$$

$$V_{1-\text{loop}} = e^{4\Gamma(\varphi)}\left\{-\frac{3M_t(\varphi)^4}{16\pi^2}\left(\ln\frac{M_t(\varphi)^2}{\mu^2} - \frac{3}{2} + 2\Gamma(\varphi)\right)\right.$$

$$+ \frac{6M_W(\varphi)^4}{64\pi^2} \left(\ln \frac{M_W(\varphi)^2}{\mu^2} - \frac{5}{6} + 2\Gamma(\varphi) \right) + \frac{3M_Z(\varphi)^4}{64\pi^2} \left(\ln \frac{M_Z(\varphi)^2}{\mu^2} - \frac{5}{6} + 2\Gamma(\varphi) \right) \Bigg\},$$

$$\tag{2.3}$$

$$\Gamma(\varphi) = \int_{M_t}^{\varphi} \gamma \, d \ln \mu, \tag{2.4}$$

$$\gamma = \frac{1}{(4\pi)^2} \left(\frac{9}{4} g_2^2 + \frac{3}{4} g_Y^2 - 3 y_t^2 \right), \tag{2.5}$$

where φ is the field value of the Higgs, $H = \varphi/\sqrt{2}$, $M_W(\varphi) = g_2 \varphi/2$, $M_Z(\varphi) = \sqrt{g_Y^2 + g_2^2} \, \varphi/2$, and $M_t(\varphi) = y_t \varphi/\sqrt{2}$.

From above expression, we can define the effective quartic coupling of the Higgs potential as follows.

$$\lambda_{\text{eff}}(\varphi, \mu) = e^{4\Gamma(\varphi)} \lambda(\mu) + e^{4\Gamma(\varphi)} \frac{1}{16\pi^2} \Bigg[-3 y_t^4 \left(\ln \frac{y_t^2 \varphi^2}{2\mu^2} - \frac{3}{2} + 2\Gamma(\varphi) \right)$$

$$+ \frac{3 g_2^4}{8} \left(\ln \frac{g_2^2 \varphi^2}{4\mu^2} - \frac{5}{6} + 2\Gamma(\varphi) \right) + \frac{3 \left(g_Y^2 + g_2^2 \right)^2}{16} \left(\ln \frac{\left(g_Y^2 + g_2^2 \right) \varphi^2}{4\mu^2} - \frac{5}{6} + 2\Gamma(\varphi) \right) \Bigg].$$

$$\tag{2.6}$$

The two loop formula is given in Ref. [3], and we use it for our analysis.

2.1.1   Scheme Independence of the Coleman-Weinberg Potential

In this section, we comment on the scheme independence of the Coleman-Weinberg potential by taking ϕ^4 theory Lagrangian as an example,

$$\mathcal{L} = \frac{1}{2} (\partial_\mu \phi)^2 - \frac{1}{2} m^2 \phi^2 - \frac{\lambda}{4!} \phi^4. \tag{2.7}$$

The Coleman-Weinberg potential is

$$-i V_{1-\text{loop}} = -\frac{1}{2} \int \frac{d^d p}{(2\pi)^d} \log \left(-p^2 + \frac{\lambda \varphi^2}{2} \right)$$

$$= -\frac{i}{2} \int dp_E \frac{\Omega_d \, p_E^{d-1}}{(2\pi)^d} \log \left(p_E^2 + \frac{\lambda \varphi^2}{2} \right), \tag{2.8}$$

where $\Omega_d = 2\pi^{d/2}/\Gamma(d/2)$. Then, we have

$$
\begin{aligned}
V_{1-\text{loop}} &= \frac{1}{\Gamma(\frac{d}{2})}\frac{1}{2}\int dp_E^2 \frac{(p_E^2)^{d/2-1}}{(4\pi)^{d/2}}\log\left(p_E^2 + \frac{\lambda\varphi^2}{2}\right)\\
&= \frac{1}{\Gamma(\frac{d}{2})}\frac{1}{2}\frac{1}{(4\pi)^{d/2}}\frac{2}{d}\left((p_E^2)^{d/2}\log\left(p_E^2 + \frac{\lambda\varphi^2}{2}\right)\Big|_0^\infty - \int dp_E^2 \frac{(p_E^2)^{d/2}}{p_E^2 + \frac{\lambda\varphi^2}{2}}\right)\\
&= -\frac{1}{\Gamma(\frac{d}{2})}\frac{1}{2}\frac{1}{(4\pi)^{d/2}}\frac{2}{d}\left(\frac{\lambda\varphi^2}{2}\right)^{d/2}\int dx\frac{x^{d/2}}{1+x}\\
&= -\frac{1}{\Gamma(\frac{d}{2})}\frac{1}{2}\frac{1}{(4\pi)^{d/2}}\frac{2}{d}\left(\frac{\lambda\varphi^2}{2}\right)^{d/2}\int dy\, y^{d/2}(1-y)^{-1-d/2}\\
&= -\frac{1}{2}\frac{1}{(4\pi)^{2-\epsilon}}\frac{2}{d}\left(\frac{\lambda\varphi^2}{2}\right)^{2-\epsilon}\frac{d}{2}\Gamma\left(-\frac{d}{2}\right)\\
&= -\frac{1}{2}\frac{1}{(4\pi)^2}\left(\frac{\lambda\varphi^2}{2}\right)^2\left(1+\epsilon\log(4\pi)-\epsilon\log\left(\frac{\lambda\varphi^2}{2}\right)\right)\frac{\frac{1}{\epsilon}-\gamma}{(-2+\epsilon)(-1+\epsilon)}\\
&= \frac{1}{64\pi^2}\left(\frac{\lambda\varphi^2}{2}\right)^2\left(-\frac{1}{\epsilon}+\gamma-\log(4\pi)+\log\left(\frac{\lambda\varphi^2}{2}\right)-\frac{3}{2}\right). \qquad (2.9)
\end{aligned}
$$

In the MS and $\overline{\text{MS}}$ schemes, the divergence is subtracted as follows.

$$
-\frac{1}{\epsilon} \to -\log(\mu^2) \quad \text{(MS scheme)}
$$

$$
-\frac{1}{\epsilon}+\gamma-\log(4\pi) \to -\log(\mu^2) \quad (\overline{\text{MS}}\text{ scheme}). \qquad (2.10)
$$

Therefore, Coleman-Weinberg potential becomes

$$
V = V_{\text{tree}} + V_{1-\text{loop}}
$$

$$
= \begin{cases}
\dfrac{\varphi^4}{4!}\left\{\lambda_{\text{MS}}+\dfrac{3}{32\pi^2}(\lambda_{\text{MS}}\varphi^2)^2\left(\log\left(\dfrac{\lambda_{\text{MS}}\varphi^2}{2\mu^2}\right)+\gamma-\log(4\pi)-\dfrac{3}{2}\right)\right\} & \text{for MS}\\[4ex]
\dfrac{\varphi^4}{4!}\left\{\lambda_{\overline{\text{MS}}}+\dfrac{3}{32\pi^2}(\lambda_{\overline{\text{MS}}}\varphi^2)^2\left(\log\left(\dfrac{\lambda_{\overline{\text{MS}}}\varphi^2}{2\mu^2}\right)-\dfrac{3}{2}\right)\right\} & \text{for }\overline{\text{MS}}
\end{cases}
$$

$$(2.11)$$

In order to compare λ_{MS} and $\lambda_{\overline{\text{MS}}}$, let us calculate four point function with external momentum $(p_1 + p_2)^2 = (p_1 + p_3)^2 = (p_1 + p_4)^2 = P^2$:

$$
\begin{aligned}
\langle \phi(p_1)\phi(p_2)\phi(p_3)\phi(p_4) \rangle &= -i\lambda + \frac{(-i\lambda)^2}{2}\mu^\epsilon \int \frac{d^d k}{(2\pi)^d} \frac{i^2}{k^2(P+k)^2} \times 3 \\
&= -i\lambda + \frac{3}{2} i\lambda^2 \mu^\epsilon \int \int dx \frac{d^d l_E}{(2\pi)^d} \frac{1}{(l_E^2 - x(1-x)P^2)^2} \\
&= -i\lambda + \frac{3}{32\pi^2} i\lambda^2 \left(\frac{1}{\epsilon} - \gamma + \log(4\pi) + \log\left(\frac{\mu^2}{-x(1-x)P^2} \right) \right).
\end{aligned}
\tag{2.12}
$$

Then, we obtain

$$
\lambda_{\mathrm{MS}} = \lambda_{\overline{\mathrm{MS}}} - \frac{3}{32\pi^2}\lambda_{\overline{\mathrm{MS}}}^2 (\gamma - \log(4\pi)).
\tag{2.13}
$$

Substituting Eq. (2.13) into Eq. (2.11), we can see that effective potential in MS and that in $\overline{\mathrm{MS}}$ are the same.

2.1.2 How to Calculate the Beta Function

This part is based on Refs. [4, 5]. In the previous sections, we have seen that we need the beta function and gamma function in order to evaluate the effective potential. We review the calculation of these functions using the dimensional regularization, namely $d = 4 - 2\epsilon$. Then, requiring that $F_{\mu\nu}F^{\mu\nu}$, $\bar{\psi}i\partial_\mu\gamma^\mu\psi$ and $\bar{\psi}iA_\mu\gamma^\mu\psi$ have same dimension, we can fix the dimension in unit of momentum as $[A_\mu] = 1$, $[\psi] = 3/2$, and overall $1/g_B^2$ factor has dimension $[1/g_B^2] = d - 4 = 2\epsilon$. Hence, we parameterize g_B as

$$
g_B = \bar{\mu}^\epsilon \bar{Z}_g g,
\tag{2.14}
$$

where

$$
\bar{\mu} = \frac{\mu}{\sqrt{4\pi}} e^{\gamma_E}.
\tag{2.15}
$$

Here γ_E is the Euler constant. This corresponds to the usual one loop subtraction of $(1/\epsilon - \gamma_E + \log(4\pi))/(4\pi)^2$, which can be found in the elementary textbook of quantum field theory like Ref. [6].

By using this μ, the renormalization of the coupling constant is

$$
g_B = \mu^\epsilon Z_g g, \qquad\qquad Z_g = 1 + \sum_{i=1}^{\infty} \frac{Z_g^{(i)}(g)}{\epsilon^i}.
\tag{2.16}
$$

The dimensional analysis tells us that $Z_g^{(i)}(g)$ depends on μ only through $g(\mu)$. We also note that Eq. (2.16) does not contain $\epsilon^0, \epsilon^1, \ldots$ terms. This corresponds to

the choice of the counter term in the scheme, and therefore this is nothing but the definition of $\overline{\text{MS}}$ scheme.

The definition of the beta function is

$$\beta_g = \mu \frac{\partial}{\partial \mu} g. \tag{2.17}$$

The partial derivative means that g_B and ϵ are fixed.

From the definition, we have

$$\beta_g = \mu \frac{\partial}{\partial \mu} \left(\mu^{-\epsilon} Z_g^{-1} g_B \right) = -\epsilon g - g \beta_g \frac{\partial}{\partial g} \log Z_g, \tag{2.18}$$

which becomes

$$\left(\beta_g + \epsilon g + g \beta_g \frac{\partial}{\partial g} \right) Z_g = 0. \tag{2.19}$$

We substituting Eq. (2.16) into this, and put ansatz on $\beta_g = \sum_{i=0}^{i=N} \beta_g^{(i)} \epsilon^i$, where N is some finite number. Then it turns out that

$$\begin{aligned}
\beta_g^{(i)} &= 0, \quad (2 \le i \le N) \\
\beta_g^{(1)} &= -g, \\
\beta_g^{(0)} &= -g \beta_g^{(1)} \frac{\partial}{\partial g} Z_g^{(1)}.
\end{aligned} \tag{2.20}$$

Hence, in order to calculate the beta function in $\overline{\text{MS}}$ scheme, we take the simple pole of ϵ in Z_g:

$$\lim_{\epsilon \to 0} \beta_g = g^2 \frac{\partial}{\partial g} Z_g^{(1)}. \tag{2.21}$$

The similar derivation is applicable to the gamma function. From the definition,

$$\gamma_\phi = \frac{1}{2} \mu \frac{\partial}{\partial \mu} \log Z_\phi, \tag{2.22}$$

we can derive

$$\left(\beta_g \frac{\partial}{\partial g} - 2\gamma \right) Z_\phi = 0, \tag{2.23}$$

where Z_ϕ is the wavefunction renormalization of a scale field ϕ, $\phi_B = \sqrt{Z_\phi}\phi$. As a result, we obtain

$$\gamma_\phi = -\frac{1}{4}g\frac{\partial}{\partial g}Z_\phi^{(1)}. \tag{2.24}$$

A few comments on the properties of the beta and gamma functions are in order.

1. The coefficients of $\mathcal{O}(g^3)$, $\mathcal{O}(g^5)$ terms in the beta function and $\mathcal{O}(g^3)$ term in gamma function are independent of the scheme.
   This can be seen by starting from the given beta function of some scheme,

$$\beta_g = b_0 g^3 + b_1 g^5 + \mathcal{O}(g^7). \tag{2.25}$$

   Let us calculate the beta function in different scheme, $\beta'_{g'} := \mu\partial_\mu g'$. Here $g' = g + ag^3 + \mathcal{O}(g^5)$ is taken.[1] $\beta'_{g'}$ becomes

$$\begin{aligned}
\beta'_{g'} &= \beta_g \frac{dg'}{dg} \\
&= (b_0 g^3 + b_1 g^5 + \mathcal{O}(g^7))(1 + 3ag^2 + \mathcal{O}(g^4)) \\
&= b_0 g'^3 + b_1 g'^5 + \mathcal{O}(g'^7). \tag{2.26}
\end{aligned}$$

2. The zero of the beta function, $\beta(g_*) = 0$, is independent of the scheme.
   If the beta function vanishes at $g = g_*$ in some scheme, $\beta'_{g'}(g'(g = g_*))$ also does:

$$\beta'_{g'}(g'(g = g_*)) = \beta_g(g_*)\frac{dg'}{dg} = 0. \tag{2.27}$$

   Therefore, the existence of a fixed point is scheme independent.
3. $\dfrac{d\beta}{dg}$ at $g = g_*$ is independent of the scheme.

$$\frac{d\beta'_{g'}}{dg'} = \frac{d\beta_g}{dg} + \frac{\partial g}{\partial g'}\beta_g(g_*)\frac{\partial^2 g'}{\partial g^2} = \frac{d\beta_g}{dg}. \tag{2.28}$$

   This independence is importance because $d\beta/dg$ determines the flow around a fixed point. This means that the critical exponent is scheme independent quantity.
4. The leading term of γ_ϕ is independent of the scheme.
   We write a relation between the wavefunction renormalization as

$$Z'_\phi(g') = Z_\phi(g)F_\phi(g), \qquad\qquad F_\phi(g) = 1 + \mathcal{O}(g^2) \tag{2.29}$$

---

[1] In general, scale μ' can also be different from μ. Here we assume that $\mu' \propto \mu$.

For some scheme, $\gamma_\phi(g) = c_0 g^2 + \mathcal{O}(g^4)$, then

$$
\begin{aligned}
\gamma'_\phi(g') &= \frac{1}{2}\mu\frac{\partial}{\partial\mu}\log(Z_\phi(g)F_\phi(g)) \\
&= \gamma_\phi(g) + \frac{1}{2}\beta_g\frac{\partial}{\partial g}\log F_\phi(g) \\
&= c_0 g^2 + \mathcal{O}(g^4).
\end{aligned}
\tag{2.30}
$$

5. $\gamma_\phi(g) = \gamma'_\phi(g')$ at a fixed point, $\beta_g(g_*) = 0$.
   This is obvious from the Eq. (2.30).

The leading contribution in beta function and gamma function corresponds to the summation of the leading logarithm. The renormalization group equation for the one-particle irreducible Green function $\Gamma^{(n)}$ is

$$
\left(\mu\frac{\partial}{\partial\mu} + \beta_g\frac{\partial}{\partial g} - n\gamma_\phi\right)\Gamma^{(n)} = 0.
\tag{2.31}
$$

By introducing $t := \log(\mu/Q)$ where Q is some pivot scale, we have

$$
\frac{\partial}{\partial t}\Gamma^{(n)}(t, g) = \left(\beta_g\frac{\partial}{\partial g} - n\gamma_\phi\right)\Gamma^{(n)}.
\tag{2.32}
$$

Formally we can solve it, and obtain

$$
\begin{aligned}
\Gamma^{(n)}(t, g) &= \exp\left[t\left(\beta_g\frac{\partial}{\partial g} - n\gamma_\phi\right)\right]\Gamma^{(n)}(0, g) \\
&= \sum_m \frac{1}{m!}\left(\log\frac{\mu}{Q}\right)^m\left(\beta_g\frac{\partial}{\partial g} - n\gamma_\phi\right)^m\Gamma^{(n)}(0, g)
\end{aligned}
\tag{2.33}
$$

The point is that the mass independent scheme such as $\overline{\text{MS}}$, β and γ does not have explicit dependence of μ.

The inclusion of leading term of the beta and gamma function corresponds to the summation of leading log. The next-to-leading, next-to-next-leading, ... terms correspond to next-leading log, next-to-next-leading log, ..., respectively.

2.2 Bare Higgs Mass at the Two Loop

In the following, we will estimate the bare parameters of the SM, and check the theoretical consistency. To compute the bare parameters is important because these are inputs for numerical consideration of the cutoff scale physics such as string theory. There are two kinds of the bare parameters, dimensionless coupling and dimensionful

one. The dimensionless couplings are the gauge couplings, Yukawa couplings and Higgs self coupling, while dimensionful coupling is the bare Higgs mass. As we will see in Sect. 2.4, the dimensionless couplings are well approximated by $\overline{\text{MS}}$ ones. On the other hand, the bare Higgs mass needs extra computations. In this section, we calculate the bare Higgs mass at the two loop level. See Refs. [7–11] for related topic. The dominant part of the bare Higgs mass is the quadratic divergence, so we focus on this part, and calculate it by a cutoff scheme. We have performed the two loop level calculation, and obtain the bare mass as follows:

$$m_{B,\,1-\text{loop}}^2 = -\left(6\lambda_B + \frac{3}{4}g_{YB}^2 + \frac{9}{4}g_{2B}^2 - 6y_{tB}^2\right) I_1, \tag{2.34}$$

$$m_{B,\,2-\text{loop}}^2 = -\left\{9y_{tB}^4 + y_{tB}^2\left(-\frac{7}{12}g_{YB}^2 + \frac{9}{4}g_{2B}^2 - 16g_{3B}^2\right)\right.$$

$$-\frac{87}{16}g_{YB}^4 - \frac{63}{16}g_{2B}^4 - \frac{15}{8}g_{YB}^2g_{2B}^2$$

$$\left.+ \lambda_B\left(-18y_{tB}^2 + 3g_{YB}^2 + 9g_{2B}^2\right) - 12\lambda_B^2\right\} I_2. \tag{2.35}$$

Here I_1 and I_2 are quadratic divergent loop integrals,

$$I_1 := \int \frac{d^4 p_E}{(2\pi)^4} \frac{1}{p_E^2}, \tag{2.36}$$

$$I_2 := \int \frac{d^4 p_E}{(2\pi)^4} \frac{d^4 q_E}{(2\pi)^4} \frac{1}{p_E^2 q_E^2 (p_E + q_E)^2}, \tag{2.37}$$

$y_{tB}, \lambda_B, g_{3B}, g_{2B}$ and g_{YB} are bare top Yukawa, bare Higgs self coupling, bare $SU(3)_C$ coupling, bare $SU(2)_L$ coupling and bare $U(1)_Y$ coupling, respectively.

The vanishing bare Higgs mass condition at the one loop is nothing but Veltman condition [8]. In the computation, we take the physical Higgs mass to be zero and work in symmetric phase. This is because the dimensional analysis tells us that the quadratic divergent part is same both in symmetric phase and broken phase, and is independent of physical Higgs mass. In addition, Landau gauge is taken. The use of Landau gauge drastically reduces the number of Feynman diagram. In Landau gauge, the following class of diagram vanishes since three point coupling is derivative coupling, and external momentum is zero:

$$\left.\vcenter{\hbox{}}\right|_{k=0} = 0.$$

$$\tag{2.38}$$

In Figs. 2.1 and 2.2, we show non-vanishing diagrams and their contributions.

	$5g_{YB}^4 + 9g_{2B}^4$
	$-\dfrac{51}{8}g_{2B}^4$
	$\dfrac{1}{8}g_{YB}^4 + \dfrac{3}{8}g_{2B}^4$
	$\dfrac{5}{16}g_{YB}^4 + \dfrac{15}{16}g_{2B}^4 + \dfrac{15}{8}g_{YB}^2 g_{2B}^2$
sum	$\dfrac{87}{16}g_{YB}^4 + \dfrac{63}{16}g_{2B}^4 + \dfrac{15}{8}g_{YB}^2 g_{2B}^2$

Fig. 2.1 g^4 terms in $m_{B,\,2-\text{loop}}^2$ in units of I_2

	$12\lambda_B^2$
	$-9y_{tB}^4$
	$y_{tB}^2\left(\tfrac{7}{12}g_{YB}^2 - \tfrac{9}{4}g_{2B}^2 + 16g_{3B}^2\right)$
	$\lambda_B\left(18y_{tB}^2 - 3g_{YB} - 9g_{2B}^2\right)$

Fig. 2.2 The terms other than g^4 in $m_{B,\,2-\text{loop}}^2$ in units of I_2

In order to fix the ratio of I_1 and I_2, the cutoff scheme should be specified. In this thesis, we take proper time regularization:

$$\int d^4 k_E \frac{1}{k_E^2} = \int_\varepsilon^\infty d\alpha \int d^4 k_E \, e^{-\alpha k_E^2}, \qquad (2.39)$$

By employing this regularization, the one loop and two loop integrals are calculated as

$$I_1 = \frac{1}{\varepsilon} \frac{1}{16\pi^2},$$

$$I_2 = \int \frac{d^4 k}{(2\pi)^4} \frac{d^4 p}{(2\pi)^4} \frac{1}{k^2 p^2 (p+k)^2}$$

$$= \int_\epsilon^\infty d\alpha \int_\epsilon^\infty d\beta \int_\epsilon^\infty d\gamma \frac{d^4 k}{(2\pi)^4} \frac{d^4 p}{(2\pi)^4} e^{-\alpha p^2 - \beta k^2 - \gamma(p+k)^2}$$

$$= \int_\epsilon^\infty d\alpha \int_\epsilon^\infty d\beta \int_\epsilon^\infty d\gamma \frac{\pi^4}{(2\pi)^8} \frac{1}{(\alpha\beta + \beta\gamma + \gamma\alpha)^2}$$

$$= \frac{1}{\epsilon} \int_1^\infty d\alpha' \int_1^\infty d\beta' \int_1^\infty d\gamma' \frac{\pi^4}{(2\pi)^8} \frac{1}{(\alpha'\beta' + \beta'\gamma' + \gamma'\alpha')^2}$$

$$= \frac{1}{\varepsilon} \frac{1}{(16\pi^2)^2} \ln \frac{2^6}{3^3} \simeq 0.005 \, I_1. \qquad (2.40)$$

Here $\alpha' = \epsilon \, \alpha$, $\alpha' = \epsilon \, \beta$ and $\alpha' = \epsilon \, \gamma$. If we employ the usual momentum cutoff, we obtain

$$I_1 = \frac{\Lambda^2}{16\pi^2}, \qquad (2.41)$$

which implies the relation $1/\varepsilon = \Lambda^2$. We note that the ratio Eq. (2.40) depends on the cutoff scheme. However, in the next section, we will show that the two loop effect is small, and therefore we can safely neglect the cutoff scheme dependence.

2.3 Bare Parameters at the Cutoff Scale

In this section, we numerically solve the renormalization group equations (RGEs), and evaluate the bare parameters at the cutoff scale. The values of SM couplings at the electroweak scale are given in Ref. [3]:

$$g_2(M_t) = 0.64822 + 0.00004 \left(\frac{M_t}{\text{GeV}} - 173.10 \right) + 0.00011 \left(\frac{M_W - 80.384\text{GeV}}{0.014\text{GeV}} \right), \quad (2.42)$$

$$g_Y(M_t) = 0.35761 + 0.00011 \left(\frac{M_t}{\text{GeV}} - 173.10 \right) + 0.00021 \left(\frac{M_W - 80.384\text{GeV}}{0.014\text{GeV}} \right), \quad (2.43)$$

$$g_3(M_t) = 1.1666 + 0.00314 \left(\frac{\alpha_S(M_Z) - 0.1184}{0.0007} \right) - 0.00046 \left(\frac{M_t}{\text{GeV}} - 173.10 \right), \quad (2.44)$$

$$y_t(M_t) = 0.93558 + 0.00550 \left(\frac{M_t}{\text{GeV}} - 173.10 \right) - 0.00042 \left(\frac{\alpha_S(M_Z) - 0.1184}{0.0007} \right)$$

$$- 0.00042 \left(\frac{M_W - 80.384\text{GeV}}{0.014\text{GeV}} \right) \pm 0.00050_{\text{th}}, \quad (2.45)$$

$$\lambda(M_t) = 0.12711 + 0.00206 \left(\frac{M_H}{\text{GeV}} - 125.66 \right) - 0.00004 \left(\frac{M_t}{\text{GeV}} - 173.10 \right) \pm 0.00030_{\text{th}}. \quad (2.46)$$

The RGE of the SM at two loop level is in Appendix B. The mass of the Higgs boson is

$$M_H = 125.09 \pm 0.24 \,\text{GeV} \quad (2.47)$$

at the 1σ by Particle Data Group [12]. The $SU(3)_C$ gauge coupling is

$$\alpha_S(M_W) = 0.1185 \pm 0.0006 \,\text{GeV}. \quad (2.48)$$

We note that the current error of the value of the top mass:

$$M_t^{\text{pole}} = \begin{cases} 171.2 \pm 2.4 \,\text{GeV}, & \text{MITP [13]}, \\ 176.7^{+4.0}_{-3.4} \,\text{GeV}, & \text{PDG [14]}, \end{cases} \quad (2.49)$$

$$M_t^{\text{Pythia}} = \begin{cases} 173.21 \pm 0.51 \pm 0.71 \,\text{GeV}, & \text{direct measurement, PDG [14]}, \\ 174.98 \pm 0.76 \,\text{GeV}, & \text{D0 [15]}, \\ 174.34 \pm 0.64 \,\text{GeV}, & \text{D0+CDF [16]}, \\ 173.34 \pm 0.76 \,\text{GeV}, & \text{ATLAS [17]}, \\ 172.38 \pm 0.10 \pm 0.65 \,\text{GeV}, & \text{CMS [18]}. \end{cases} \quad (2.50)$$

As we can see, there are two types of top masses, M_t^{pole} and M_t^{Pythia}. M_t^{Pythia} is measured by using Monte Carlo simulation. The experiment observes the momentum of the color singlet decay product of $t\bar{t}$, and compares with the event shape of Monte Carlo simulation. The problem is that we do not know the relation between M_t^{Pythia} and $\overline{\text{MS}}$ parameters, which is important for renormalization group (RG) evolution. Moreover, M_t^{Pythia} inevitably suffers from uncertainty of hadronization.

On the other hand, M_t^{pole} is defined as a pole of two point function of the top field. At least perturbatively, M_t^{pole} is well defined, and can be written by using $\overline{\text{MS}}$ couplings. Therefore, we use M_t^{pole} in the thesis. M_t^{pole} is measured from inclusive cross section of $t\bar{t}$, $\sigma(pp \to t\bar{t}X)$ at the LHC. We can see that M_t^{pole} still has large

uncertainty. As we will see, in order to discuss the criticality of the SM precisely, the error of M_t should become small.

The way of precision measurement of the top mass is the threshold scan of the toponium state, which can be done by, e.g. international linear collider (ILC) in which initial energy of electron and positron is controlled. In the ILC, the error of top mass is estimated as $\mathcal{O}(10\text{–}100)\,\mathrm{MeV}$. In the following, we take

$$M_t^{\mathrm{pole}} = 171.2 \pm 2.4\,\mathrm{GeV} \tag{2.51}$$

as a reference value.

Then let us move on numerical calculation. We plot the running of bare parameters in the left panel of Fig. 2.3. The largest uncertainty comes from the error of the top mass Eq. (2.51), we represent it as bands. Surprisingly, we can find triple coincidence if the top quark mass is 170 GeV: the Higgs self coupling λ, its beta function β_λ and bare Higgs mass take zero around the string/Planck scale. Figure 2.4
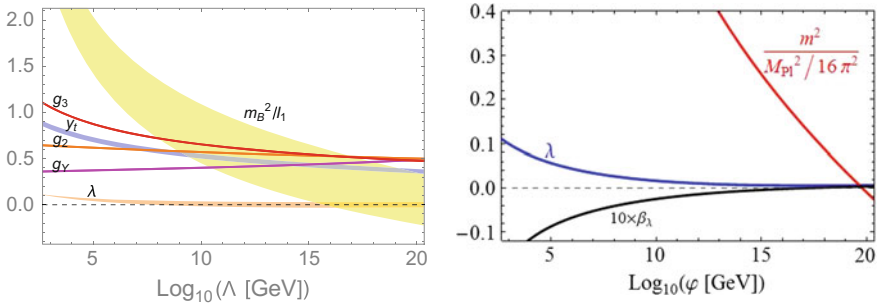
Fig. 2.3 *Left* The bare parameters as functions of the cutoff scale Λ as well as the beta function of λ. The *band* corresponds to the two sigma deviation of the top mass, Eq. (2.51). *Right* The triple coincidence occurs if $M_t = 170$ GeV

Fig. 2.4 The *light blue band* is RGE running of $\lambda_{\mathrm{eff}}(\mu)$. $\lambda_{\mathrm{eff}}(\mu)$ is defined by two loop effective potential, and we have used 2 loop RGE. The *dark blue band* is the beta function multiplied by ten, $10 \times d\lambda_{\mathrm{eff}}/d\ln\mu$. $M_H = 125.09$ GeV and $\alpha_s = 0.1185$ are taken. The band corresponds to 95% CL deviation of M_t
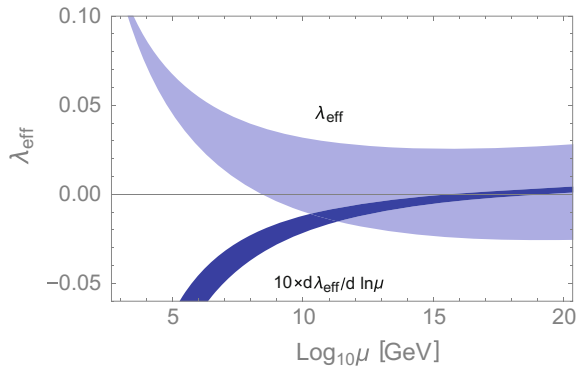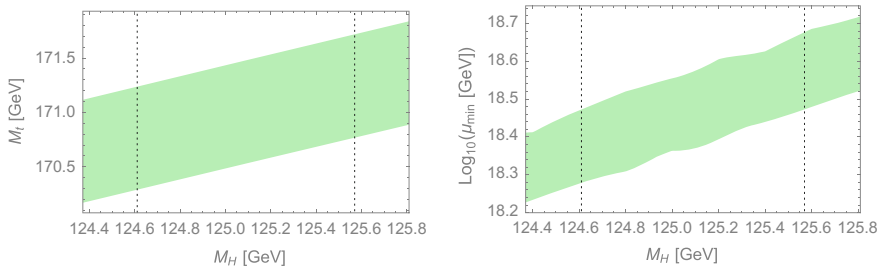
Fig. 2.5 Left: M_t realizing $\lambda_{\min} = 0$ as a function of M_H. We use the two loop RGE and effective potential. The *light green band* and *dotted line* correspond to 95% deviation of α_s and M_H, respectively. *Right* The scale $\mu_{\min}$ that realizes $\lambda_{\min} = 0$
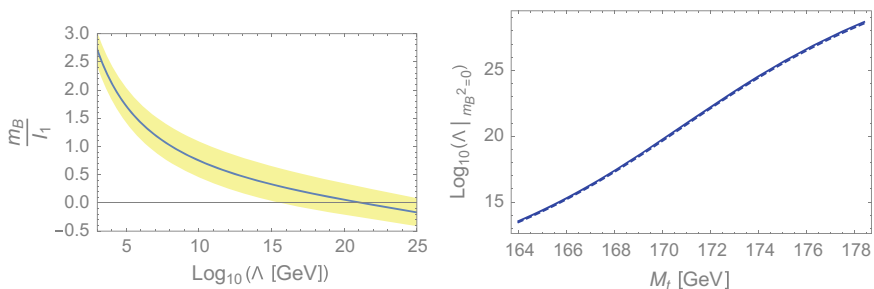
Fig. 2.6 *Left* The bare Higgs mass as a function of Λ. The *band* corresponds the deviation of the top mass at 95% C.L. *Right* The scale where the bare Higgs mass takes zero as a function of M_t

is the enlarged view of the effective self coupling λ_{eff} and its derivative as functions of the renormalization scale μ. The band is same as Fig. 2.3. In the left panel of the Fig. 2.5, M_t realizing $\lambda_{\min} = 0$ as a function of M_H is plotted. In the right panel, we can see the scale $\mu_{\min}$ that realizes $\lambda_{\min} = 0$. From this we can see that the two loop effect is small. In Fig. 2.6, we show the bare Higgs mass as a function of the cutoff scale Λ at the two loop level. The right panel represents the scale where the bare mass vanishes. The dashed and solid lines correspond to one-loop and two-loop calculations, respectively. We can see that the two loop effect is small, as we noted before. The bare mass and the self coupling at the Planck scale is shown in Fig. 2.7, as well as the beta function of the self coupling. It can be seen that there is three coincidence. The bare mass, self coupling and its beta function simultaneously become zero if the top quark mass is around 170 GeV.

Fig. 2.7 The *blue solid*
(*dashed*) *line* corresponds to
the one-plus-two-loop
(one-loop) bare mass m_B^2
($m_{B,\,1-\text{loop}}^2$) in units of
$M_P^2/16\pi^2$ for $\Lambda = M_P$. For
comparison, we also plot the
quartic coupling λ at the
Planck scale with the *red
dotted line*. The central
values $\alpha_s(m_Z) = 0.1185$ and
$m_H = 125.9$ GeV are used
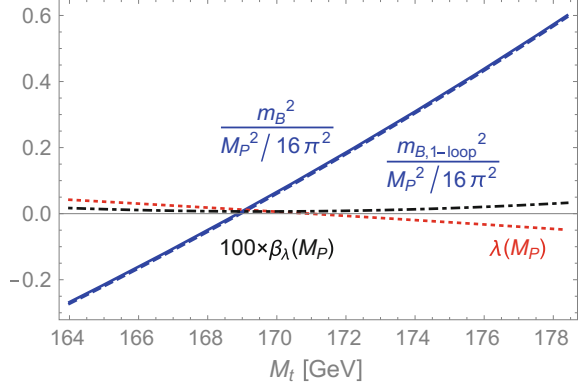
2.4 The Relation Between Dimensionless Bare Couplings and $\overline{\text{MS}}$ Couplings

We have approximated the bare couplings by $\overline{\text{MS}}$ ones. In this section, we present the justification of this approximation. The relation between dimensionless bare coupling and $\overline{\text{MS}}$ coupling can be obtained by calculating a physical quantity. Here we present the relation in ϕ^4 theory by performing the one loop integral of the four point function $\langle\phi(p_1)\phi(p_2)\phi(p_3)\phi(p_4)\rangle$. As there is no wavefunction renormalization at the one loop level, we can take $\phi_B = \phi$. The one loop calculation in the $\overline{\text{MS}}$ scheme can be found in Eq. (2.12). In the momentum cutoff scheme, we get

$$-i\lambda_B + \frac{(-i\lambda_B)^2}{2}\int \frac{d^4k}{(2\pi)^4}\frac{i^2}{k^2(P+k)^2}\times 3$$

$$= -i\lambda_B + \frac{3}{2}i\lambda_B^2\int_0^{\Lambda^2}\int_0^1 dx\,\frac{d^4l_E}{(2\pi)^4}\frac{1}{(l_E^2 - x(1-x)P^2)^2}. \tag{2.52}$$

Taking $P^2 = -\Lambda^2$, we obtain

$$\langle\phi(p_1)\phi(p_2)\phi(p_3)\phi(p_4)\rangle = -i\lambda_B + \frac{3}{32\pi^2}i\lambda_B^2\frac{\log(161 + 72\sqrt{5})}{2\sqrt{5}}$$

$$\simeq -i\lambda_B + 0.01\times i\lambda_B^2. \tag{2.53}$$

Finally we have

$$-i\lambda(\mu) + \frac{3}{32\pi^2}i\lambda(\mu)^2\left(\log\left(\frac{\mu^2}{\Lambda^2}\right) - 2\right) = -i\lambda_B + \frac{3}{32\pi^2}i\lambda_B^2\frac{\log(161 + 72\sqrt{5})}{2\sqrt{5}}, \tag{2.54}$$

and the relation between bare and $\overline{\text{MS}}$ coupling can be derived as

$$\lambda_B = \lambda(\Lambda) - \frac{3}{32\pi^2} i\lambda(\Lambda)^2 \left(2 + \frac{\log(161 + 72\sqrt{5})}{2\sqrt{5}} \right). \tag{2.55}$$

Now we have confirmed that the difference between two couplings are very small, and the approximation $\lambda_B \simeq \lambda(\Lambda)$ is justified.

Now let us evaluate the effect of above approximation on the scale where the bare Higgs mass vanishes. The relation between the bare and $\overline{\text{MS}}$ coupling in the SM is generally written as

$$\lambda^i_{\overline{\text{MS}}}(\mu) = \lambda^i_B + \sum_{jk} c^{ijk}(\mu/\Lambda) \, \lambda^j_B \lambda^k_B + O(\lambda^3_B), \tag{2.56}$$

$$c^{ijk}(x) := f^{ijk} + b^{ijk} \ln x + O(x^2), \tag{2.57}$$

where b^{ijk} represents the one loop coefficient of the beta function, f^{ijk} represents the finite correction and λ^i_B represent $(\{g^2_{YB}, g^2_{2B}, g^2_{3B}, y^2_{tB}, \lambda_B\})$. Since the all SM couplings are perturbative up to the Planck scale, we have

$$\mu \ll \Lambda, \qquad\qquad \left| \frac{\lambda^i_{\overline{\text{MS}}}}{16\pi^2} \ln(\mu/\Lambda) \right| \ll 1, \tag{2.58}$$

and therefore

$$\lambda^i_{\overline{\text{MS}}}(\mu) = \lambda^i_B + \sum_{jk} \left(f^{ijk} + b^{ijk} \ln \frac{\mu}{\Lambda} \right) \lambda^j_B \lambda^k_B, \tag{2.59}$$

is the good approximation. On the other hand, the scale dependence of $\overline{\text{MS}}$ coupling can be written by using beta function,

$$\lambda^i_{\overline{\text{MS}}}(\Lambda) = \lambda^i_{\overline{\text{MS}}}(\mu) + \sum_{jk} b^{ijk} \lambda^j_{\overline{\text{MS}}}(\mu) \, \lambda^k_{\overline{\text{MS}}}(\mu) \ln \frac{\Lambda}{\mu}, \tag{2.60}$$

at one loop level. Combining Eqs. (2.59) and (2.60), we obtain the following formula:

$$\lambda^i_{\overline{\text{MS}}}(\Lambda) = \lambda^i_B + \sum_{jk} f^{ijk} \lambda^j_B \lambda^k_B. \tag{2.61}$$

This is generalization of Eq. (2.55).

As a result, the correction to the bare Higgs mass is given by

$$\Delta m^2_B = \left(a^i \lambda^i_{\overline{\text{MS}}}(\Lambda) - \sum_{ijk} a^i f^{ijk} \lambda^j_{\overline{\text{MS}}}(\Lambda) \, \lambda^k_{\overline{\text{MS}}}(\Lambda) \right) I_1, \tag{2.62}$$

Here a_i is the coefficient of the one loop bare mass. We denote the scale where the bare mass without correction vanishes by Λ_0,

$$a^i \lambda^i_{\overline{\text{MS}}}(\Lambda_0) = 0. \tag{2.63}$$

Then, the scale where the corrected bare mass takes zero becomes

$$\Lambda|_{m_B^2=0} := e^{\delta t}\Lambda_0, \qquad \delta t = \frac{\sum_{ijk} a^i f^{ijk} \lambda^j_{\overline{\text{MS}}}(\Lambda_0) \lambda^k_{\overline{\text{MS}}}(\Lambda_0)}{\sum_{ijk} a^i b^{ijk} \lambda^j_{\overline{\text{MS}}}(\Lambda_0) \lambda^k_{\overline{\text{MS}}}(\Lambda_0)}. \tag{2.64}$$

Since δt is the order of one, we expect that

$$0.1 \lesssim \frac{\Lambda|_{m_B^2=0}}{\Lambda_0} \lesssim 10. \tag{2.65}$$

This is the uncertainty coming from the difference between the bare and $\overline{\text{MS}}$ couplings.

2.5 The Effect of the Graviton

Since we consider the scale close to the Planck scale, the effect of the gravitational interaction may become relevant. Here, we estimate the impact on the bare Higgs mass from gravity. When we take into the gravity, the action becomes

$$S \ni \int d^4x \sqrt{-g}\, \mathcal{L}_{\text{SM}}. \tag{2.66}$$

We expand the $g_{\mu\nu}$ around the flat space:

$$g_{\mu\nu} = \eta_{\mu\nu} + \frac{1}{M_P}h_{\mu\nu}, \tag{2.67}$$

where $\eta_{\mu\nu}$ is the flat space metric, diag$(+ - - -)$, and $h_{\mu\nu}$ is the fluctuation corresponding to the graviton. It is found that the interaction is

$$\int d^4x \left(\frac{\delta}{\delta g_{\mu\nu}}(\sqrt{-g}\,\mathcal{L}_{\text{SM}})\bigg|_{g=\eta} h_{\mu\nu} + \frac{1}{2}\frac{\delta}{\delta g_{\rho\sigma}}\frac{\delta}{\delta g_{\mu\nu}}(\sqrt{-g}\,\mathcal{L}_{\text{SM}})\bigg|_{g=\eta} h_{\mu\nu}h_{\rho\sigma} + \cdots \right)$$

$$= \int d^4x \sqrt{-g}\left(T^{\mu\nu}h_{\mu\nu} + \cdots \right). \tag{2.68}$$

In the second line, we have used the definition of the energy momentum tensor, $T_{\mu\nu} := \frac{1}{\sqrt{-g}}\frac{\delta}{\delta g_{\mu\nu}}(\sqrt{-g}\,\mathcal{L}_{\text{SM}})$.

The part of $T_{\mu\nu}$ related to the Higgs is given by

$$
\begin{aligned}
T_{\mu\nu} \sim &(D_\mu H)^\dagger (D^\nu H) + (D_\nu H)^\dagger (D^\mu H) \\
&- g_{\mu\nu} \left((D_\mu H)^\dagger (D^\mu H) - m_B^2 H^\dagger H - \lambda_B (H^\dagger H)^2 y_u \bar{Q} \tilde{H} U + y_d \bar{Q} H D + y_l \bar{L} H E + \text{h.c.} \right).
\end{aligned}
\tag{2.69}
$$

Among the terms in Eq. (2.69), only the kinetic term is relevant for one loop calculation of the bare mass. However, this contribution vanishes since the momentum of the external line is zero, and there are no correction to the bare mass at the one loop level. As for the second term in Eq. (2.68), the possible interaction is the type of $hh\partial H\partial H$, which gives no contribution at one loop level.

In general, gravitons give the correction to the Higgs mass of the order of $\mathcal{O}(\Lambda^4/M_P^2)$ at the two loop level. If the theory of gravity is weak coupled, this contribution is two loop suppressed. For example, in perturbative string theory, the string coupling, determined by the dilation background, is small and the perturbative expansion is valid. In this sense, our analysis of the bare Higgs mass is valid taking into account the gravitational effect. If the physics around the Planck scale is strong coupled or the cutoff scale becomes much higher than the Planck scale, we can not neglect the effect of gravitons.

2.6 Metastability of the Electroweak Vacuum

We have seen that our electroweak vacuum is in the critical point, the border between stable and unstable vacuum. However, in practice, even if the electroweak vacuum is unstable, there are no problems provided that the lifetime is sufficiently large compared with the age of the universe. In this case, we call the electroweak vacuum is metastable. Therefore, it is phenomenologically important to determine the lifetime of false vacuum. The way of calculation is developed by Coleman [19].

In the actual calculation, the bounce solution of the Euclidean equation of the motion plays the crucial role. By using the bounce action S_0, the decay rate per unit volume is

$$
\frac{\Gamma}{V} \sim \frac{1}{R^4} e^{-S_0},
\tag{2.70}
$$

where R is a typical size of the bounce solution.

At the tree level, the equation of the motion is

$$
-\frac{d^2}{dr^2}\varphi - \frac{3}{r}\frac{d}{dr}\varphi + \lambda\varphi^3 = 0.
\tag{2.71}
$$

The boundary condition of the bounce solution is given by

$$
\varphi'(0) = 0, \qquad\qquad \varphi(\infty) = 0,
\tag{2.72}
$$

The solution of the equation is [20]

$$\varphi(r) = \sqrt{\frac{2}{|\lambda|}} \frac{2R}{r^2 + R^2}, \qquad\qquad S_{\text{bounce}} = \frac{8\pi^2}{3\,|\lambda(\mu)|}, \qquad (2.73)$$

Note that the action has the scale invariance at the classical level,

$$\varphi(r) \rightarrow \frac{1}{C}\varphi(Cr). \qquad\qquad (2.74)$$

Hence, if $\varphi(r)$ is a solution of the equation, $\frac{1}{C}\varphi(Cr)$ is also a solution for arbitrary constant C. This means that, at the classical level, there is huge uncertainty due to the arbitrary choice of scales R and μ. In order to resolve the situation, the one-loop level calculation is needed. The resultant one-loop calculation suggests that the tunneling probability becomes [20]

$$p \sim \text{Max}_R \frac{1}{H_0^4 R^4} \exp\left(-\frac{8\pi^2}{3\,|\lambda(\mu = 1/R)|}\right), \qquad (2.75)$$

where H_0 is the current Hubble parameter. Here we have not included the one-loop correction to the exponent for simplicity. Figure 2.8 shows the phase structure of the SM. We can see that the error of the top mass is larger than that of the Higgs mass, and that we indeed live in the stable or metastable vacuum depending on the mass of the top quark.

Fig. 2.8 The phase diagram of the SM. The *upper*, *middle* and *lower region* correspond to unstable, metastable and stable electroweak vacuum. The *red* and *blue circles* represent the 1σ and 2σ deviations
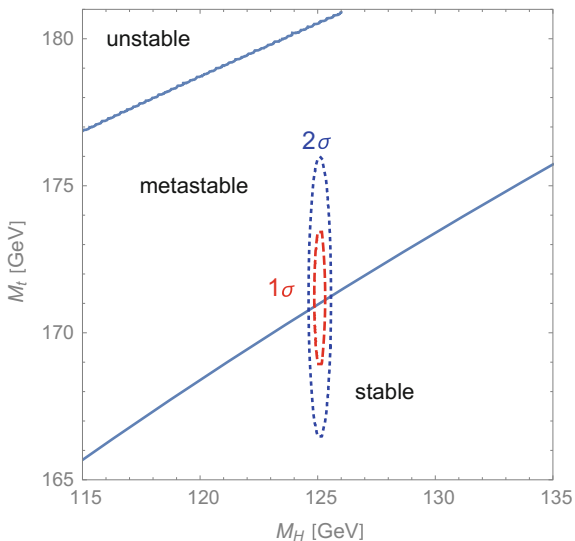
We note that the above estimate is valid when we consider the zero temperature field theory and vacuum to vacuum transition. The condition of the metastability becomes severe if we take into account the finite temperature effect or dynamical evolution of Higgs field during inflation and preheating, although these estimations highly depend on the assumption of cosmological history. In this sense, Eq. (2.75) gives conservative condition of metastability of electroweak vacuum.

References

1. S.R. Coleman, E.J. Weinberg, Radiative corrections as the origin of spontaneous symmetry breaking. Phys. Rev. D **7**, 1888–1910 (1973)
2. S.P. Martin, A supersymmetry primer (1997). arXiv:hep-ph/9709356. (Adv. Ser. Direct. High Energy Phys. 18(1) (1998))
3. D. Buttazzo, G. Degrassi, P.P. Giardino, G.F. Giudice, F. Sala, A. Salvio, A. Strumia, Investigating the near-criticality of the Higgs boson. JHEP **12**, 089 (2013). arXiv:1307.3536
4. Y. Sumino, *Intensive Lecture*
5. D.J. Gross, *Applications of the Renormalization Group*
6. M.E. Peskin, D.V. Schroeder, *An Introduction to Quantum Field Theory*
7. K.G. Wilson, The renormalization group and strong interactions. Phys. Rev. D **3**, 1818 (1971)
8. M. Veltman, The infrared—ultraviolet connection. Acta Phys. Polon. B **12**, 437 (1981)
9. M. Al-sarhi, I. Jack, D. Jones, Quadratic divergences in gauge theories. Z. Phys. C **55**, 283–288 (1992)
10. Y. Hamada, H. Kawai, K.-Y. Oda, Bare Higgs mass at Planck scale. Phys. Rev. D **87**(5), 053009 (2013). arXiv:1210.2538
11. D. Jones, *The quadratic divergence in the Higgs mass revisited*. Phys. Rev. D **88**, 098301 (2013). arXiv:1309.7335
12. Particle Data Group, K.A. Olive et al., Review of particle physics. Chin. Phys. C**38**, 090001 (2014)
13. S. Moch, S. Weinzierl, S. Alekhin, J. Blumlein, L. de la Cruz, et al., High precision fundamental constants at the TeV scale (2014). arXiv:1405.4781
14. Particle Data Group, K. Olive et al., Review of particle physics. Chin. Phys. C **38**, 090001 (2014)
15. (D0 Collaboration), V.E. Abazov, Precision measurement of the top quark mass in lepton +jets final states. Phys. Rev. Lett. **113**, 032002 (2014)
16. Tevatron Electroweak Working Group, T.E.W. Group, Combination of CDF and D0 results on the mass of the top quark using up to 9.7 fb^{-1} at the Tevatron (2014). arXiv:1407.2682
17. D0 Collaborations, T. ATLAS, CDF, and CMS, First combination of Tevatron and LHC measurements of the top-quark mass (2014). arXiv:1403.4427
18. CMS Collaboration, C. collaboration, Measurement of the top-quark mass in t t-bar events with all-jets final states in pp collisions at sqrt(s)=8 TeV (2014)
19. S.R. Coleman, *The Uses of Instantons*
20. G. Isidori, G. Ridolfi, A. Strumia, On the metastability of the standard model vacuum. Nucl. Phys. B **609**, 387–409 (2001). arXiv:hep-ph/0104016

Chapter 3
Higgs Inflation and Standard Model Criticality

Abstract In this chapter, we investigate the possibility that the SM Higgs boson plays the role of an inflation in light of the discovery of the Higgs boson. In 2007, Bezurkov and Shaposhnikov first pointed out this possibility. The successful Higgs inflation is realized if the non-minimal coupling between the Higgs H and scalar curvature $\mathcal{R}$, $\xi|H|^2\mathcal{R}$, is introduced. ξ is the coupling constant, and very large value, $\xi \sim 10^5$, is required for successful inflation. However, the observation of the Higgs and determination of its mass changes the situation. As we have seen in Chap. 2, the Higgs self coupling and its beta function becomes zero at very high scale, which means that the Higgs potential is very flat around string/Planck scale. This opens up the new possibilities of the Higgs inflation, which we will present here. In Sect. 3.1, we present the general argument of the Higgs inflation above the SM cutoff Λ. In Sect. 3.2, we show that non-minimal coupling ξ can be as small as $\mathcal{O}(10)$.

3.1 Minimal Higgs Inflation

In the last chapter, we have shown that the Higgs self coupling λ, its beta function and the bare Higgs mass simultaneously become zero around the string/Planck scale, which means the Higgs potential,

$$V_{SM} = \frac{1}{4}\lambda_{\text{eff}}(\mu = \varphi)\varphi^4, \tag{3.1}$$

is very flat at this scale. Here φ is the field value of the physical Higgs, $H = \varphi/\sqrt{2}$. We plot the figure of the Higgs potential in Fig. 3.1 for various top masses. We can see that the potential actually has plateau.

Fig. 3.1 The Higgs potential as functions of Higgs field φ. We take $M_H = 125.09\,\text{GeV}$ and $\alpha_S = 0.1185$. We have used two loop effective potential and two loop RGE
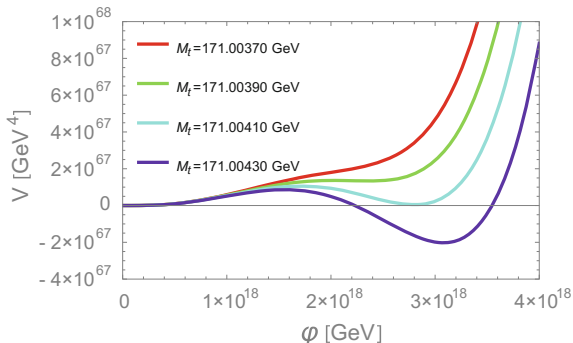
3.1.1 Is the Saddle Point Inflation in the SM Possible?

By tuning the top mass or adding Planck suppressed operator, the saddle point, where the first and second derivative of the potential vanish, appears. The potential is very flat around the saddle point, and one might be tempted to think that the inflation can occur here. However, this naive expectation is not true. Strictly speaking, the exponential expansion of the universe can be realized, but the observed density perturbation can not be reproduced. In this section, we clarify this point.

For the field value φ which is much larger than the electroweak scale, the Higgs potential can be written as

$$V_{\text{SM}} = \frac{\lambda_{\text{eff}}(\varphi)}{4}\varphi^4. \tag{3.2}$$

Let us expand the λ_{eff} around the minimum μ_{min}:

$$\lambda_{\text{eff}}(\mu) = \lambda_{\text{min}} + \sum_{n=2}^{\infty} \frac{\beta_n}{(16\pi^2)^n} \left(\ln \frac{\mu}{\mu_{\text{min}}} \right)^2, \tag{3.3}$$

where β_n is the $\mathcal{O}(1)$ quantity.

If the λ_{min} is larger than a critical value λ_c,

$$\lambda_c := \frac{\beta_2}{(64\pi^2)^2}, \tag{3.4}$$

the Higgs potential is monotonically increasing function. When $\lambda_{\text{min}} = \lambda_c$, the potential indeed has the saddle point φ_c,

$$\varphi_c = e^{-1/4}\mu_{\text{min}}. \tag{3.5}$$

In the following, we assume the existence of the saddle point by tuning $\lambda_{\min}$ or adding φ^6, φ^8, ... terms. The conclusion does not depend on how to realize the saddle point. Then, the potential around the saddle point is written as

$$V(\varphi) = V_c + \frac{V_c'''}{3!}\delta\varphi^3 + \ldots, \tag{3.6}$$

where $\delta\varphi := \varphi - \varphi_c$, the prime represents the derivative with respect to φ and the subscript c indicates that the function is estimated at $\varphi = \varphi_c$. The slow roll parameter ϵ is calculated as

$$\epsilon = \frac{M_P^2}{8}\left(\frac{V_c'''}{V_c}\right)^2 \delta\varphi^4 + \mathcal{O}(\delta\varphi^5). \tag{3.7}$$

The e-folding number becomes

$$\begin{aligned}
N_* &= \frac{1}{M_P}\int^{\delta\varphi_*} \frac{d\delta\varphi}{\sqrt{2\epsilon}} \\
&= \frac{2}{M_P^2}\frac{V_c}{V_c'''}\frac{1}{|\delta\varphi_*|}.
\end{aligned} \tag{3.8}$$

Now the density perturbation A_s can be expressed by N_*, V_c, V_c''' by using above equations.

$$\epsilon = \frac{2V_c^2}{N_*^4 M_P^6 \left(V_c'''\right)^2}, \tag{3.9}$$

and we obtain

$$A_s = \frac{N_*^4 M_P^2 \left(V_c'''\right)^2}{48\pi^2 V_c}. \tag{3.10}$$

In the SM, typical order of V_c and V_c''' are estimated as

$$V_c \sim 10^{-6}\varphi^4, \qquad\qquad V_c''' \sim 10^{-5}\varphi_c, \tag{3.11}$$

and therefore the expected order of A_s becomes

$$A_s \simeq 100\left(\frac{N_*}{60}\right)^4 \left(\frac{10^{-6}\varphi_c^4}{V_c}\right) \left(\frac{V_c'''}{10^{-5}\varphi_c}\right)^2 \left(\frac{0.1M_P}{\varphi_c}\right)^2, \tag{3.12}$$

which is much larger than the observed value, $A_s \sim 10^{-9}$ [1]. This is why the SM Higgs cannot be responsible for the cosmic inflation in the early universe. We emphasize that this conclusion is only valid under the assumption that the SM can be trusted up to the very high scale.

3.1.2 Constraints on M_t and Λ

In principle, it may be possible to realize the flat potential by the new physics such as string theory above the cutoff scale Λ. In this section, we examine the general possibility of the Higgs inflation, and constrain the parameters in the SM. We assume that the Higgs inflation occurs in the region where the Higgs field value is larger than the cutoff scale, $\varphi > \Lambda$. Even in this case, we have constraints on the low energy Higgs potential in order not to prevent the successful inflation.

The potential can be evaluated by the standard calculation of field theory for $\varphi < \Lambda$. Unless the Higgs potential is the monotonically increasing function, the Higgs field can not reach the electroweak vacuum after the inflation. This monotonicity condition gives us

$$\frac{dV_{\text{SM}}}{d\varphi} = \frac{1}{4}\left(\beta_\lambda + 4\lambda\right)\varphi^3 > 0, \tag{3.13}$$

for $\varphi < \Lambda$. Another constraint comes from the constraint on the tensor perturbation, that is, gravitational wave. The non-observation of the tensor mode puts the upper bound on the tensor to scalar ratio r, and the height of the SM Higgs potential is bounded from above:

$$V_{\text{SM}}(\Lambda) < V_{\text{max}}, \qquad\qquad V_{\text{max}} \simeq 10^{65}\,\text{GeV}^4\left(\frac{r}{0.1}\right) \tag{3.14}$$

In the Fig. 3.2, we shows the constraint on M_t and Λ in the SM. The larger value of M_t is excluded because the large top Yukawa coupling induces the instability of the Higgs potential, while the smaller M_t is excluded because the Higgs self coupling λ tends to large due to small top Yukawa. One can see that the there is an upper bound on Λ, $\Lambda \lesssim 5 \times 10^{17}\,\text{GeV}$.

Fig. 3.2 The region excluded by the value of the potential (*left*, *red*) and by the monotonicity (*right*, *blue*) in the Λ versus M_t plane in order to realize the flat potential Higgs inflation within the SM. This figure is taken from Ref. [12]
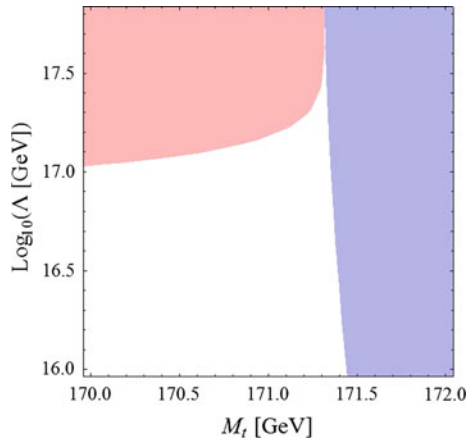
In Chap. 2, we have shown that the SM can be valid very high scale which may be close to the string scale. Interestingly, the upper bound on Λ is close to the string scale $M_s \sim 10^{17}$ GeV. If the signal of the gravitational wave is detected, the scale of the inflation is determined. This may be achieved in near future if r is not very small compared with 0.1.

3.1.3 Log Type Potential

Here we illustrate the possible potential above Λ. As an example, we take following log type potential above Λ.

$$V = V_0 + V_1 \log \frac{\varphi}{\Lambda} =: \tilde{V}_0 + V_1 \log \frac{\varphi}{M_P}. \tag{3.15}$$

The motivation of this type of potential is the Coleman-Weinberg potential in the momentum cutoff scheme,

$$V_{\text{eff}}(\varphi) = \frac{m_B^2}{2}\varphi^2 + \frac{\lambda_B}{4}\varphi^4 + \sum_i \frac{N_i}{2} \int \frac{d^4 p}{(2\pi)^4} \ln \frac{p^2 + c_i\varphi^2}{p^2}, \tag{3.16}$$

where N_i is the degrees of freedom of particles which couple with the Higgs, and $c_i\varphi^2$ represents the mass squared in the presence of the Higgs vacuum expectation value. We have added the bare cosmological constant term to get $V_{\text{eff}}(\varphi = 0) = 0$, and omitted small negative φ^2 term for simplicity. The bare mass is fixed in such a way that the mass of the Higgs vanishes. To see this, the derivative of the effective potential with respect to φ^2 is

$$\frac{dV_{\text{eff}}}{d\varphi^2} = \frac{1}{2}\left[m_B^2 + \lambda_B\varphi^2 + \sum_i \frac{N_i c_i}{16\pi^2}\left(\Lambda^2 - c_i\varphi^2 \log \frac{\Lambda^2 + c_i\varphi^2}{c_i\varphi^2}\right)\right]. \tag{3.17}$$

The mass of Higgs is given by the curvature around the minimum:

$$m_R^2 := 2 \left.\frac{dV_{\text{eff}}}{d\varphi^2}\right|_{\varphi^2 \to 0}, \tag{3.18}$$

from which we obtain

$$m_B^2 = -\frac{\Lambda^2}{16\pi^2}\sum_i N_i c_i. \tag{3.19}$$

Now the effective potential becomes

Table 3.1 The degrees of freedom, N_i, and the effective mass, $c_i \varphi^2$, of each particle

i	φ	χ	W	Z	t
N_i	1	3	6	3	-12
c_i	$3\lambda_B$	λ_B	$\dfrac{g_{2B}^2}{4}$	$\dfrac{g_{YB}^2 + g_{2B}^2}{4}$	$\dfrac{y_{tB}^2}{2}$

$$\frac{dV_{\text{eff}}}{d\varphi^2} = \frac{\varphi^2}{2}\left[\lambda_B - \sum_i \frac{N_i c_i^2}{16\pi^2} \log \frac{\Lambda^2 + c_i\varphi^2}{c_i\varphi^2}\right]. \tag{3.20}$$

For the large field value, $\varphi \gg \Lambda$, we can expand the log term as a power series in Λ^2/φ^2, and get

$$\frac{dV_{\text{eff}}}{d\varphi^2} \to \frac{1}{2}\left[m_B^2 + \lambda_B^2\varphi^2 + \frac{\Lambda^4}{16\pi^2\varphi^2}\sum_{j:c_j\varphi^2 \gg \Lambda^2} \frac{N_j}{2}\right]. \tag{3.21}$$

By assuming the criticality of the SM, $m_B^2 \sim \lambda_B \sim 0$, then, the effective potential becomes the log type potential.

$$V_{\text{eff}} \to V_0 + \frac{\Lambda^4}{16\pi^2} \log \frac{\varphi}{\Lambda} \sum_{j:c_j\varphi^2 \gg \Lambda^2} \frac{N_j}{2}$$

$$= V_0 - \frac{3\Lambda^4}{32\pi^2} \log \frac{\varphi}{\Lambda}. \tag{3.22}$$

Here we put the values in Table 3.1.

As a result, we have

$$V(\varphi) = V_1\left(C + \log \frac{\varphi}{M_P}\right), \tag{3.23}$$

with

$$V_1 = -\frac{3}{32\pi^2}\Lambda^4, \tag{3.24}$$

where C is a constant. The slow roll parameters are calculated as

$$\epsilon = \frac{1}{2}\left(\frac{M_P}{\varphi}\right)^2\left(\frac{1}{C + \ln \frac{\varphi}{M_P}}\right)^2, \qquad \eta = -\left(\frac{M_P}{\varphi}\right)^2 \frac{1}{C + \ln \frac{\varphi}{M_P}},$$

$$\xi^2 = 2\left(\frac{M_P}{\varphi}\right)^4\left(\frac{1}{C + \ln \frac{\varphi}{M_P}}\right)^2, \qquad \varpi^3 = -6\left(\frac{M_P}{\varphi}\right)^6\left(\frac{1}{C + \ln \frac{\varphi}{M_P}}\right)^3. \tag{3.25}$$

The end point of the inflation, φ_{end}, is determined from the condition,

$$\max \left\{ \epsilon(\varphi_{\text{end}}), \left| \eta(\varphi_{\text{end}}) \right| \right\} = 1. \tag{3.26}$$

Then,

$$\varphi_{\text{end}} = \begin{cases} \dfrac{M_P}{\sqrt{2}\, W\left(e^C/\sqrt{2}\right)} & \text{for } 0 < C < 0.153, \\[20pt] \sqrt{\dfrac{2}{W\left(2e^{2C}\right)}}\, M_P & \text{for } C > 0.153. \end{cases} \tag{3.27}$$

In other words, we have

$$C = \begin{cases} \dfrac{M_P}{\sqrt{2}\varphi_{\text{end}}} - \log \dfrac{\varphi_{\text{end}}}{M_P} & \text{for } \varphi_{\text{end}} \geq \sqrt{2}M_P, \\[20pt] \left(\dfrac{M_P}{\varphi_{\text{end}}}\right)^2 - \log \dfrac{\varphi_{\text{end}}}{M_P} & \text{for } \varphi_{\text{end}} \leq \sqrt{2}M_P. \end{cases} \tag{3.28}$$

Here W is the Lambert function which satisfies $x = W(x)e^{W(x)}$, and the upper bound on $\varphi_{\text{end}} \gtrsim 1.57 M_P$ can be seen from Eq. (3.27). The e-folding number can be written by φ_* and φ_{end},

$$\begin{aligned} N_* &= \frac{2C-1}{4} \frac{\varphi_*^2 - \varphi_{\text{end}}^2}{M_P^2} + \frac{\varphi_*^2}{2M_P^2} \ln \frac{\varphi_*}{M_P} - \frac{\varphi_{\text{end}}^2}{2M_P^2} \log \frac{\varphi_{\text{end}}}{M_P} \\ &= \frac{\varphi_*^2}{2M_P^2} \ln \frac{\varphi_*}{\varphi_{\text{end}}} - \frac{\varphi_*^2 - \varphi_{\text{end}}^2}{4M_P^2} \times \begin{cases} \left(1 - \sqrt{2}M_P/\varphi_{\text{end}}\right) & \text{for } \varphi_{\text{end}} \geq \sqrt{2}M_P, \\ \left(1 - 2M_P^2/\varphi_{\text{end}}^2\right) & \text{for } \varphi_{\text{end}} \leq \sqrt{2}M_P. \end{cases} \end{aligned} \tag{3.29}$$

The thing we have to do is to express the slow-roll parameters by N_*, which is achieved by solving Eq. (3.29),

$$\varphi_* = \begin{cases} \dfrac{\sqrt{4N_* + \sqrt{2}\varphi_{\text{end}} - \varphi_{\text{end}}^2}}{\sqrt{W\left(e^{-1+\sqrt{2}/\varphi_{\text{end}}} \left(4N_* + \sqrt{2}\varphi_{\text{end}} - \varphi_{\text{end}}^2\right)/\varphi_{\text{end}}^2\right)}} & \text{for } \varphi_{\text{end}} \geq \sqrt{2}M_P, \\[30pt] \dfrac{\sqrt{4N_* + 2 - \varphi_{\text{end}}^2}}{\sqrt{W\left(e^{-1+\sqrt{2}/\varphi_{\text{end}}^2} \left(4N_* + 2 - \varphi_{\text{end}}^2\right)/\varphi_{\text{end}}^2\right)}} & \text{for } \varphi_{\text{end}} \leq \sqrt{2}M_P. \end{cases} \tag{3.30}$$
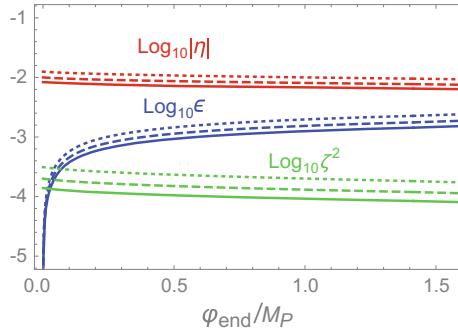
Fig. 3.3 The slow roll parameters as functions of φ_{end}. The *dotted*, *dashed* and *solid lines* correspond to $N_* = 40$, 50 and 60, respectively

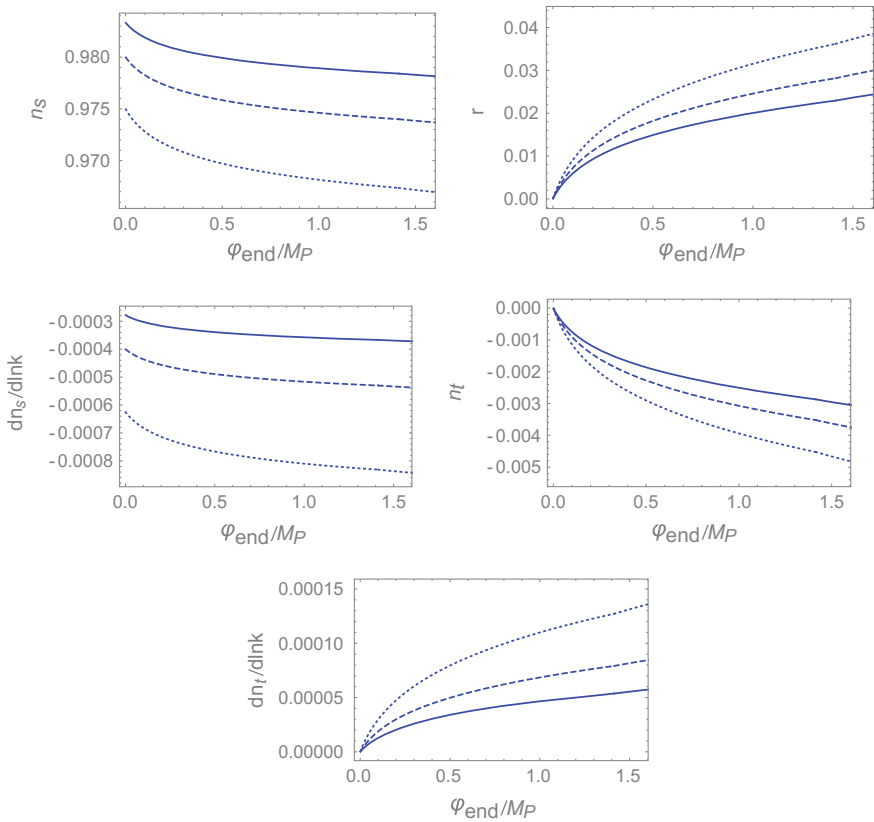**Fig. 3.4** The inflationary parameters as functions of φ_{end}. The *dotted*, *dashed* and *solid lines* correspond to $N_* = 40$, 50 and 60, respectively

The slow roll parameters as functions of φ_{end} and N_* are obtained by substituting Eq. (3.30) into Eq. (3.25), which we plot in the Fig. 3.3. We note that the observed overall amplitude $A_{s,\text{obs}}$ can be reproduced by taking

$$V_1 = 12\pi^2 A_{s,\text{obs}} M_P^4 \left(\frac{\varphi_*}{M_P}\right)^{-2} \left(C + \log\frac{\varphi_*}{M_P}\right)^{-3}. \tag{3.31}$$

We can also calculate the tensor to scalar ratio, running spectral index and so on. As a result, we get

$$0.980\text{--}\text{--}0.984 > n_s > 0.974\text{--}\text{--}0.979, \qquad\qquad 0 < r < 0.029\text{--}\text{--}0.024,$$

$$-(4.0\text{--}\text{--}2.7) \times 10^{-4} > \frac{dn_s}{d\ln k} > -(5.3\text{--}\text{--}3.7) \times 10^{-4}, \qquad 0 > n_t > -(3.7\text{--}\text{--}3.0) \times 10^{-3},$$

$$-(1.6\text{--}\text{--}0.9) \times 10^{-5} > \frac{d^2 n_s}{d\ln k^2} > -(2.2\text{--}\text{--}1.2) \times 10^{-5}, \quad 0 < \frac{dn_t}{d\ln k} < (8.2\text{--}\text{--}5.6) \times 10^{-5},$$

$$\tag{3.32}$$

for $50 \leq N_* \leq 60$ and $0 < \varphi_{\text{end}} < 1.57 M_P$. See also Fig. 3.4. These values are marginally consistent with the recent Planck 2015 data [2], see also Appendix C.

3.2 Higgs Inflation from Standard Model Criticality

In this section, we consider a possible concrete example of the potential beyond Λ in the previous general argument.

We introduce the non-minimal coupling ξ between Higgs and Ricci scalar [3–10]. Then, the action becomes

$$S = \int d^4x \sqrt{-g} \left\{ -\frac{M_P^2 + \xi\varphi^2}{2}\mathcal{R} + \frac{(\partial_\mu\varphi)^2}{2} - \frac{\lambda}{4}\varphi^4 \right\}. \tag{3.33}$$

For simplicity, we neglect the Higgs mass term, Yukawa sector and gauge sector. This frame is called Jordan frame. The $\varphi^2\mathcal{R}$ term can be eliminated by performing the redefinition of the metric, $\hat{g}_{\mu\nu} = \Omega^2 g_{\mu\nu}$, $\Omega^2 = 1 + \frac{\xi\varphi^2}{M_P^2}$. As a result, we have

$$S = \int d^4x \sqrt{-\hat{g}} \left\{ -\frac{M_P^2}{2}\hat{\mathcal{R}} + \frac{(\partial_\mu\chi)^2}{2} - \frac{\lambda}{4}\frac{\varphi^4}{(1+\xi\varphi^2/M_P^2)^2} \right\}. \tag{3.34}$$

This frame is called Einstein frame. Here, χ is the canonical field in the Einstein frame, the relation between χ and φ is

$$\frac{d\chi}{d\varphi} = \sqrt{\frac{\Omega^2 + 6\xi^2\varphi^2/M_P^2}{\Omega^4}}. \tag{3.35}$$

For the large field value, this becomes simple:

$$\frac{d\chi}{d\varphi} = \sqrt{6}\frac{M_P}{\varphi},$$

(3.36)

from which we have

$$\varphi = \varphi_* \exp\left(\frac{1}{\sqrt{6}M_P}(\chi - \chi_*)\right),$$

(3.37)

where χ_* and φ_* are integration constants. If we take $\chi_* = \varphi_* = \frac{M_P}{\sqrt{\xi}}$ and for sufficiently large ξ, then

$$\varphi \simeq \frac{M_P}{\sqrt{\xi}} \exp\left(\frac{\chi}{\sqrt{6}M_P}\right), \quad \text{for} \quad \varphi \gg \frac{M_P}{\sqrt{\xi}}.$$

(3.38)

Thanks to ξ term, we can obtain flat potential for high field value. From Eq. (3.34), the potential in Einstein frame U is given by the last term,

$$U = \frac{\lambda}{4}\frac{\varphi^4}{(1 + \xi\varphi^2/M_P^2)^2},$$

(3.39)

which becomes constant for $\varphi \gg M_P/\sqrt{\xi}$. If we ignore the running effect, the prediction is obtained as [4]

$$n_s = 1 - 6\epsilon + 2\eta \simeq 0.967,$$
$$r = 16\epsilon \simeq 3 \times 10^{-3},$$
$$\frac{dn_s}{d\ln k} = 16\epsilon\eta - 24\epsilon^2 - 2\zeta^2 \simeq -5.4 \times 10^{-4},$$

(3.40)

where the definition of slow roll parameters are

$$\epsilon = \frac{M_P^2}{2}\left(\frac{dU/d\chi}{U}\right)^2,$$

(3.41)

$$\eta = M_P^2\frac{d^2U/d\chi^2}{U},$$

(3.42)

$$\zeta^2 = M_P^4\frac{(d^3U/d\chi^3)(dU/d\chi)}{U^2}.$$

(3.43)

We note that scalar perturbation A_s is correctly realized in above calculation:

$$A_s = \frac{V}{24\pi^2\epsilon M_P^4} \simeq 2.2 \times 10^{-9}.$$

(3.44)

Now let us consider the effect of the running of λ. From the result of previous chapter, the Higgs self coupling has local minimum around string/Planck scale. Then, by expand the λ_{eff} around its minimum μ_{min}, we have

$$\lambda_{\text{eff}}(\mu) = \lambda_{\text{min}} + \sum_{n=2}^{\infty} \frac{\beta_n}{(16\pi^2)^n} \left(\ln \frac{\mu}{\mu_{\text{min}}} \right)^2. \tag{3.45}$$

In the vicinity of μ_{min}, we can safely neglect $n \geq 3$ terms.

Then, the Higgs potential is approximated as

$$V(\varphi) = \frac{\lambda_{\text{eff}}(\mu)}{4} \varphi^4. \tag{3.46}$$

The requirement that potential should be moronically increasing function, we obtain the lower bound on λ_{min}:

$$\lambda_{\text{min}} \geq \lambda_c := \frac{\beta_2}{(64\pi^2)^2}. \tag{3.47}$$

We should note that there are two choices of way to take renormalization scale μ. The prescription I is

$$\mu = \frac{\varphi}{\sqrt{1 + \xi\varphi^2/M_P^2}}, \tag{3.48}$$

while the prescription II is

$$\mu = \varphi. \tag{3.49}$$

These two prescriptions correspond the effective mass in Einstein frame and Jordan frame, respectively. See Sect. 3.3 for the detail. In the following sections, we numerically calculate inflationary parameters in both prescriptions.

3.2.1 Prescription I

In our potential, Eq. (3.45), we have four parameters: λ_{min}, μ_{min}, β_2 and ξ. β_2 is the order of one quantity, and we fix $\beta_2 = 0.5$ in our analysis. In order to realize $A_s \simeq 2 \times 10^{-9}$, we must tune one parameter. We tune λ_{min} to reproduce correct A_s. As a result, our prediction depends on two parameters, μ_{min} and ξ.

We show the detailed predictions of the Higgs inflation in Fig. 3.5. In the figure, we defined
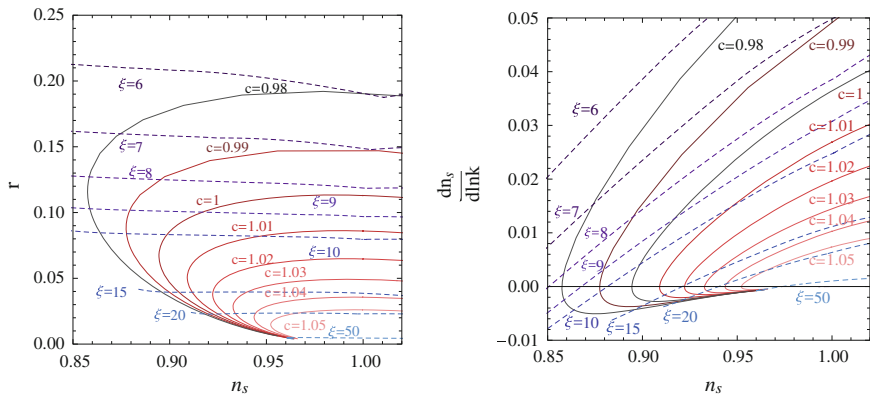
Fig. 3.5 *Left* Predictions on inflationary parameters, r and n_s in prescription I. *Right* Same as *left figure*, but $dn_s/d\ln k$ versus n_s. These figures are taken from Ref. [7]

$$c = \frac{\mu_{\min}}{M_P/\sqrt{\xi}}. \tag{3.50}$$

The solid line corresponds to the constant c, and dashed one corresponds to the constant ξ. One can see that the relation between n_s, r and $dn_s/d\ln k$. Some of the region is consistent with current bound, and the future detection of the tensor perturbation might be strong hint on this inflation model. In the left panel of Fig. 3.6, the field value corresponding to the observed cosmic microwave background, φ_*, is presented. We can see that φ_* is around the Planck scale.

Next, we evaluate the effect of higher dimensional operator, and see how the higher dimensional term should be small in order not to violate successful inflation.[1] As an example, we take

$$\Delta V = \lambda_6 \frac{\varphi^6}{M_P^2} \tag{3.51}$$

in Jordan frame. In Einstein frame, the potential becomes

$$\Delta U = \lambda_6 \frac{\varphi^6}{\left(1 + \xi\varphi^2/M_P^2\right)^2}. \tag{3.52}$$

Figure 3.7 shows the predictions on n_s and r in the case of $c = 0.98$ (left) and $c = 1$ (right). Each solid line corresponds to constant λ_6, and dashed one corresponds to constant ξ. We can see that λ_6 needs to be sufficiently small in order to realize

---

[1]The smallness of higher dimensional term would be related to asymptotic scale (shift) symmetry in Jordan (Einstein) frame [11].
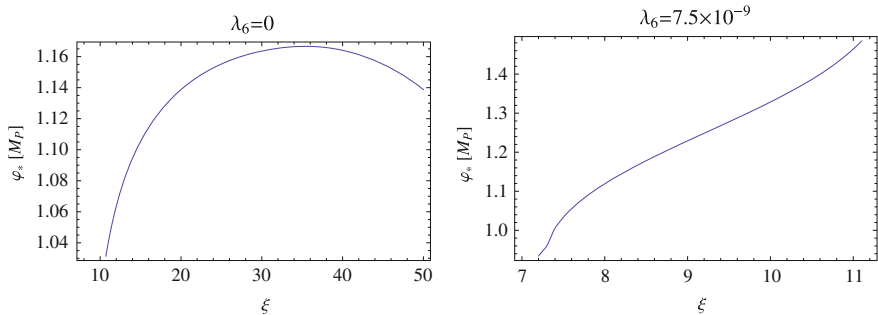
Fig. 3.6 *Left* φ_* as a function of ξ. We can see that φ_* is around the Planck scale. *Right* same as *left figure*, except for introducing $\lambda_6 = 7.5 \times 10^{-9}$. This figure is taken from Ref. [7]
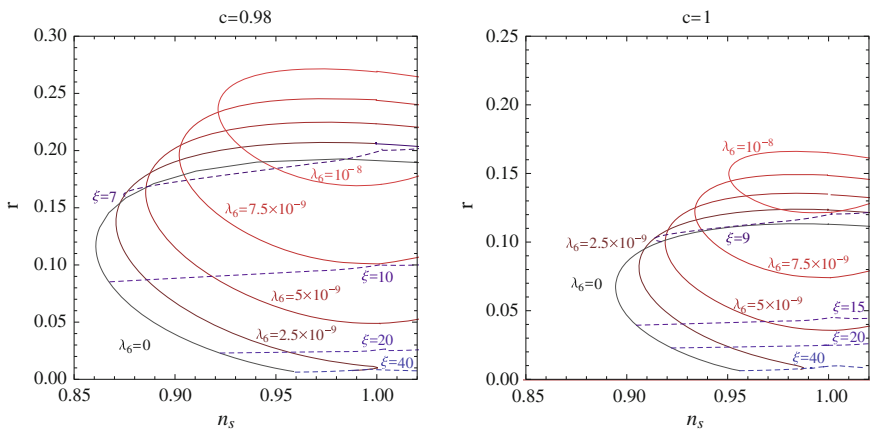
Fig. 3.7 Same as the left panel of Fig. 3.5, but introducing λ_6 term. We take $c = 0.98$ and $c = 1$ in the *left* and *right panels*, respectively. These figure are taken from Ref. [7]

successful inflation. In the Fig. 3.8, the predictions on $dn_s/d\ln k$ and n_s are shown, and φ_* is plotted in the right panel of Fig. 3.6.

3.2.2 Prescription II

In this section, we present the numerical estimation of the prescription II. In this case, we can show that the potential becomes almost quadratic one. From Eqs. (3.39), (3.45) and (3.49), the potential is
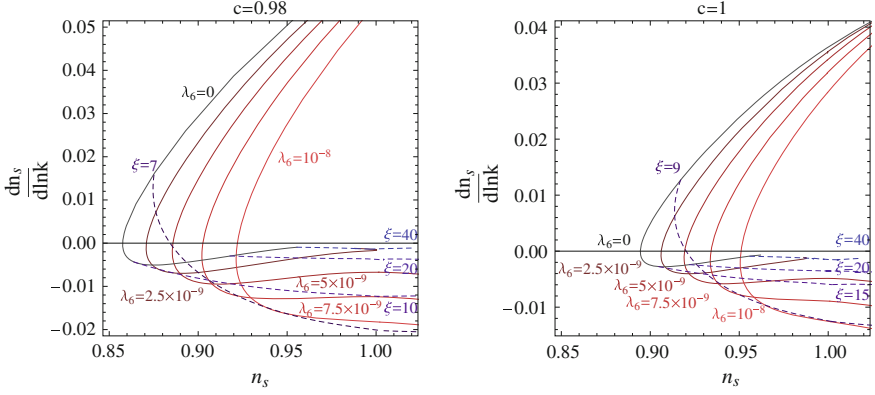
Fig. 3.8 Same as the right panel of Fig. 3.5, but introducing λ_6 term. We take $c = 0.98$ and $c = 1$ in the *left* and *right panels*, respectively. These figure are taken from Ref. [7]

$$
\begin{aligned}
U &= \frac{1}{4}\varphi^4 \left(\lambda_{\min} + \frac{\beta_2}{(16\pi)^2} \left(\ln \frac{\varphi}{\mu_{\min}} \right)^2 \right) \frac{1}{\left(1 + \xi\varphi^2/M_P^2\right)^2} \\
&= \frac{1}{4} \frac{\varphi^4}{\left(1 + \xi\varphi^2/M_P^2\right)^2} \left(\lambda_{\min} + \frac{\beta_2}{(16\pi)^2} \left(\frac{\chi}{\sqrt{6}M_P} - \ln c \right)^2 \right) \\
&\simeq \frac{1}{4} \frac{M_P^4}{\xi^2} \left(\lambda_{\min} + \frac{\beta_2}{(16\pi)^2} \left(\frac{\chi}{\sqrt{6}M_P} - \ln c \right)^2 \right).
\end{aligned}
\tag{3.53}
$$

In the last line, we have taken $\varphi \gg M_P/\sqrt{\xi}$.

In the Fig. 3.9, the slow roll parameters are plotted as functions of $X = \varphi/$ $(M_P/\sqrt{\xi})$ in the prescription II. Here we take $c = 1$. In the Fig. 3.10, the predictions on n_s and r are shown. The small and large dots represent $N_* = 50$ and 65. We

Fig. 3.9 ϵ and η as functions of $X = \varphi/(M_P/\sqrt{\xi})$. This figure is taken from Ref. [7]
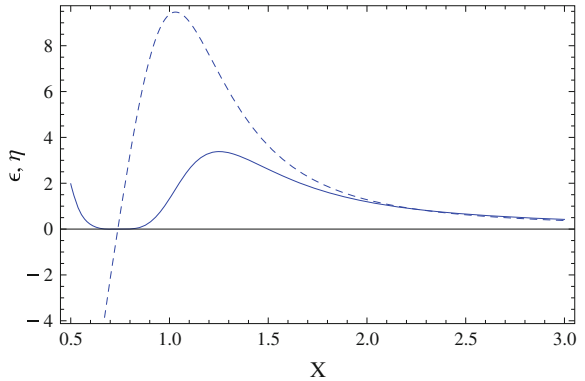
Fig. 3.10 The predictions of n_s versus r in prescription II. The *small* and *large dots* are $N_* = 50$ and 65, respectively. This figure is taken from Ref. [7]
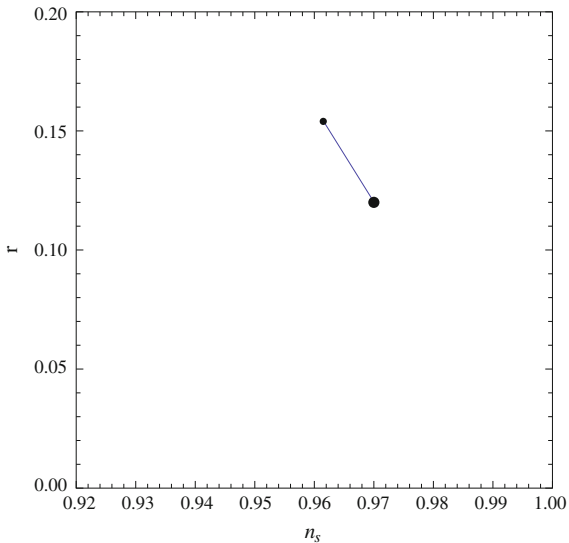
note that this prediction is almost same as that of quadratic chaotic inflation, which is marginal under the recent Planck 2015 result.

3.3 The Difference Between Prescription I and II

What is the physical meaning of the prescription I and II? In this section, we try to answer this question.

For simplicity, we consider the massless ϕ^4 theory.

$$\mathcal{L} = \frac{1}{2}\partial_\mu\phi\,\partial^\mu\phi - \frac{1}{4!}\lambda\,\phi^4. \tag{3.54}$$

with non-minimal coupling $\xi\mathcal{R}\phi^2$. Let us consider the Coleman-Weinberg potential of this model. The effective mass is given by

$$m_{\text{eff}}^2 = \begin{cases} m_J^2 = \dfrac{1}{2}\lambda\varphi^2, & \text{Jordan frame,} \\[2mm] m_E^2 = \dfrac{1}{2}\lambda\varphi^2\,\dfrac{1}{(1+\xi^2/M_P^2)^2}, & \text{Einstein frame,} \end{cases} \tag{3.55}$$

Therefore, by utilizing the momentum cutoff scheme, the effective potential in the Jordan frame becomes

$$
\begin{aligned}
V_{\mathrm{J,eff}} &= \frac{1}{4!}\lambda\,\varphi^4 + \int_{|p|<\Lambda_J} \frac{d^4 p}{(2\pi)^4}\,\log(p^2 + m_J^2) \\
&\simeq \frac{1}{4!}\lambda\,\varphi^4 + \frac{m_J^4}{32\pi^2}\lambda^2\varphi^4\,\log\left(\frac{\Lambda_J^2}{m_J^2}\right) \\
&= \frac{1}{4!}\varphi^4\left(\lambda + \frac{3}{16\pi^2}\lambda^2\,\log\left(\frac{\Lambda_J^2}{\mu^2}\right)\right) + \frac{1}{128\pi^2}\lambda^2\varphi^4\,\log\left(\frac{\mu^2}{m_J^2}\right) \\
&=: \frac{1}{4!}\lambda(\mu)\varphi^4 + \frac{1}{128\pi^2}\lambda^2\varphi^2\,\log\left(\frac{\mu^2}{m_J^2}\right).
\end{aligned}
\tag{3.56}
$$

In the second line, we have omitted the quartic divergent and quadratic divergent terms, which should be removed by the bare cosmological constant and bare mass term. In the last line, we have defined renormalized coupling $\lambda(\mu)$. If the Λ_J is constant respect for φ, $\mu = m_J$ gives good approximation.

On the other hand, in the Einstein frame, we obtain

$$
V_{\mathrm{E,eff}} = \frac{1}{(1 + \xi\varphi^2/M_P^2)^2}\left\{\frac{1}{4!}\varphi^4\left(\lambda + \frac{3}{16\pi^2}\lambda^2\,\log\left(\frac{\Lambda_E^2}{\mu^2}\right)\right) + \frac{1}{128\pi^2}\lambda^2\varphi^4\,\log\left(\frac{\mu^2}{m_E^2}\right)\right\}.
\tag{3.57}
$$

The relation between the cutoff in the Jordan frame and Einstein frame is given by

$$
\Lambda_J = \Omega^2\Lambda_E.
\tag{3.58}
$$

We can see this by following expression:

$$
\begin{aligned}
\int_{g^{\mu\nu}p_\mu p_\nu < \Lambda_J} \frac{d^4 p}{(2\pi)^4}\,\log(g^{\mu\nu}p_\mu p_\nu + m_J^2) &= \int_{\Omega^2\hat{g}^{\mu\nu}p_\mu p_\nu < \Lambda_J} \frac{d^4 p}{(2\pi)^4}\,\log(\Omega^2\hat{g}^{\mu\nu}p_\mu p_\nu + m_J^2) \\
&= \int_{\Omega^2\hat{g}^{\mu\nu}p_\mu p_\nu < \Lambda_J} \frac{d^4 p}{(2\pi)^4}\,\log(\hat{g}^{\mu\nu}p_\mu p_\nu + m_E^2) + \mathrm{const.} \\
&= \int_{\hat{g}^{\mu\nu}p_\mu p_\nu < \Omega^{-2}\Lambda_J} \frac{d^4 p}{(2\pi)^4}\,\log(\hat{g}^{\mu\nu}p_\mu p_\nu + m_E^2) + \mathrm{const.}
\end{aligned}
\tag{3.59}
$$

Hence, if we take the constant cutoff in the Jordan frame, the cutoff in the Einstein frame depends on φ, and vice versa. The problem is that which frame we have to take the constant cutoff Λ.

When we take the constant cutoff in the Jordan frame, we can improve the effective potential by putting $\mu = m_J$, which is nothing but the prescription II. The prescription I corresponds to the constant cutoff in the Einstein frame. This is the physical meaning of two prescriptions.

References

1. Planck, P.A.R. Ade et al., Planck 2015 results. XIII. Cosmological parameters (2015). arXiv:1502.01589
2. Planck, P.A.R. Ade et al., Planck 2015 results. XX. Constraints on inflation (2015). arXiv:1502.02114
3. D.S. Salopek, J.R. Bond, J.M. Bardeen, Designing density fluctuation spectra in inflation. Phys. Rev. D **40**, 1753 (1989)
4. F.L. Bezrukov, M. Shaposhnikov, The standard model Higgs boson as the inflaton. Phys. Lett. B **659**, 703–706 (2008). arXiv:0710.3755
5. Y. Hamada, H. Kawai, K.-Y. Oda, S.C. Park, Higgs inflation still alive. Phys. Rev. Lett. **112**, 241301 (2014). arXiv:1403.5043
6. F. Bezrukov, M. Shaposhnikov, Higgs inflation at the critical point. Phys. Lett. B **734**, 249–254 (2014). arXiv:1403.6078
7. Y. Hamada, H. Kawai, K.-Y. Oda, S.C. Park, Higgs inflation from standard model criticality. Phys. Rev. D **91**, 053008 (2015). arXiv:1408.4864
8. K. Allison, Higgs xi-inflation for the 125-126 GeV Higgs: a two-loop analysis. JHEP **1402**, 040 (2014). arXiv:1306.6931
9. J.L. Cook, L.M. Krauss, A.J. Long, S. Sabharwal, Is Higgs inflation dead? Phys. Rev. D **89**, 103525 (2014). arXiv:1403.4971
10. Y. Hamada, H. Kawai, K.-Y. Oda, Eternal Higgs inflation and the cosmological constant problem. Phys. Rev. D **92**, 045009 (2015). arXiv:1501.04455
11. F. Bezrukov, The Higgs field as an inflaton. Class. Quantum Gravitation **30**, 214001 (2013). arXiv:1307.0708
12. Y. Hamada, H. Kawai, K.-Y. Oda, Minimal Higgs inflation. PTEP **2014**, 023B02 (2014). arXiv:1308.6651

Chapter 4
Naturalness Problem and Quantum Gravity

Abstract In this chapter, we try to solve the naturalness problem based on the principle beyond ordinary field theory, maximum entropy principle and saddle/non analytical point of vacuum energy. In Sect. 4.1, we briefly review the naturalness problem of Higgs boson. In Sect. 4.2, we explain the original idea given by Coleman. In Sect. 4.3, we present a solution to the cosmological constant problem and Higgs mass using maximum entropy principle. In Sect. 4.4, we show a solution to the strong CP problem and cosmological constant problem based on the argument about vacuum energy.

4.1 Naturalness Problem

It is well known that the mass of the SM Higgs boson has a serious problem. The one-loop correction to the Higgs mass contains the quadratic divergence, and therefore the natural scale of the Higgs mass is around the cutoff scale. Because the natural cutoff scale of the theory is the string scale, the observed value of the Higgs mass, 125 GeV, is unnaturally small. This is so-called gauge hierarchy problem.

One of the most natural solutions to this problem is introducing the supersymmetry, which is the symmetry between bosons and fermions. By introducing this symmetry, the quadratic divergence to the Higgs mass is canceled. For example, the top quark contributions are canceled by stop contribution. Supersymmetry should be spontaneously broken because we do not know the scalar partner of the electron at the same mass. Then, the Higgs mass receives the radiative correction which is proportional to the mass of supersymmetry particle, which should be around TeV scale in order to solve the fine-tuning problem. However, no significant deviations from the SM is found in the LHC results, which means that it becomes difficult to solve the fine-tuning problem by considering the supersymmetry. Although there are other solutions to fine-tuning problem within field theory such as gauge Higgs unification, Randall-Sundrum model and composite Higgs, all of these kind scenarios require new physics around TeV scale.

Taking into account above situation, it is good time to seek for solution beyond the ordinary local field theory. Probably, the most popular one is the anthropic principle,

which is based on the landscape and multiverse in string theory. A problem of the anthropic principle is that how to define the probability measure in the multiverse is unclear. In this thesis, we focus on another possibility, the baby universe mechanism which is originally proposed by Coleman many years ago [1], see also Refs. [2, 3]. The original idea is given by Euclidean gravity, and hence has the problem of the conformal mode. Let us see this problem concretely. For the homogenous, isotropic and closed universe is described by

$$ds^2 = dt^2 - a^2 \left(\frac{dr^2}{1 - r^2} + r^2 d\Omega_2 \right). \tag{4.1}$$

Then the action of gravity with a scalar field system becomes

$$S = \int d^4x \left\{ \frac{1}{2} M_P^2 \left(\mathcal{R} - 2\Lambda \right) + \frac{1}{2} \partial_\mu \phi \partial^\mu \phi \right\}$$
$$\ni \int dt \left(-\frac{1}{2} a \dot{a}^2 \right) + \int d^4x \left(\frac{1}{2} \partial_\mu \phi \partial^\mu \phi \right). \tag{4.2}$$

We can see that the coefficient of the kinetic term of a is negative. On the other hand, the kinetic term of a scalar field has positive coefficient, which leads to the fact that we can not take bounded Hamiltonian by rotating the time coordinate.

Recently, Kawai and Okada revisited the baby universe mechanism and formulated it in the Lorentzian universe [4], and proposed the maximum entropy principle(MEP). Succeeding Kawai and Okada's work, we find that the Fermi constant(Higgs vacuum expectation value) is indeed fixed by the MEP [5, 6]. Furthermore, we find another mechanism to fix the parameters in the SM, and present how to fix the θ parameter in $SU(3)_C$, Higgs quartic coupling in the string/Planck scale and cosmological constant [7].

4.2 Coleman's Argument

We first review the original argument given by Coleman.

$$\sum_{\text{topology}} \int \mathcal{D}g \exp(-S_E), \qquad S_E = \frac{M_P^2}{2} \int d^4x \sqrt{g} \left(\mathcal{R} + 2\Lambda + \text{matter} \right) \tag{4.3}$$

As we have mentioned in the beginning of this chapter, the Euclidean gravity has the problem of wrong sign kinetic term. Let us remember why we cannot justify Wick rotation by using the one dimensional system of the two free particles, one of which has wrong sign kinetic term [8]. That is,

$$H = \frac{1}{2m_1^2} p_1^2 - \frac{1}{2m_2^2} p_2^2, \tag{4.4}$$

$$i\partial_t \psi = \left(-\partial_{x_1}^2 + \partial_{x_2}^2\right)\psi. \tag{4.5}$$

Performing Fourier transformation, we have

$$i\partial_t \tilde{\psi} + (-k_1^2 + k_2^2)\tilde{\psi} = 0, \qquad \text{Lorentzian} \tag{4.6}$$
$$-\partial_{t_E} \tilde{\psi}_E + (-k_1^2 + k_2^2)\tilde{\psi}_E = 0. \qquad \text{Euclidean} \tag{4.7}$$

We can easily solve above equations:

$$\tilde{\psi} = \exp\left[-i(k_1^2 - k_2^2)t\right], \qquad \text{Lorentzian} \tag{4.8}$$
$$\tilde{\psi}_E = \exp\left[-(k_1^2 - k_2^2)t_E\right]. \qquad \text{Euclidean} \tag{4.9}$$

In the coordinate space, the wavefunctions are written by

$$\psi = \int dk_1 dk_2 \exp\left[-i(k_1^2 - k_2^2)t\right] e^{-i(k_1+k_2)(x_1+x_2)} \qquad \text{Lorentzian} \tag{4.10}$$

$$\psi_E = \int dk_1 dk_2 \exp\left[-(k_1^2 - k_2^2)t_E\right] e^{-i(k_1+k_2)(x_1+x_2)} \qquad \text{Euclidean.} \tag{4.11}$$

The integral is divergent in Euclidean with both $t_E < 0$ and $t_E > 0$.

On the other hand, in the Lorentzian universe, there are no problems. In fact, this is why the universe expands. If this is not the case, the universe does not continue expanding but stabilizes at some point.

In the following in this section, we consider in the Euclidean gravity based on Coleman's work although above problem exists, because it is instructive to move to consideration in Lorentzian universe from the next section.

Let us consider the closed universe with Euclidianization $t \to it_E$ and cosmological constant Λ. Friedmann equation becomes

$$-\left(\frac{da/dt_E}{a}\right)^2 = \frac{\Lambda}{3} - \frac{1}{a^2}, \tag{4.12}$$

from which we obtain

$$\int_0^a \frac{da}{\sqrt{1 - a^2\Lambda/3}} = \int_0^T dt_E. \tag{4.13}$$

Here we impose $a(t_E = 0) = 0$ as a initial condition. We have

$$\text{LHS} = \sqrt{\frac{3}{\Lambda}} \int_0^{\sqrt{\Lambda/3}a} \frac{da'}{\sqrt{1-a'^2}} = \sqrt{\frac{3}{\Lambda}} \arcsin\left(\sqrt{\frac{\Lambda}{3}}a\right). \tag{4.14}$$

Hence, we obtain a as a function of t:

$$a = \sqrt{\frac{3}{\Lambda}} \sin\left(\sqrt{\frac{\Lambda}{3}}t_E\right). \tag{4.15}$$

The metric is

$$ds^2 = dt_E^2 + a^2 \left(\frac{dr^2}{1-r^2} + r^2 d\Omega_2\right). \tag{4.16}$$

By putting $r = \sin\rho$, we get

$$\begin{aligned} ds^2 &= dt_E^2 + a^2 \left(d\rho^2 + \sin^2\rho d\Omega_2\right) \\ &= dt_E^2 + a^2 d\Omega_3. \end{aligned} \tag{4.17}$$

By performing the transformation of variable,

$$t_E' \equiv \sqrt{\frac{3}{\Lambda}}t_E, \tag{4.18}$$

the metric becomes

$$\begin{aligned} ds^2 &= \frac{\Lambda}{3} \left(dt_E'^2 + \sin^2 t_E' d\Omega_3\right) \\ &= \frac{\Lambda}{3} d\Omega_4. \end{aligned} \tag{4.19}$$

In this sense, Euclidean gravity has the solution of S^4 topology. Note that we can understand the metric of S^n iteratively.

$$\begin{aligned} d\Omega_2 &= d\theta_2^2 + \sin^2\theta_2 d\phi^2, \\ d\Omega_3 &= d\theta_3^2 + \sin^2\theta_3 d\Omega_2, \\ &\quad\cdots \end{aligned} \tag{4.20}$$

Let us consider the action of this solution. From Eq. (4.3), we have

$$\mathcal{R}_{\mu\nu} - \frac{1}{2}\mathcal{R}g_{\mu\nu} = \Lambda g_{\mu\nu} \underset{\text{contraction by } g^{\mu\nu}}{\longrightarrow} \Lambda = -4\mathcal{R}, \tag{4.21}$$

then the action becomes

$$S_E = \frac{1}{2} M_P^2 \int \sqrt{g_E} d^4 x (\mathcal{R} + 2\Lambda)$$

$$= \frac{1}{2} M_P^2 \frac{8\pi^2}{3} \left(\sqrt{\frac{3M_P^2}{\Lambda}} \right)^4 (-2\Lambda)$$

$$= -\frac{24\pi^2}{\Lambda} M_P^6. \tag{4.22}$$

Next, let us consider the situation that some large S^4 universes are connected by small tube. We call such tube wormhole. The typical size of wormhole is expected to be the Planck scale, and hence we try to sum up wormhole configuration in order to obtain low energy effective action. If one wormhole is inserted, from the view point of large universe, the non-local interaction is induced, so the effect on partition function is given by

$$\int \mathcal{D}g \left(\sum_{ij} c_{ij} \int d^4 x d^4 y \sqrt{g(x)} \sqrt{g(y)} \mathcal{O}^i(x) \mathcal{O}^j(y) \right) \exp[-S_W] \exp[-S_E].$$

$$\tag{4.23}$$

Here S_W is the wormhole action, c_{ij} is numerical constant and $\mathcal{O}^i$ is any local operator in the theory. By considering the multiple insertion of the wormhole, we obtain

$$\int \mathcal{D}g \exp \left[\left(\sum_{ij} c_{ij} \int d^4 x d^4 y \sqrt{g(x)} \sqrt{g(y)} \mathcal{O}^i(x) \mathcal{O}^j(y) \right) \exp[-S_W] \right] \exp[-S_E],$$

$$\tag{4.24}$$

as the partition function. This means that the action of the theory is modified to

$$S_{\text{eff}} = S_E + c_{ij} S_i S_j + \cdots, \qquad S_i = \int d^4 x \, \mathcal{O}(x). \tag{4.25}$$

Here $\cdots$ represents the effect of the three, four, ..., legs wormholes. As we will see in the next section, the key observation of the multi-local action is that parameter in the theory becomes dynamical variable.

Provided that we assume the existence of the multiverse, the partition function of the multiverse becomes

$$Z = \int d\vec{\lambda}\,\omega(\vec{\lambda}) \int \mathcal{D}g\mathcal{D}\phi \exp[-\lambda_i S_i]$$

$$= \int d\vec{\lambda}\,\omega(\vec{\lambda}) \exp[Z_1(\vec{\lambda})], \tag{4.26}$$

because each universe is independent of each other after the summation of wormhole configuration. Here Z_1 is the partition function of single universe.

We use saddle point approximation to estimate Z_1. Putting S^4 solution into Z_1, as a single universe action, we obtain

$$-\frac{24\pi^2}{\Lambda} M_P^2, \tag{4.27}$$

from which one can see that $\Lambda \to 0$ is exponentially dominated in the path integral. Then, Coleman concludes that Λ is dynamically tunes to be zero.

In the following discussion, we utilize the Lorentzian version multi-local action,

$$\int \mathcal{D}g\mathcal{D}\phi \exp[i\,S_{\text{eff}}], \tag{4.28}$$

which would be justified by matrix model [9].

4.3   Maximum Entropy Principle

The starting point is the path integral of the multiverse:

$$Z = \int d\vec{\lambda}\,\omega(\vec{\lambda}) \int \mathcal{D}g\mathcal{D}\phi \exp\left(i\sum_i \lambda_i S_i\right) = \int d\vec{\lambda}\,\omega(\vec{\lambda}) \exp[Z_1(\vec{\lambda})], \quad (4.29)$$

where Z_1 is

$$Z_1 = \int \mathcal{D}g\mathcal{D}\phi_{\text{singleuniverse}} \exp\left[i\sum_i \lambda_i S_i\right]. \tag{4.30}$$

Therefore, what we should do is to calculate the partition function of single universe. If some value of λ dominates in the integral, the parameter of theory is dynamically fixed at that point. Z_1 is calculated as

$$Z_1(\lambda) = \int \mathcal{D}p_z \mathcal{D}z \mathcal{D}N \exp[i\,S]$$

$$= \int_{-\infty}^{\infty} dT \int \mathcal{D}p_z \mathcal{D}z \exp\left[i\int dt\,(p_z\dot{z} - TH)\right]$$

$$= \langle f | \int_{-\infty}^{\infty} dT \exp\left[-iT\hat{H}\right] |i\rangle$$

$$= \langle f | \delta(\hat{H}) | i \rangle$$

$$= \langle f | \phi_{E=0} \rangle \langle \phi_{E=0} | i \rangle, \tag{4.31}$$

where we introduce variable $z = a^3$. In the second line, we take the gauge

$$N(t) = T, \tag{4.32}$$

and N integral becomes T integral. The normalization of the wavefunction is

$$\langle \phi_{E'} | \phi_E \rangle = \delta(E - E'), \tag{4.33}$$

and Hamiltonian is given by

$$\hat{H} = z\left(-\frac{1}{2}p_z^2 - U(z)\right), \tag{4.34}$$

with

$$U(z) = \frac{M_P^4}{z^{2/3}} - M_P^4 \Lambda - \frac{C_{\text{rad}}}{z^{4/3}} M_P^2, \tag{4.35}$$

where we assume matter term has only radiation component. Note that we have treated matter fields classically. The wavefunction is the solution of one dimensional Schrodinger equation:

$$\hat{H} | \phi_{E=0} \rangle = 0. \tag{4.36}$$

The WKB solution is

$$\phi_{E=0}(z) \simeq \frac{1}{\sqrt{z k_{E=0}(z)}} \sin\left(\int_0^z dz' k_{E=0}(z')\right),$$

$$k_{E=0}^2(z) = -2U(z) = -2\left(\frac{M_P^4}{z^{2/3}} - M_P^4 \Lambda - \frac{C_{\text{rad}}}{z^{4/3}} M_P^2\right) \tag{4.37}$$

Therefore, we can calculate Eq. (4.31) provided that initial and final scale factor are specified. As for initial condition, we take $a_{\text{ini}} = \epsilon$, where ϵ is very small value. a_{finial} depends on the cosmological history. If Λ is smaller than $\Lambda_{\text{cri}} = M_P^2/(4C_{\text{rad}})$, then the universe shrinks back and we take $a_{\text{finial}} = \epsilon$. On the contrary, if $\Lambda > \Lambda_{\text{cri}}$, the universe eternally expands. In this case, as an ad hoc assumption, we use IR cutoff a_{IR} as a value of a_{finial}.

As a result, we obtain

$$Z_1 \simeq \phi(z_{\text{final}})\phi^*(z_{\text{ini}})$$

$$\simeq \begin{cases} \text{const}|\phi_{\epsilon=0}(\epsilon)|^2, & \text{for} \quad \Lambda < \Lambda_{\text{cr}} \\ \dfrac{1}{\sqrt{\Lambda^{1/4}}} \sin(a_{\text{IR}}^3 \Lambda^{1/2} + \alpha')\phi_{E=0}^*(\epsilon), & \text{for} \quad \Lambda > \Lambda_{\text{cr}} \end{cases} \tag{4.38}$$

One can see that Λ becomes maximum at $\Lambda = \Lambda_{\text{cri}}$. As a result, we obtain the multiverse partition function as

$$Z = \int d\vec{\lambda}\, \omega(\vec{\lambda}) \exp[Z_1(\vec{\lambda})] \tag{4.39}$$

$$\sim \exp\left(\text{const}\, \frac{1}{\Lambda_{\text{cri}}^{1/4}}\right) \sim \exp\left(\text{const}\, C_{\text{rad}}^{1/4}\right). \tag{4.40}$$

The energy density of the radiation appears in the exponent, which means that the parameter of the SM is fixed in such a way that the radiation energy of late stage of the universe is maximized, which we call MEP.

4.3.1   Big Fix of the Fermi Constant

In this subsection, we show how to fix the Fermi constant starting from the MEP. We denote Higgs vacuum expectation value by v. We fix the other parameters in the SM, gauge couplings, Yukawa couplings and Higgs quartic coupling and only vary v.[1]

In the following argument, we assume that the v dependence of dark energy and dark matter is smaller than that of baryon. This assumption would be reasonable if dark sector is irreverent of electroweak physics.

First, to illustrate our procedure, we consider the case that all baryons are proton. After that, we add the effect of helium. If all baryons are proton, the produced entropy by baryon decay is

$$\frac{N_B m_p}{a^3(\tau_p)} = \frac{C_{\text{rad}}}{a^3(\tau_p)}, \tag{4.41}$$

then we have

$$C_{\text{rad}} = N_B m_p a(\tau_p). \tag{4.42}$$

---

[1] Similar argument can be done if we fix gauge couplings, quark mass and Higgs quartic coupling [5].

Here m_p is the proton mass, N_B is the baryon number of the universe. Friedmann equation tells us

$$\frac{1}{\tau_p^2} = \frac{1}{M_P^2} \frac{N_B m_p}{a^3},$$
(4.43)

from which we have

$$C_{\text{rad}} \propto N_B^{4/3} \tau_p^{2/3} m_p^{4/3}.$$
(4.44)

Here τ_p is the lifetime of proton.

When we take into account the existence of helium nuclei, Boltzmann equations are given as follows. By solving the following Boltzmann equations, we obtain the entropy at the late stage of the universe,

$$\frac{dN_p}{dt} = -\tau_p^{-1} N_p + 3\tau_{He}^{-1} N_{He},$$

$$\frac{dN_{He}}{dt} = -\tau_{He}^{-1} N_{He},$$

$$\frac{da/dt}{a} = \sqrt{\frac{1}{3M_P^2} \left(\frac{M}{a^3} + \frac{C_{\text{rad}}}{a^4} - \frac{M_P^2}{a^2} \right)},$$

$$M = m_p N_p + m_{He} N_{He},$$

$$\frac{dC_{\text{rad}}}{dt} = a \, m_p \left(\tau_p^{-1} N_p + (1 - 2\epsilon)\tau_{He}^{-1} N_{He} \right),$$
(4.45)

with initial conditions

$$N_p(0) = N_B(1 - 2X_n), \qquad\qquad N_{He}(0) = N_B \frac{X_n}{2},$$
(4.46)

where N_p and N_{He} are the number of the proton and helium, m_{He} and τ_{He} are the mass and lifetime of helium, respectively. When the helium decays into the pion, pion loses its energy by the collision with other nucleon. This effect is represented by ϵ.

What we want to know is the v dependence of C_{rad}. Numerically, C_{rad} is written as

$$C_{\text{rad}} \propto \left(N_B m_p \right)^{4/3} \tau_p^{2/3} \left\{ 1 - c \left(\epsilon, \tau_{He}/\tau_p, m_{He}/m_p \right) X_n \right\},$$
(4.47)

where c is the numerical constant which is around 0.01 [6]. The first factor is the same as Eq. (4.44). The second factor represents the effect of helium nuclei. If baryon number is created at the scale much higher than the electroweak scale, see for example Refs. [10–13], the resultant baryon number is independent of v, which we assume in the following. Moreover, we can check numerically that the v dependence of c is so

small that we can treat c as a constant. After all, we only take care of v dependence of m_p, τ_p and X_n.

First, let us consider $m_p^{4/3} \tau_p^{2/3}$ part. In order to estimate τ_p, we consider the process $p \rightarrow e^+ + \pi^0$. Then, we get

$$\tau_p^{-1} \propto \frac{m_p^5}{M_P^4} \left(1 - \frac{m_\pi^2}{m_p^2}\right)^2. \tag{4.48}$$

As a phenomenological expression, we use

$$m_p = \alpha \Lambda_{\text{QCD}} + \beta(2m_u + m_d), \quad m_n = \alpha \Lambda_{\text{QCD}} + \beta(m_u + 2m_d) + m_{em},$$
$$Q = \beta(m_d - m_u) - m_{em}, \quad m_\pi^2 = \gamma \Lambda_{\text{QCD}}(m_u + m_d). \tag{4.49}$$

In the thesis, we use the following typical values reproducing observed up and down quark masses:

$$\alpha = 3.1, \quad \beta = 1.4, \quad \gamma = 16, \quad m_{em} = 2.2 \,\text{MeV}, \quad \Lambda_{\text{QCD}} = 300 \,\text{MeV}. \tag{4.50}$$

The choice of Λ_{QCD} is just the convention. We have to comment on why we choose $m_{em} = 2.2 \,\text{MeV}$. We assume the model of nucleon as follows: three quarks exists, and the distances between two quarks are about proton charge radius, $r_N = 0.86 \text{fm}$. Then we can roughly estimate the electromagnetic energy of the neutron and proton as

$$-m_{em}^{(n)}/\alpha_{em} \sim -\frac{1}{3} \times \frac{2}{3} - \frac{1}{3} \times \frac{2}{3} + \frac{1}{3} \times \frac{1}{3} = -\frac{1}{3},$$
$$-m_{em}^{(p)}/\alpha_{em} \sim \frac{2}{3} \times \frac{2}{3} - \frac{1}{3} \times \frac{2}{3} - \frac{1}{3} \times \frac{2}{3} = 0. \tag{4.51}$$

In the region where $m_{u,d} \ll \Lambda_{\text{QCD}}$, we have

$$m_p^{4/3} \tau_p^{2/3} \propto \left(1 - \left(\frac{4\beta}{\alpha} - \frac{2\gamma}{3\alpha^2}\right) \frac{m_u}{\Lambda_{\text{QCD}}} - \left(2\beta - \frac{2\gamma}{3\alpha^2}\right) \frac{m_d}{\Lambda_{\text{QCD}}}\right). \tag{4.52}$$

By putting Eq. (4.50) and $(m_u, m_d) = (2.3 \,\text{MeV}, 4.8 \,\text{MeV})$, one can see that $m_p^{4/3} \tau_p^{2/3}$ is decreasing function of v. We plot $m_p^{4/3} \tau_p^{2/3}$ in the Fig. 4.1.

Next, let us move on the evaluation of v dependence of X_n. When the interaction rate of the weak interaction becomes smaller than the Hubble parameter, proton-neutron conversion process is not effective, and X_n is almost fixed. Succeedingly, until the time of big bang nucleosynthesis(BBN), some neutrons decay via $n \rightarrow p \, e^+ \, \nu_e$. Finally, the X_n is fixed at the time when the BBN starts, $t = t_{\text{BBN}}$. Hence, X_n is given by

Fig. 4.1 $m_p^{4/3}\tau_p^{2/3}$ as a function of the Higgs VEV v. Here we ignore the overall constant, and only plot v dependent factor, see Eq. (4.52)
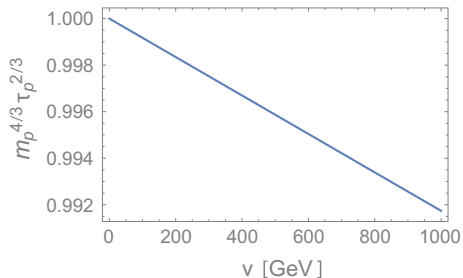
$$X_n(t \to \infty) = e^{-(t_{\text{BBN}}-t_{\text{dec}})/\tau_n} \frac{1}{1+e^{Q/T_{\text{dec}}}}. \tag{4.53}$$

Here $Q = m_n - m_p$, τ_n is the lifetime of the neutron, t_{dec} is the freeze out time of the weak interaction.

t_{dec} is determined by equating the interaction rate and Hubble parameter. The interaction rate of the proton-neutron conversion process,

$$n + \nu \leftrightarrow p + e^-, \quad n + e^+ \leftrightarrow p + \bar{\nu}, \quad n \leftrightarrow p + e^- + \bar{\nu}, \tag{4.54}$$

is

$$\Gamma(p \to n) = (2.5\text{sec})^{-1} \left(\frac{T}{1\,\text{MeV}}\right)^5 \left(\frac{246\,\text{GeV}}{v}\right)^4 \frac{P(m_e/T, Q/T)}{P(0,0)}, \tag{4.55}$$

with

$$P(x, y) = \int_0^\infty dz \sqrt{1 - \left(\frac{x^2}{y+z}\right)^2} \frac{(y+z)^2 z^2}{(1+e^{-zT/T_\nu})(1+e^{y+z})}, \tag{4.56}$$

where m_e is the electron mass and T_ν is the temperature of the neutrino

$$T_\nu = T \times \frac{S(m_e/T)}{S(0)}, \quad S(x) = 1 + \frac{45}{2\pi^4}\int_0^\infty dy\, y^2 \left(\sqrt{x^2+y^2} + \frac{y^2}{3\sqrt{x^2+y^2}} \frac{1}{1+e^{\sqrt{x^2+y^2}}}\right). \tag{4.57}$$

On the other hand, Hubble parameter is

$$H \simeq \frac{1}{2}\sqrt{\frac{43\pi^2}{90}\frac{T^2}{M_P}} \simeq \frac{1}{2}\frac{1}{t} \tag{4.58}$$

From Eqs. (4.55) and (4.58), we can calculate t_{dec} numerically. We plot t_{dec} as a function of v in the Fig. 4.2.

Fig. 4.2 T_{dec} as a function of the Higgs VEV v. We can see that the decoupling temperature is around MeV
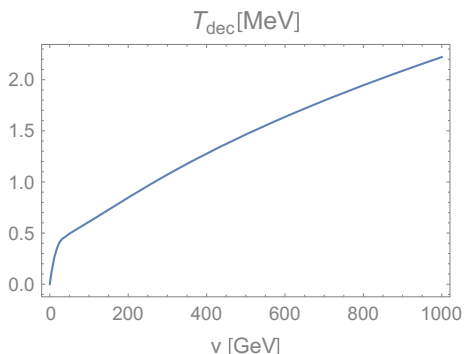
The lifetime of the neutron is calculated as

$$\tau_n^{-1} = (885\,\text{sec})^{-1} \left(\frac{m_e}{0.51\,\text{MeV}}\right)^5 \left(\frac{246\,\text{GeV}}{v}\right)^4 \frac{F(Q/m_e)}{F(1.29\,\text{MeV}/0.51\,\text{MeV})}, \quad (4.59)$$

with

$$F(x) = \int_1^x dy \, y(y^2 - 1)^{1/2}(x - y)^2. \quad (4.60)$$

Since BBN time rarely depends on v, we fix

$$T_{\text{BBN}} = 0.1\,\text{MeV}. \quad (4.61)$$

The relation between T_{BBN} and t_{BBN} is given by Eq. (4.58). Now Eq. (4.53) can be estimated as a function of v and we plot it in Fig. 4.3. We note that, if v is too small, the neutron becomes heavier than the proton, and therefore we only plot the range $v \gtrsim 200\,\text{GeV}$.

Combining all the ingredients, we can evaluate C_{rad} as a function of v. Figure 4.4 shows v dependence of C_{rad}. We can see that v is fixed around the electroweak scale, $v = \mathcal{O}(100)\,\text{GeV}$. The hierarchy problem of the Higgs mass is solved. The electroweak scale comes from $\tau_n \sim t_{\text{BBN}}$, which is rewritten as

$$v_h \sim \frac{T_{\text{BBN}}^2}{M_P \, y_e^5}. \quad (4.62)$$

Fig. 4.3 X_n as a function of the Higgs VEV v_h
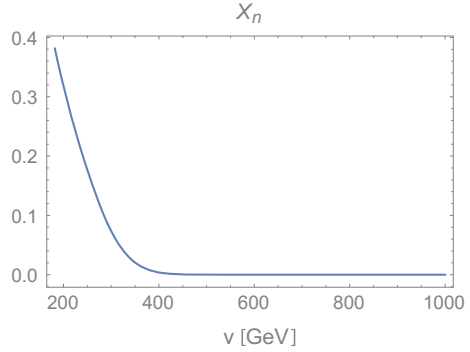
Fig. 4.4 C_{rad} as a function of the Higgs VEV v_h. We can see that v_h is fixed to be the order of $100\,\text{GeV}$. Here we take $c = 1/100$
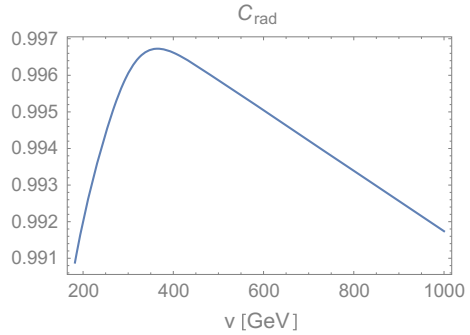
4.4 Fixing Parameters from Vacuum Energy

4.4.1 Formulation

In this section, we present another point of view of the fixing of the parameters of theory. We note that the argument in this section does not assume the existence of the multiverse. Our starting point is the multi-local action which may appears after the integration of various wormhole configurations,

$$S_M = \sum_i c_i\, S_i + \sum_{i,j} c_{i,j}\, S_i S_j + \sum_{i,j,k} c_{i,j,k}\, S_i S_j S_k + \cdots . \tag{4.63}$$

Here S_i is a usual local action,

$$S_i = \int_0^\infty dt \int d^3x\, \mathcal{O}_i(t, \mathbf{x}), \tag{4.64}$$

and c_i is a constant.

In general, it is very difficult to treat theory without locality. However, fortunately, multi-local action can be interpreted as a superposition of various values of coupling constants,

$$e^{i S_M} = \int d\vec{\lambda}\, f(\vec{\lambda})\, e^{i \sum \lambda_i S_i}, \tag{4.65}$$

by performing the Fourier transformation. In fact, the variable λ_i corresponds to coupling constant of S_i. Here we treat coupling constants collectively, and denote by $\vec{\lambda}$. By using the Eq. (4.65), the partition function of multi-local action can be expressed as

$$\begin{aligned}
Z &= \int_{t=0}^{t=\infty} \mathcal{D}\phi\, e^{i S_M} \psi_f^* \psi_i \\
&= \int d\vec{\lambda}\, f(\vec{\lambda}) \int_{t=0}^{t=\infty} \mathcal{D}\phi\, e^{i \sum \lambda_i S_i} \psi_f^* \psi_i \\
&= \int d\vec{\lambda}\, f(\vec{\lambda})\, \langle f | T e^{-i \int_0^{+\infty} dt\, \hat{H}(\vec{\lambda}; a_{cl}(t))} | i \rangle,
\end{aligned} \tag{4.66}$$

where H is the Hamiltonian, a_{cl} is the classical solution of the scale factor, and ψ_i and ψ_f represent the initial and final wavefunctions, $|i\rangle$ and $|j\rangle$ are the initial and final state, respectively. The point is that now coupling constants $\vec{\lambda}$ are not the constants but the variables. If a some value of $\vec{\lambda}$, $\vec{\lambda}_0$ dominates in the integral, we get

$$Z \sim f(\vec{\lambda}_0) \langle f | T e^{-i \int_0^{+\infty} dt\, \hat{H}(\vec{\lambda}_0; a_{cl}(t))} | i \rangle, \tag{4.67}$$

and hence the parameters are dynamically fixed.

Assuming the spacetime background which is exponentially expanding universe, we have

$$T e^{-i \int_0^{+\infty} dt\, \hat{H}(\vec{\lambda}; a_{cl}(t))} | i \rangle \sim e^{-i\epsilon(\vec{\lambda}) \int_{t^*}^{+\infty} dt\, V_3(a_{cl}(t))} | \psi(t^*; \vec{\lambda}) \rangle, \tag{4.68}$$

with V_3 being the space volume of the universe, ϵ being vacuum energy of the universe. $|\psi(t^*; \vec{\lambda})\rangle$ is

$$|\psi(t^*; \vec{\lambda})\rangle = T e^{-i \int_0^{t^*} dt\, \hat{H}(\vec{\lambda}; a_{cl}(t))} | i \rangle, \tag{4.69}$$

and t^* is time when the vacuum energy dominated era starts. Substituting Eqs. (4.68) and (4.69) into Eq. (4.66), we get

$$Z \sim \int d\vec{\lambda}\, f(\vec{\lambda})\, e^{-i\epsilon(\vec{\lambda}) \int_{t^*}^{+\infty} dt\, V_3(a_{cl}(t))} \langle f | \psi(t^*; \vec{\lambda}) \rangle \sim \int d\vec{\lambda}\, f(\vec{\lambda})\, e^{-i\epsilon(\vec{\lambda}) V_4} \langle f | \psi(t^*; \vec{\lambda}) \rangle. \tag{4.70}$$

Consequently, we should evaluate the integration in this expression to check the fixing of parameters. For this purpose, the following formulas are useful thanks to

the largeness of spacetime volume V_4. If the vacuum energy $\epsilon(\lambda)$ has a saddle point, λ_0,

$$e^{i\epsilon(\lambda)V_4} \underset{V_4 \to \infty}{\sim} \sqrt{\frac{2\pi}{i\,\epsilon''(\lambda)V_4}} e^{ik\epsilon(\lambda)} \delta(\lambda - \lambda_0), \tag{4.71}$$

by using the saddle point approximation. On the other hand, if $\epsilon(\lambda)$ is continuous but $\epsilon'(\lambda)$ is not continuous at some point, λ_0, then

$$e^{i\epsilon(\lambda)V_4} \underset{V_4 \to \infty}{\sim} \frac{i}{V_4} \left[e^{iV_4\epsilon(\lambda)} \left(\frac{d\epsilon}{d\lambda}\right)^{-1} \bigg|_{\lambda_0+} - e^{iV_4\epsilon(\lambda)} \left(\frac{d\epsilon}{d\lambda}\right)^{-1} \bigg|_{\lambda_0-} \right] \delta(\lambda - \lambda_0). \tag{4.72}$$

4.4.2 Strong CP Problem

It is natural that the dimensionless parameters in Lagrangian takes $\mathcal{O}(1)$. However, the $SU(3)_C$ θ term,

$$S_\theta := \frac{\theta}{32\pi^2} \int d^4x\, F^a_{\mu\nu} \tilde{F}^{a\mu\nu}, \tag{4.73}$$

should take $\theta < 10^{-10}$ by the measurement of the neutron electric dipole moment [14]. This is strong CP problem, see App. 10 for the detailed review of this subject. This problem can be solved starting from the Eq. (4.70),

$$Z \sim \int_0^{2\pi} d\theta\, f(\theta) e^{-i\epsilon(\theta)V_4} \langle f|\psi(t^*; \theta)\rangle, \tag{4.74}$$

where the energy density ϵ is

$$\epsilon \sim m_\pi^2 \Lambda_{\text{QCD}}^2 \cos\theta. \tag{4.75}$$

$\epsilon(\theta)$ has saddle points at $\theta = 0$ and $\theta = \pi$, and hence by using Eq. (4.71), the partition function is dominated by saddle points,

$$Z \sim \sqrt{\frac{2\pi}{i\,V_4\Lambda_{\text{QCD}}}} \left[f(0)e^{-i\epsilon(0)V_4} \langle f|\psi(t^*; 0)\rangle + f(\pi)e^{-i\epsilon(\pi)V_4} \langle f|\psi(t^*; \pi)\rangle \right], \tag{4.76}$$

which indicates that θ is fixed at 0 or π with almost same probability. Then, we can conclude that $\theta = 0$ is naturally realized.

We note that $\theta = \pi$ is already excluded although $\theta = \pi$ does not induce the CP violation. In the case of $\theta = \pi$, the relation between hadron masses do not agree with experiment, see App. 10 for the detail.

4.4.3 Multiple Point Criticality Principle

In this subsection, we show that the situation of the MPP is natural in the context of the vacuum energy argument.

We take Higgs quartic coupling λ_{EW} at the electroweak scale as a variable, and fix the other parameters.

$$V = -\frac{1}{2}\mu^2\varphi^2 + \frac{1}{4}\lambda\varphi^4 = \frac{1}{4}\lambda\left(\varphi^2 - \frac{\mu^2}{\lambda}\right)^2 - \frac{\mu^4}{4\lambda}. \tag{4.77}$$

We denote λ_* as the value of λ_{EW} realizing the MPP. We also write the position of the minimum at electroweak and Planck scale as φ_{EW} and φ_{M_P}, respectively.

The position of the true vacuum, $\langle\varphi\rangle$, depends λ_{EW},

$$\langle\varphi\rangle \simeq \begin{cases} \varphi_{EW}, & \text{for } \lambda_* < \lambda_{EW} \\ \\ \varphi_{M_P}. & \text{for } \lambda_{EW} < \lambda_* \end{cases} \tag{4.78}$$

The vacuum energy becomes

$$\epsilon(\lambda_{EW}) \simeq \begin{cases} -\dfrac{\mu^4}{4\lambda_{EW}}, & \text{for } \lambda_* < \lambda_{EW} \\ \\ \dfrac{1}{4}\lambda_{M_P}\varphi_{M_P}^4. & \text{for } \lambda_{EW} < \lambda_* \end{cases} \tag{4.79}$$

up to the constant term. Therefore, the partition function becomes

$$Z = \int d\lambda_{EW}\, f(\lambda_{EW})e^{-i\epsilon V_4}\langle f|\psi(t^*; \lambda_{EW})\rangle. \tag{4.80}$$

From the Eq. (4.79), $\epsilon(\lambda_{EW})$ is the monotonic function for $\lambda_* < \lambda_{EW}$ and $\lambda_{EW} < \lambda_*$, respectively.

As a result, we get

$$Z \sim \frac{f(0)}{V_4}e^{-i\epsilon(0)V_4}\langle f|\psi(t^*; 0)\rangle, \tag{4.81}$$

by using

$$
e^{-i\epsilon(\lambda_{EW})V_4} \sim \frac{ie^{-i\epsilon(\lambda_*)V_4}}{V_4} \left[\left(\frac{d\epsilon(\lambda_{EW})}{d\lambda_{EW}} \right)^{-1} \bigg|_{\lambda_*+} - \left(\frac{d\epsilon(\lambda_{EW})}{d\lambda_{EW}} \right)^{-1} \bigg|_{\lambda_*-} \right] \delta(\lambda_{EW} - \lambda_*)
$$

(4.82)

This is nothing but the situation of the MPP.

4.4.4 Generalization to Wheeler-DeWitt Wavefunction and Cosmological Constant

Since we would like to treat the cosmological constant Λ, we generalize previous discussion to the Wheeler-DeWitt wavefunction. Namely, by taking the gauge in which lapse function is constant, we should integrate over the time T,

$$
Z_{WD} = \int d\Lambda_B \int d\vec{\lambda}\, f(\Lambda_B, \vec{\lambda})\theta(\Lambda) \int_0^\infty dT \, \langle f_a| \otimes \langle f_{MR}|e^{-i(\hat{H}_G(\Lambda_B)+\hat{H}_{MR}(\vec{\lambda};\hat{a}))T}|\epsilon\rangle \otimes |i_{MR}\rangle.
$$

(4.83)

Here H_G and H_{MR} are the Hamiltonian of gravity and matter/radiation, and we insert step function $\theta(\Lambda)$ and only consider the region $\Lambda \geq 0$ because we can not deal with the big crunch, unfortunately. The tensor production means product of scale factor and matter/radiation Hilbert space. Let us assume that the parameters of matter and radiation sector is fixed, and focus on the integration over Λ,

$$
Z = \int_0^\infty dT \int_0^\infty d\Lambda \, f(\Lambda)\langle a_\infty|e^{-i\hat{H}(\Lambda)T}|\epsilon\rangle.
$$

(4.84)

Here the Hamiltonian for the scale factor is

$$
\hat{H}(\Lambda) = -\frac{\hat{p}_a^2}{2\hat{a}M_P^2} + \frac{\hat{a}^3\rho(\hat{a})}{6}, \qquad \rho(\hat{a}) = \Lambda + \rho_{MR}(\hat{a}),
$$

(4.85)

where $\hat{p}_a$ is the momentum of $\hat{a}$ and ρ_{MR} is the energy density coming from matter and radiation.

Inserting the complete set into Eq. (4.84),

$$
1 = \int_{-\infty}^{+\infty} dE \, |E; \Lambda\rangle\langle E; \Lambda|, \qquad \hat{H}(\Lambda)|E; \Lambda\rangle = E|E; \Lambda\rangle,
$$

(4.86)

and remembering the standard formula,

$$
\lim_{t\to+\infty} \frac{e^{-iEt} - 1}{-iE} = \pi\delta(E) + PV\frac{1}{E},
$$

(4.87)

we obtain

$$
Z = \int_0^\infty d\Lambda \, f(\Lambda) \int_0^\infty dt \int_{-\infty}^\infty dE \, e^{-iEt} \langle a_\infty | E; \Lambda \rangle \langle E; \Lambda | \epsilon \rangle
$$
$$
= \int_0^\infty d\Lambda \, f(\Lambda) \left(\pi \langle a_\infty | 0; \Lambda \rangle \langle 0; \Lambda | \epsilon \rangle + PV \int_{-\infty}^\infty \frac{dE}{E} \langle a_\infty | E; \Lambda \rangle \langle E; \Lambda | \epsilon \rangle \right).
$$
$$(4.88)$$

Here PV represents the principle value integral. In the App. 12, we show that the second term in Eq. (4.88) can be ignored, and therefore we only take the first term hereafter. Intuitively, this is understood that the classical Friedmann equation (Hamiltonian constraint) describes our universe very well.

As a result, path integral becomes

$$
Z = \int_0^\infty d\Lambda \, f(\Lambda) \pi \langle a_\infty | 0; \Lambda \rangle \langle 0; \Lambda | \epsilon \rangle. \tag{4.89}
$$

In the WKB approximation, the wavefunction becomes

$$
\langle a | 0; \Lambda \rangle = M_P \sqrt{\frac{a}{p_{cl}}} \exp \left(i \int^a da' \, p_{cl}(a') \right), \quad p_{cl}(a) := M_P a^2 \sqrt{\frac{\rho(a)}{3}}. \tag{4.90}
$$

If the energy density consists of the cosmological constant and matter,

$$
\rho(a) = \Lambda + \frac{M}{a^3} := \Lambda + \rho_M(a), \tag{4.91}
$$

the integral can be performed:

$$
\int_{a_M}^a da' \, p_{cl}(a') = \frac{M_P}{3^{\frac{3}{2}}} \left(a^3 \sqrt{\rho(a)} - a_M^3 \sqrt{\rho(a_M)} + \frac{M}{\sqrt{\Lambda}} \log \left[\frac{a^{\frac{3}{2}}(\Lambda + \sqrt{\Lambda \rho(a)})}{a_M^{\frac{3}{2}}(\Lambda + \sqrt{\Lambda \rho(a_M)})} \right] \right)
$$
$$
:= \frac{M_P a^3}{3^{\frac{3}{2}}} g(\Lambda, a), \tag{4.92}
$$

The property of g is as follows.

$$
g(0, a) = 2 \left(\sqrt{\rho_M(a)} - \left(\frac{a_M}{a} \right)^3 \sqrt{\rho_M(a_M)} \right), \qquad \lim_{a \to \infty} g(\Lambda, a) = \sqrt{\Lambda},
$$
$$
\left. \frac{dg(\Lambda, a)}{d\Lambda} \right|_{\Lambda=0} = \frac{1}{3} \left(\frac{1}{\sqrt{\rho_M(a)}} - \left(\frac{a_M}{a} \right)^3 \frac{1}{\sqrt{\rho_M(a_M)}} \right). \tag{4.93}
$$

So we can use the approximation Eq. (4.72):

$$\langle a|0; \Lambda \rangle \underset{a \to \infty}{\sim} \frac{3^{\frac{3}{2}} i}{M_P a^3} \left(\frac{dg(\Lambda, a)}{d\Lambda} \right)^{-1} \bigg|_{\Lambda=0} M_P \sqrt{\frac{a}{p_{cl}(a)}} \exp \left(i \frac{M_P a^3}{3^{\frac{3}{2}}} g(0, a) \right) \delta(\Lambda)$$

$$= \frac{3^{\frac{3}{2}} i}{M_P a^3} \left(\frac{dg(\Lambda, a)}{d\Lambda} \right)^{-1} \bigg|_{\Lambda=0} \delta(\Lambda) \langle a|0; 0 \rangle. \tag{4.94}$$

Finally, we obtain the following expression of the partition function by substituting Eq. (4.94) into Eq (4.89):

$$Z \sim \frac{1}{a_\infty^3} \left(\frac{dg(\Lambda, a_\infty)}{d\Lambda} \bigg|_{\Lambda=0} \right)^{-1} \langle a_\infty|0; 0 \rangle \langle 0; 0|\epsilon \rangle$$

$$\sim \frac{1}{a_\infty^3} \left(\frac{dg(\Lambda, a_\infty)}{d\Lambda} \bigg|_{\Lambda=0} \right)^{-1} \int_0^\infty dt \, \langle a_\infty|e^{-i\hat{H}(0)t}|\epsilon \rangle. \tag{4.95}$$

Therefore, the cosmological constant is fixed to be zero.

4.4.5 A Possible Way to Obtain Nonzero Cosmological Constant

In the previous subsection, we conclude that the cosmological constant is peaked at zero. However the observation indicates the small but nonzero value of the cosmological constant [15]. Here we discuss a possible way to obtain nonzero cosmological constant.

In the following, we assume the existence of the multiverse. In this case, the partition function after integrating out the wormhole configuration becomes

$$Z_M := \sum_{N=0}^{\infty} \int dg \frac{f(g)}{N!} Z_U(g)^N = \int dg f(g) \exp \left(Z_U(g) \right), \tag{4.96}$$

because universes are independent of each other without wormhole effect. Let us expand $Z_U(g)$ around the saddle point $g = g_*$. Then, we obtain

$$Z_U(g) = Z_U(g^*) + \frac{1}{2} \frac{d^2 Z_U}{dg^2} \bigg|_{g=g^*} (g - g^*)^2 + \mathcal{O} \left((g - g^*)^3 \right). \tag{4.97}$$

Here, the single universe partition function $Z_U(g)$ can be written as

$$Z_U(g) = \int \mathcal{D}\phi e^{igS_g + \cdots} \times \psi_f^* \psi_i, \tag{4.98}$$

where S_g is the interaction term corresponding to the coupling g. Therefore, the second derivative of the partition function is given by the correlation function of S_g:

$$\frac{d^2 Z_U}{dg^2}\bigg|_{g=g^*} = -\int \mathcal{D}\phi e^{ig^* S_{g^*}+\cdots} S_{g^*}^2 \times \psi_f^* \psi_i$$

$$:= -\langle \hat{S}_{g^*}^2 \rangle Z_U(g^*). \tag{4.99}$$

This is nothing but fluctuation of the coupling g,

$$\Delta g \sim \left(\frac{d^2 Z_U}{dg^2}\right)^{-\frac{1}{2}}\bigg|_{g=g^*} = \frac{1}{\sqrt{\langle \hat{S}_{g^*}^2 \rangle Z_U(g^*)}}. \tag{4.100}$$

The order of $\langle \hat{S}_{g^*}^2 \rangle$ is estimated as

$$\langle \hat{S}_{g^*}^2 \rangle = \int d^4 x \int d^4 y \underbrace{\langle \hat{O}_{g^*}(x) \hat{O}_{g^*}(y) \rangle}_{\text{contract}}$$

$$= \int d^4 x \int d^4 y\, W(x-y)$$

$$= V_4 \int d^4 X\, W(X) \sim V_4 M_P^4. \tag{4.101}$$

In the second line, we use the translation invariance of the vacuum. In the last line, we change the variables x, y into $X = x - y$ and $Y = x + y$.

We can confirm this relation by considering the concrete model. For example, if we think the free scalar theory,

$$\int d^d x d^d y \langle (\partial_\mu \phi(x))^2 (\partial_\nu \phi(y))^2 \rangle = 2 (\partial_{x_\mu})^2 (\partial_{y_\mu})^2 \left(\frac{\Gamma(d/2)}{2\pi^{d/2}} \frac{1}{|x-y|^{d-2}}\right)^2$$

$$= \int d^d x d^d y\, 8 \left(\frac{\Gamma(d/2)}{2\pi^{d/2}}\right)^2 (2d^2 - 11d + 14)(2d^2 - 2d + 5) \frac{1}{|x-y|^{2d}}$$

$$= \int d\,|x-y|\, \frac{\Gamma(d/2)}{2\pi^{d/2}} (2d^2 - 11d + 14)(2d^2 - 2d + 5)$$

$$\times V_d \frac{1}{|x-y|^{d+1}}$$

$$= \frac{\Gamma(d/2)}{2d\,\pi^{d/2}} (2d^2 - 11d + 14)(2d^2 - 2d + 5) V_d \Lambda^d$$

$$= \frac{29}{4\pi^2} V_4 \Lambda^4. \tag{4.102}$$

In the last line, we have put $d = 4$. We note that the two point function of the d-dimensional free scalar theory is

$$G(x - y) := \langle \phi(x)\phi(y) \rangle = \frac{\Gamma(d/2)}{2\pi^{d/2}} \frac{1}{|x - y|^{d-2}}. \tag{4.103}$$

The derivation of this expression is the following. The Green function satisfies the equation of motion with delta functional source term:

$$\partial_\mu \partial^\mu G(x) = -\delta^{(d)}(x). \tag{4.104}$$

Then, in the momentum, $G(x)$ is expressed as

$$G(x) = \int \frac{d^d k}{(2\pi)^d} \frac{1}{k^2} e^{-ik \cdot x}, \tag{4.105}$$

which implies that $G(x)$ only depends on the radial component of x, i.e., $|x|$. The integration of Eq. (4.104) becomes

$$\int d^d x \partial_\mu \partial^\mu G(x) = -1. \tag{4.106}$$

By using

$$\int d^d x \partial_\mu \partial^\mu G(x) = \int d^{d-1} S \hat{x}_\mu \partial^\mu G(x), \tag{4.107}$$

we obtain

$$\int d^{d-1} S \partial_r G(x) = -1. \tag{4.108}$$

After all, we reach the

$$\partial_r G(x) = -\frac{1}{\int d^{d-1} S} = -\frac{\Gamma(d/2)}{r^{d-1} 2\pi^{d/2}}, \tag{4.109}$$

from which we get Eq. (4.103).

Let us return to the argument of meaning of fluctuation. Now we have seen that the fluctuation of the dimensionless coupling g is the order of $1/\sqrt{V_4}$. Then, the fluctuation of the cosmological constant may be given by

$$\Delta \rho_0 \sim M_P^4 \Delta g \sim \frac{M_P^4}{\sqrt{V_4 M_P^4 Z_U(g^*)}} \sim \frac{M_P^2 H_0^2}{\sqrt{Z_U(g^*)}}. \tag{4.110}$$

The current cosmological constant is given by $\sim M_P^2 H_0^2$ because the current universe is dominated by the vacuum energy. Therefore, if $Z_U(g_*)$ is the order of one, we can understand the nonzero cosmological constant as a quantum fluctuation from zero.

References

1. S.R. Coleman, Why there is nothing rather than something: a theory of the cosmological constant. Nucl. Phys. B **310**, 643 (1988)
2. I.R. Klebanov, L. Susskind, T. Banks, Wormholes and the cosmological constant. Nucl. Phys. B **317**, 665–692 (1989)
3. J. Preskill, Wormholes in space-time and the constants of nature. Nucl. Phys. B **323**, 141 (1989)
4. H. Kawai, T. Okada, Solving the naturalness problem by baby universes in the lorentzian multiverse. Prog. Theor. Phys. **127**(2012), 689–721. arXiv:1110.2303
5. Y. Hamada, H. Kawai, K. Kawana, Evidence of the big fix, Int. J. Mod. Phys. **A29** (2014), no. 17, 1450099. arXiv:1405.1310
6. Y. Hamada, H. Kawai, K. Kawana, Weak scale from the maximum entropy principle. PTEP **2015**, 033B06 (2015). arXiv:1409.6508
7. Y. Hamada, H. Kawai, K. Kawana, *Natural solution to the naturalness problem—Universe does fine-tuning* (2015). arXiv:1509.05955
8. H. Kawai, *Private communication*
9. Y. Asano, H. Kawai, A. Tsuchiya, Factorization of the effective action in the IIB matrix model. Int. J. Mod. Phys. **A27**, 1250089 (2012). arXiv:1205.1468
10. M. Yoshimura, Unified gauge theories and the baryon number of the universe. Phys. Rev. Lett. **41**, 281–284 (1978). [Erratum: Phys. Rev. Lett. 42, 746 (1979)]
11. M. Fukugita, T. Yanagida, Baryogenesis without grand unification. Phys. Lett. B **174**, 45 (1986)
12. H. Aoki, H. Kawai, String scale baryogenesis, Prog. Theor. Phys. **98**, 449–456 (1997). arXiv:hep-ph/9703421
13. Y. Hamada, K. Kawana, *Minimal leptogenesis* (2015). arXiv:1510.05186
14. C.A. Baker et al., An improved experimental limit on the electric dipole moment of the neutron. Phys. Rev. Lett. **97**, 131801 (2006). arXiv:hep-ex/0602020
15. Planck, P.A.R. Ade et al., *Planck 2015 results. XIII. Cosmological parameters* (2015). arXiv:1502.01589

Chapter 5
Dark Matter and Higgs Potential

Abstract Although the SM can describe the almost all experiments, there remain phenomena that can not be explained within the SM. That is, dark matter of the universe, baryon asymmetry and mass of the neutrino. Among them, in this chapter, we focus on the dark matter. we investigate the scenario to include the dark matter by extending the SM minimally, and discuss the implications on the SM criticality. In Sects. 5.1 and 5.2, we consider the impact on the Higgs potential by singlet and weakly interacting dark matters, respectively.

5.1 Singlet Dark Matter

The minimal extension of the SM to include the dark matter is to add a stable particle, S, to the SM. Namely, the Lagrangian becomes [1–9]

$$\mathcal{L} = \mathcal{L}_{\mathrm{SM}} + \frac{1}{2}(\partial_\mu S)^2 - \frac{1}{2}m_S^2 S^2 - \frac{\rho}{4!}S^4 - \frac{\kappa}{2}S^2 H^\dagger H. \qquad (5.1)$$

Here S is the real singlet scalar. S is stable thanks to Z_2 symmetry, $S \to -S$. After the electroweak symmetry breaking, the mass of the dark matter is

$$M_{\mathrm{DM}}^2 = m_S^2 + \frac{\kappa v^2}{2}. \qquad (5.2)$$

Because S has the interaction term, $\kappa S^2 H^\dagger H$, with the Higgs field, it is thermally produced in the early universe. Assuming that the thermal production explains the current abundance of the dark matter, we get the relation between κ and M_{DM} [10],

$$\log_{10} \kappa \simeq -3.63 + 1.04 \log_{10} \frac{M_{\mathrm{DM}}}{\mathrm{GeV}}, \qquad (5.3)$$

for $M_{\mathrm{DM}} \gtrsim 100\,\mathrm{GeV}$, from which we obtain $M_{\mathrm{DM}} \sim 330\,\mathrm{GeV} \times (\kappa/0.1)$.

Fig. 5.1 The contour plot of $\kappa(\mu = 10^{17}\,\text{GeV})$ and $\rho(\mu = 10^{17}\,\text{GeV})$. The red region corresponds to the strong coupling. In the following, we only consider the white region
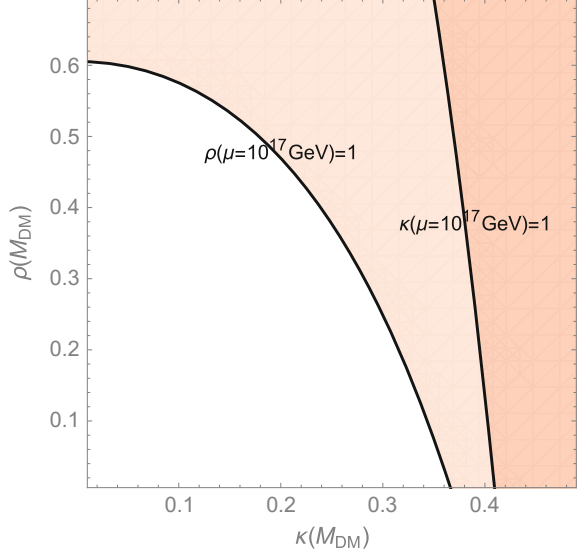
We have two new parameter, κ and ρ. In order to avoid the strong coupling regime, we consider the region where $\kappa, \rho \leq 1$ for $\mu \leq 10^{17}\,\text{GeV}$. In Fig. 5.1, we show the region realizing $\kappa(\mu = 10^{17}\,\text{GeV})$, $\rho(\mu = 10^{17}\,\text{GeV}) \leq 1$. In the red region $\kappa(\mu = 10^{17}\,\text{GeV}) \geq 1$ or $\rho(\mu = 10^{17}\,\text{GeV}) \geq 1$. Therefore, we take $\kappa(\mu = M_{\text{DM}}) \leq 0.4$ and $\rho(\mu = M_{\text{DM}}) \leq 0.6$.

Let us consider the Higgs potential of this model. The one-loop effective potential is given by

$$V = V_{\text{tree}} + \Delta V_{1-\text{loop, DM}}, \tag{5.4}$$

where V_{tree} and $\Delta V_{1-\text{loop, DM}}$ are

$$V_{\text{tree}} = e^{4\Gamma(\varphi)} \frac{\lambda(\mu)}{4} \varphi^4,$$

$$\Delta V_{1-\text{loop, DM}} = \Delta V_{1-\text{loop}} + \frac{M_{\text{DM}}^4}{64\pi^2} \left(\ln \frac{M_{\text{DM}}(\varphi)^2}{\mu^2} - \frac{3}{2} \right). \tag{5.5}$$

Here $M_{\text{DM}}(\varphi) = \sqrt{\frac{\kappa\varphi^2}{2} e^{2\Gamma(\varphi)} + m_S^2}$. The wavefunction renormalization $\Gamma(\varphi)$ of this model is same as that of the SM at one loop level.

The introduction of S changes the running of the Higgs self coupling as follows:

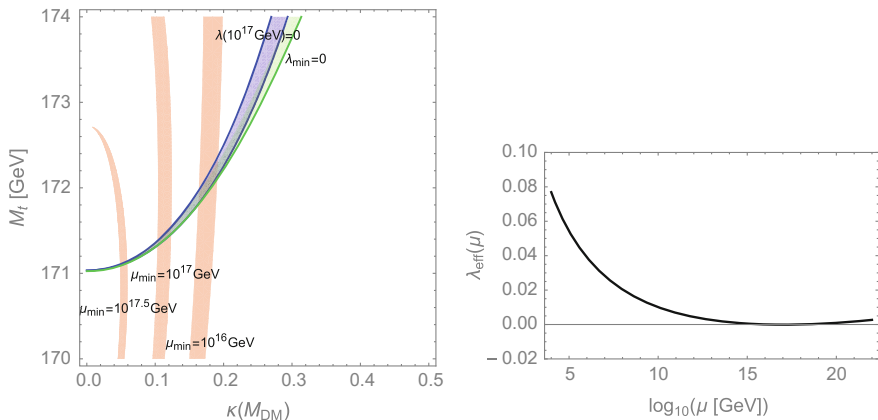$$\beta_\lambda = \beta_{\lambda, \text{SM}} + \frac{1}{16\pi^2} \frac{1}{2} \kappa^2, \tag{5.6}$$

Fig. 5.2 *Left* The contour plot of $\lambda_{\min}$ and $\mu_{\min}$ in M_t-$\kappa(M_{\mathrm{DM}})$ plane. *Right* Running of $\lambda_{\mathrm{eff}}(\mu)$ for $M_t = 172\,\mathrm{GeV}$, $\kappa(M_{\mathrm{DM}}) = 0.17$ and $\rho(M_{\mathrm{DM}}) = 0.1$. λ takes the minimum value 0 at around $10^{17}\,\mathrm{GeV}$

see Appendix B for runnings of the other coupling constants. We can see that the dark matter helps the stability of the electroweak vacuum.

We define $\lambda_{\mathrm{eff},\mathrm{DM}}$ as

$$\lambda_{\mathrm{eff},\mathrm{DM}} = \frac{V_{\mathrm{tree}} + \Delta V_{1-\mathrm{loop}}}{\varphi^4}, \tag{5.7}$$

and examine its running. Figure 5.2 shows the contour of the running of $\lambda_{\mathrm{eff},\mathrm{DM}}$. The red band corresponds to the constant $\mu_{\min} = 10^{16}$, 10^{17} and $10^{17.5}\,\mathrm{GeV}$. The green band represents the contour which satisfies $\lambda_{\min} = 0$. The right hand side of the green line corresponds the unstable electroweak vacuum. The width of band is the uncertainty of $\rho(M_{\mathrm{DM}})$. The formula of the bare Higgs mass is also modified.

$$m_B^2 = -\left(6\lambda + \frac{3}{4}g_Y^2 + \frac{9}{4}g_2^2 - 6y_t^2 + \frac{1}{2}\kappa\right) I_1, \tag{5.8}$$

Figure 5.3 indicates the scale where the bare Higgs mass becomes zero. The width of the red band corresponds to the uncertainty of $\rho(M_{\mathrm{DM}}) = 0$–$0.6$.

A way to detect this model is the direct detection experiment. The spin independent cross section of the model is given by [10]

$$\sigma_{\mathrm{SI}} = 9.5 \times 10^{-46}\,\mathrm{cm}^2 \left[\frac{\kappa}{0.05}\right]^2 \left[\frac{200\,\mathrm{GeV}}{m_{\mathrm{DM}}}\right]^2 = 8.4 \times 10^{-46}\,\mathrm{cm}^2. \tag{5.9}$$

This value can be detected by the LUX [11, 12] or XENON1T [13] experiment. The current bound from LUX [12] gives $M_{\mathrm{DM}} \gtrsim 100\,\mathrm{GeV}$. XENON1T can detect the dark matter whose mass is around 1 TeV.
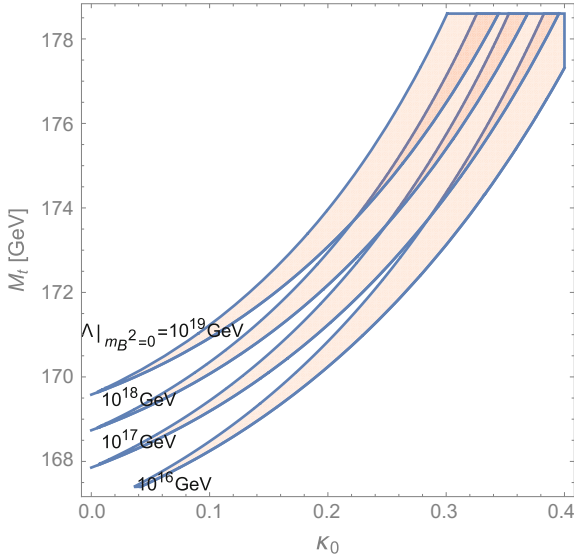
Fig. 5.3 The plot of the scale where $m_B^2 = 0$ in M_t-$\kappa(M_{\mathrm{DM}})$ plane. The width of the blue band corresponds to the uncertainty of $\rho(M_{\mathrm{DM}}) = 0$–0.6
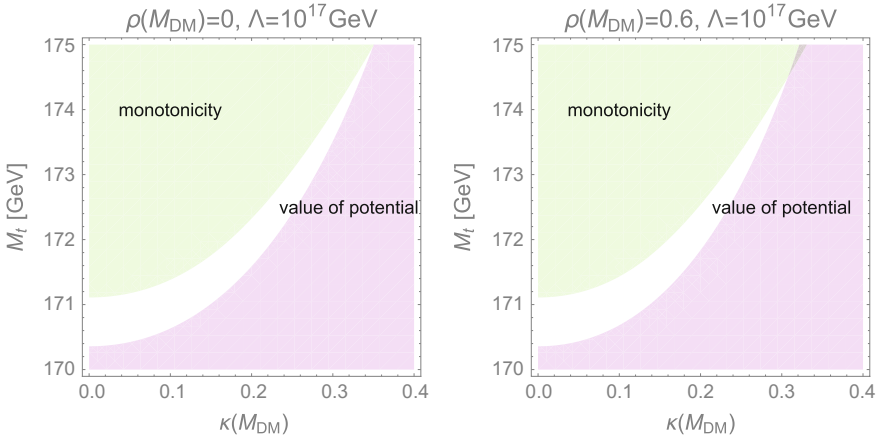
Fig. 5.4 The constraints from Higgs inflation in the SM with Higgs portal singlet scalar. The green and magenta regions are prohibited by the monotonicity and value of potential, respectively

We can also put the Higgs inflation constraint on this SM with singlet dark matter model. We show the constraints from monotonicity and the value of the potential in Figs. 5.4 and 5.5. We take $\rho(M_{\mathrm{DM}}) = 0$ and 0.6 in left and right panels, respectively. The colored region is excluded, and one can see that the top mass and $\kappa(M_{\mathrm{DM}})$ are corelated in the allowed region, which is our prediction.

Fig. 5.5 Same as Fig. 5.4, except for replacing $\kappa(M_{\mathrm{DM}})$ by M_{DM}

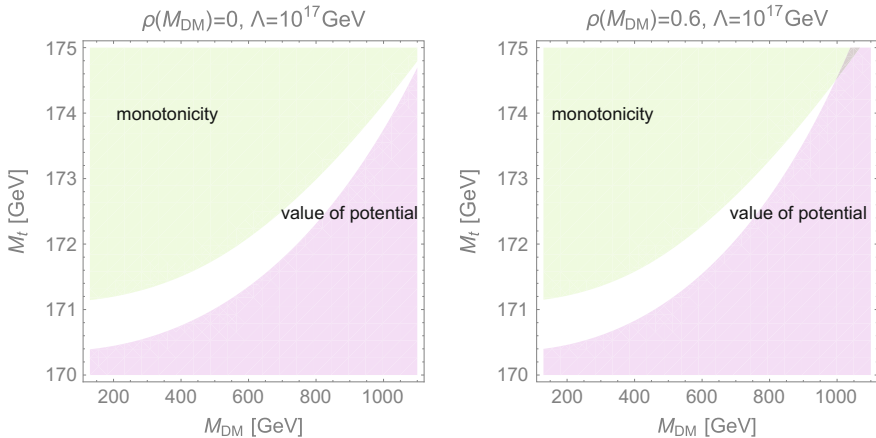If we introduce the right handed neutrino,

$$\Delta\mathcal{L} = \bar{\nu}_R i\gamma^\mu \partial_\mu \nu_R - M_R \bar{\nu}_R^c \nu_R - \left(y_\nu \bar{L} H^\dagger \nu_R + \mathrm{h.c.}\right). \tag{5.10}$$

the running is further modified. For simplicity, we introduce one right handed neutrino, and its mass is determined by the seesaw mechanism [14–18]:

$$\frac{y_\nu^2 v^2}{2M_R} = \frac{m_\nu}{2}, \quad \text{with} \quad v \simeq 246\,\mathrm{GeV}. \tag{5.11}$$

In the figure, we take $m_\nu = 0.1\,\mathrm{eV}$ as a reference value. We show the running of λ in the SM with singlet scalar and right handed neutrino in Fig. 5.6.

5.2 Weakly Interacting Dark Matter

The dark matter can be charged under the SM $SU(2)_L$ gauge interaction. This class of dark matter is often called Minimal dark matter [19–24]. Here we examine the impact on the Higgs potential in this class of dark matter models.

In order to make the dark matter neutral, we should assign the hypercharge $Y = $ (integer or half integer) depending on $SU(2)_L$ representation $n_L = $ (even or odd). Among them, $Y \neq 0$ is already excluded by the direct detection experiment due to

Fig. 5.6 The running of λ in the SM with singlet scalar and right handed neutrino. This figure is taken from Ref. [31]
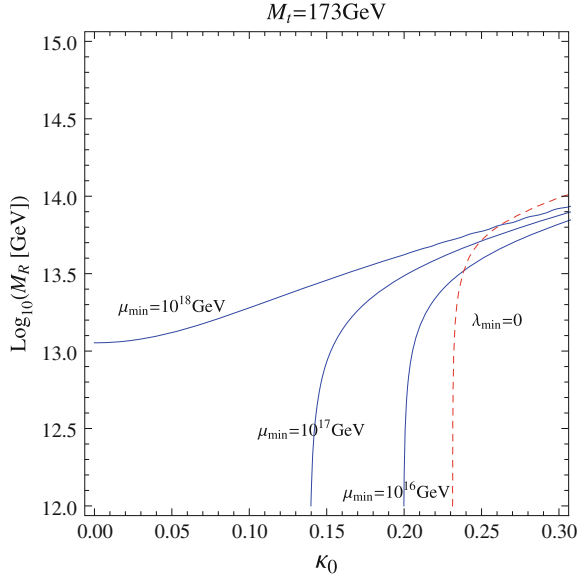
the exchange of the Z boson.[1] Therefore, we only consider $Y = 0$ dark matter with $n_L = 3, 5, \ldots$.

First, let us consider scalar dark matter X whose $SU(2)_L$ representation is $3, 5, \ldots$ and hypercharge is zero. Under the assumption of Z_2 symmetry, the general scalar potential is written as

$$
\begin{aligned}
V = & -\mu^2 \Phi^\dagger \Phi + \lambda (\Phi^\dagger \Phi)^2 + M_X^2 X^\dagger X + \lambda_X |X^\dagger X|^2 \\
& + \kappa |X^\dagger X| |\Phi^\dagger \Phi| + \kappa' (X^\dagger T_X^a X)(\Phi^\dagger T_\Phi^a \Phi) \\
& + \lambda_X' (X^\dagger T_X^a X)^2 + \lambda_X'' (X^\dagger T_X^a T_X^b X)^2 + \cdots .
\end{aligned}
\tag{5.12}
$$

The running of λ is modified by scalar couplings κ and κ'. Moreover, for the case of $n_L = 5, 7, \ldots$, the scalar quartic coupling of the dark matter hits the Landau pole much below the Planck scale even if we take scalar coupling to be zero at $\mu = M_{DM}$, see Table 5.1. Since the one-loop correction to the scalar coupling depends on the charge to the fourth power, the position of the Landau pole is significantly lower for higher representation of $SU(2)_L$.

---

[1] The exception is doublet and $Y = 1/2$ scalar dark matter. In this case, we can write the dimension 4 operator which splits the real and imaginary component of the dark matter. This model is called Inert Higgs, which we do not consider in the thesis.

Table 5.1 The positions of the Landau pole in quintet and septet dark matter models when we take all new scalar couplings to be zero at $\mu = M_{DM}$. The poles calculating using the one-loop RGE of the gauge couplings are also shown. In the case of the quintet dark matter, the $SU(2)_L$ gauge coupling is asymptotic free

(n_X, Y_X)	Landau pole (GeV)	Λ_{g_Y} (GeV)	Λ_{g_2} (GeV)
(5, real)	$9.5 \times 10^{11}\,(M_{DM}/100\,\text{GeV})^{1.38}$	9.6×10^{42}	–
(7, real)	$1.0 \times 10^{6}\,(M_{DM}/100\,\text{GeV})^{1.13}$	9.6×10^{42}	1.3×10^{56}
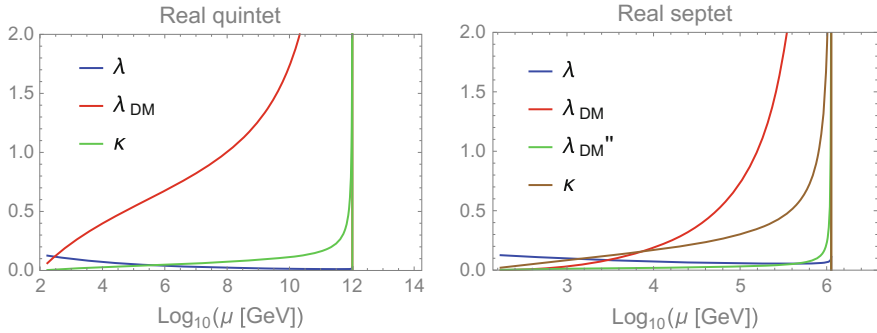
Fig. 5.7 The typical behavior of the running couplings in quintet and septet dark matter. We take $M_{DM} = 100\,\text{GeV}$. One can see that the Landau pole indeed exists
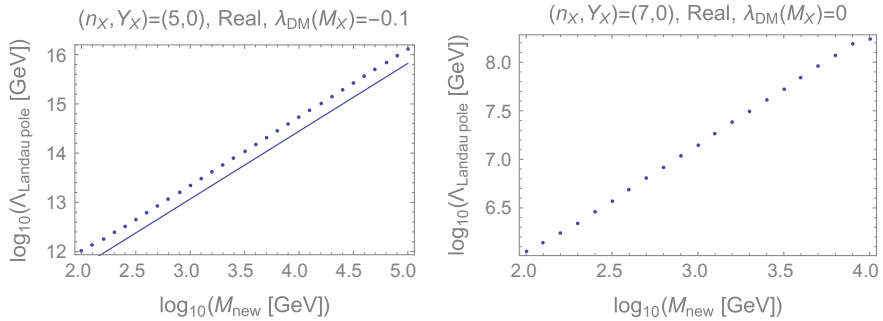
Fig. 5.8 The position of the Landau pole as a function of the dark matter mass M_{DM}

In Fig. 5.7, we plot the typical behavior of scalar couplings in quintet and septet scalar dark matters as functions of renormalization scale μ. We can see that the Landau pole actually appears below the Planck scale. As shown in Fig. 5.8, the position of Landau pole is almost proportional to the mass of the dark matter. The derivation from proportional relation comes from the running of gauge coupling g_2.

We would like to emphasize that the position of the Landau pole from scalar coupling is much smaller than that from gauge couplings Λ_{g_i},

$$\Lambda_{g_i} = M_X \exp\left(\frac{1}{2B_i}\frac{1}{g_i^2(M_X)}\right)$$

$$= M_X \left(\frac{M_t}{M_X}\right)^{B_{i,\mathrm{SM}}/B_i} \exp\left(\frac{1}{2B_i}\frac{1}{g_i^2(M_t)}\right). \tag{5.13}$$

Here $i = Y, 2$ and B_i means the coefficient of the one-loop beta function. We note that Eq. (5.13) is valid only if all other couplings are perturbative up to Λ_{g_i}.

Next, we consider the real triplet scalar dark matter model. In this case, the model can be valid up to the Planck scale. The scalar potential is written as

$$V = -\frac{1}{2}M_H^2\,|H|^2 + \frac{1}{2}M_{\mathrm{DM},3}^2\left(X^T X\right) + \lambda\left(|H|^2\right)^2 + \lambda_{\mathrm{DM},3}\left(X^T X\right)^2 + \kappa_3\,|H|^2\left(X^T X\right) \tag{5.14}$$

The contribution to the one-loop effective potential from the dark matter is given by

$$\Delta V_{\mathrm{trplet}}(\phi) = \frac{3m_{\mathrm{DM},3}(\phi)^4}{64\pi^2}\left(\ln\left(\frac{m_{\mathrm{DM},3}(\phi)^2}{\phi^2}\right) - \frac{3}{2}\right) \tag{5.15}$$

where $m_{\mathrm{DM},3}$ is the effective mass of the triplet dark matter:

$$m_{\mathrm{DM},3}(\phi) = \sqrt{M_{\mathrm{DM},3}^2 + \kappa_3(\phi)e^{2\Gamma(\phi)}\phi^2}. \tag{5.16}$$

In the left panel of the Fig. 5.9, we plot the typical running of scalar couplings. We can see that all couplings remain perturbative up to the Planck scale. The right

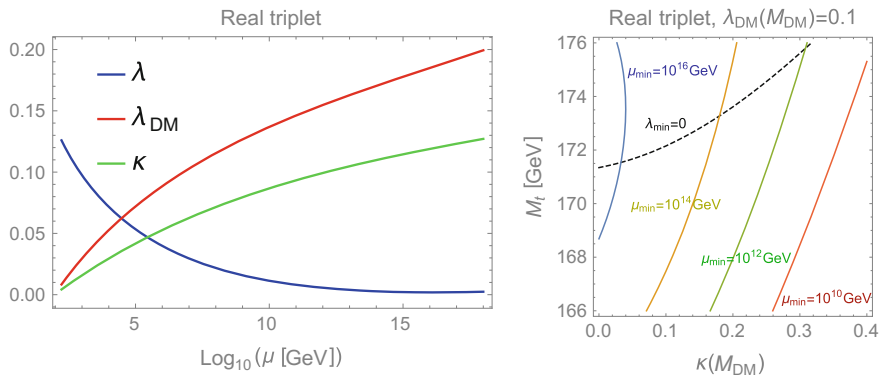**Fig. 5.9** *Left* The running of the couplings in the triplet dark matter model. *Right* The conditions $\lambda_{\min} = 0$, $\mu_{\min} = 10^{10}$ GeV, $\mu_{\min} = 10^{12}$ GeV, $\mu_{\min} = 10^{14}$ GeV and $\mu_{\min} = 10^{16}$ GeV are plotted. $\lambda_{\mathrm{DM}}(M_{\mathrm{DM}}) = 0.1$ is taken
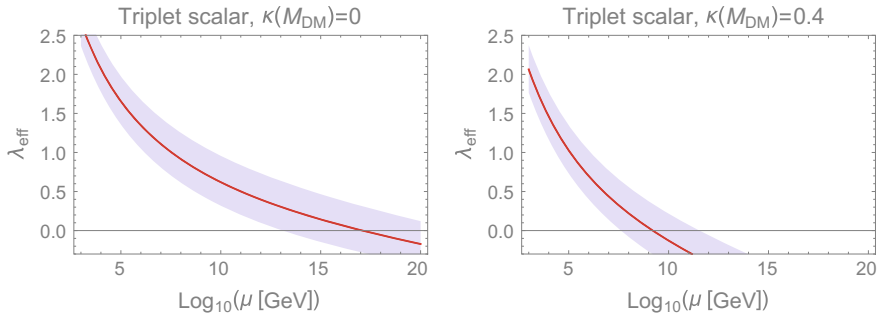
Fig. 5.10 The bare Higgs mass as a function of Λ in the real triplet dark matter model. We take $\kappa = 0$ and 0.4 in the left and right panels, respectively

panel shows the stability of the Higgs potential in M_t-κ_3 plane. The dashed black line corresponds to the situation where MPP is realized.

The one loop bare Higgs mass in this model is given by

$$\frac{m_B^2|_{1-\text{loop}}}{\Lambda^2/16\pi^2} = -\left(6\lambda + \frac{3}{4}g_Y^2 + \frac{9}{4}g_2^2 - 6y_t^2 + \frac{3}{2}\kappa_3\right). \tag{5.17}$$

We plot the Eq. (5.17) as a function of Λ in the Fig. 5.10. In the left panel, we take $\kappa(M_{\text{DM}}) = 0$ while $\kappa(M_{\text{DM}}) = 0.4$ in the right panel. The width of blue band represents the uncertainty of the top mass M_t.

Finally, let us move to the triplet and quintet fermion dark matter scenarios. The triplet Majorana fermion[2] is often studied in the text of supersymmetry [25] although our picture is different from supersymmetric scenario. The superpartner of W boson, wino, becomes the lightest supersymmetric particle in anomaly mediated supersymmetry breaking model [26, 27].

On the other hand, the advantage of the quintet fermion dark matter is its stability [20]. In the SM with quintet fermion, we can not write the operator describing dark matter decay whose dimension is less than 6. Therefore, the dark matter is stable without introducing ad hoc Z_2 symmetry.[3]

By assuming the thermal production of the dark matter, we obtain the dark matter mass as [21, 25]

$$M_\chi \simeq \begin{cases} 2.8\,\text{TeV} & (\text{for } n_\chi = 3), \\ 10\,\text{TeV} & (\text{for } n_\chi = 5). \end{cases} \tag{5.18}$$

---

[2]We review the quantization of Majorana field in Appendix E.

[3]In the case of the scalar dark matter, we can not obtain this type of the dark matter even if $n_L = 7$ [28, 29].
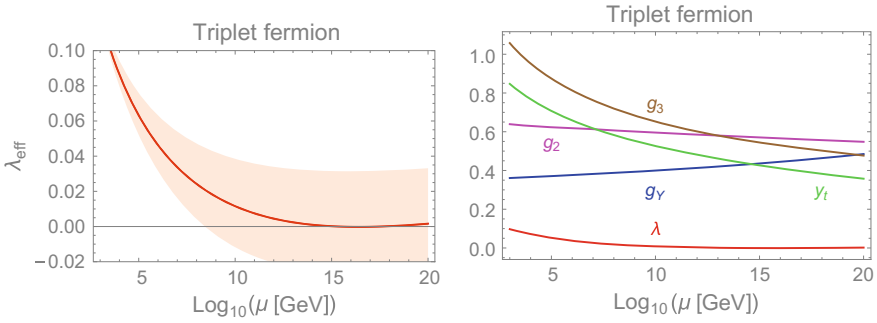
Fig. 5.11 *Left* The running of the effective coupling λ_{eff} in the triplet dark matter model for $M_t = 171.9\,\text{GeV}$. *Right* The running of the couplings in the triplet dark matter model

Fig. 5.12 The bare Higgs mass as a function of Λ in the triplet Majorana dark matter model
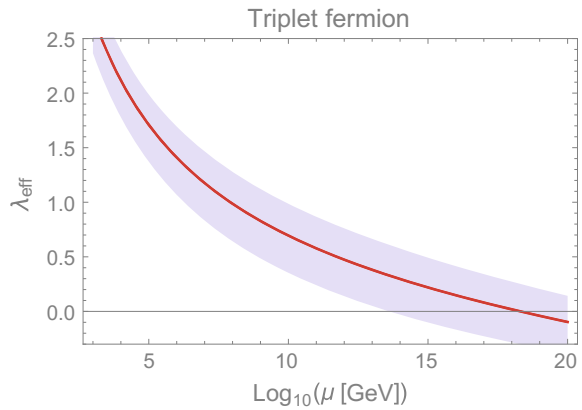
At first sight, it seems that the dark matter does not affect the running of λ because there is no coupling between the dark matter and Higgs. However, through the modification of the beta function of g_2, the Higgs potential tends to be stabilized. As shown in the left panel of the Fig. 5.11, if $M_t = 171.9\,\text{GeV}$, the degenerate vacuum appears at $\mu = 2.6 \times 10^{16}\,\text{GeV}$. The MPP predicts this situation. The right panel of the Fig. 5.11, dimensionless couplings are plotted as functions of scale μ for $M_t = 171.9\,\text{GeV}$. In the Fig. 5.12, we also show the bare Higgs mass as a function of Λ. We can see that the bare mass vanishes around the string/Planck scale.

In the case of the quintet dark matter, the Higgs potential becomes more stable than the triplet case due to the large $SU(2)_L$ charge. As a result, the degenerate vacuum appears at $\mu = 1.2 \times 10^{11}\,\text{GeV}$ for $M_t = 175\,\text{GeV}$ as in the left panel of the Fig. 5.13. We show the runnings of the other couplings in the right panel of the Fig. 5.13. The bare Higgs mass as the function of Λ can be seen in the Fig. 5.14.
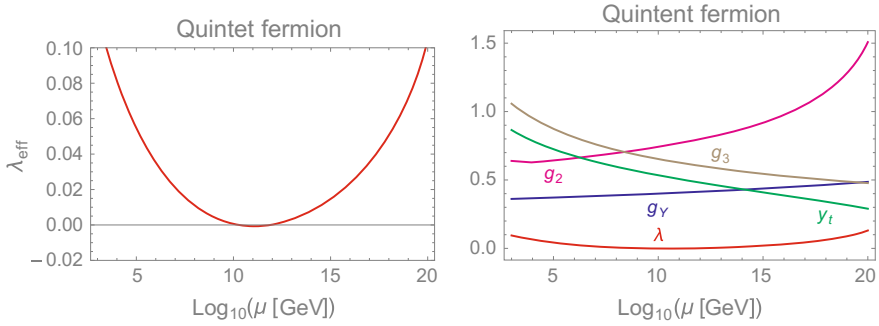
Fig. 5.13 *Left* The running of the effective coupling λ_{eff} in the quintet dark matter model for $M_t = 175\,\text{GeV}$. *Right* The running of the couplings in the quintet dark matter model

Fig. 5.14 The bare Higgs mass as a function of Λ in the quintet Majorana dark matter model
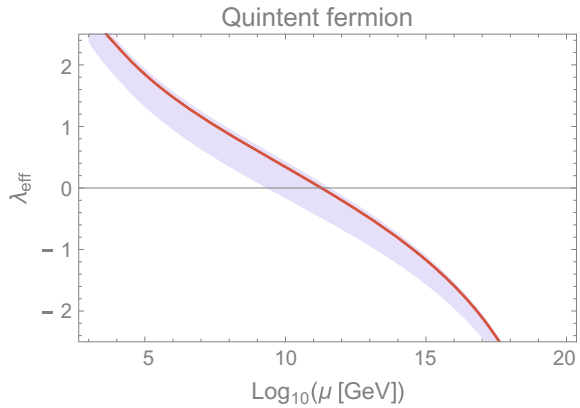
To summarize, we have

$$(M_t, \Lambda_{\text{MPP}}) = \begin{cases} (171.9, \ 2.6 \times 10^{16})\,\text{GeV} & \text{for } n_\chi = 3, \\ (175.0, \ 1.2 \times 10^{11})\,\text{GeV} & \text{for } n_\chi = 5. \end{cases} \qquad (5.19)$$

It is very interesting that the only triplet representation is allowed by requiring the perturbativity and criticality around the Planck scale.

The most plausible way to detect the weakly interacting dark matter is indirect detection. In the current universe, the cosmic ray may be produced by the pair annihilation of the dark matter in the, for example, center of our galaxy. Therefore, by examining the spectrum of the cosmic ray, we can get the hint of the dark matter. Thanks to rather large gauge interaction of the dark matter, we expect that the dark matter originated cosmic ray is detectable in the future observation. Cherenkov Telescope Array(CTA) [30] can probe these simple dark matter models.

References

1. V. Silveira, A. Zee, Scalar phantoms. Phys. Lett. **B161**, 136 (1985)
2. J. McDonald, Gauge singlet scalars as cold dark matter. Phys. Rev. **D50**, 3637–3649 (1994). arXiv:hep-ph/0702143
3. C. Burgess, M. Pospelov, T. ter Veldhuis, The Minimal model of nonbaryonic dark matter: a singlet scalar. Nucl. Phys. **B619**, 709–728 (2001). arXiv:hep-ph/0011335
4. H. Davoudiasl, R. Kitano, T. Li, H. Murayama, The new minimal standard model. Phys. Lett. **B609**, 117–123 (2005). arXiv:hep-ph/0405097
5. B. Patt, F. Wilczek, *Higgs-field portal into hidden sectors* (2006). arXiv:hep-ph/0605188
6. B. Grzadkowski, J. Wudka, Pragmatic approach to the little hierarchy problem: the case for dark matter and neutrino physics. Phys. Rev. Lett. **103**, 091802 (2009). arXiv:0902.0628
7. A. Drozd, B. Grzadkowski, J. Wudka, Multi-scalar-singlet extension of the standard model—the case for dark matter and an invisible Higgs Boson. JHEP **04**, 006 (2012). arXiv:1112.2582. [Erratum: JHEP11,130(2014)]
8. K. Kawana, Multiple point principle of the standard model with scalar singlet dark matter and right handed neutrinos. PTEP **2015**, 023B04 (2015). arXiv:1411.2097
9. K. Kawana, Criticality and inflation of the gauged B—L model. PTEP **2015**, 073B04 (2015). arXiv:1501.04482
10. J.M. Cline, K. Kainulainen, P. Scott, C. Weniger, Update on scalar singlet dark matter. Phys. Rev. **D88**, 055025 (2013). arXiv:1306.4710
11. LUX, D.S. Akerib et al., First results from the LUX dark matter experiment at the sanford underground research facility. Phys. Rev. Lett. **112**, 091303 (2014). arXiv:1310.8214
12. LUX, D.S. Akerib et al., *Improved WIMP scattering limits from the LUX experiment* (2015). arXiv:1512.03506
13. XENON1T, E. Aprile, The XENON1T dark matter search experiment. Springer Proc. Phys. **148**, 93–96 (2013). arXiv:1206.6288
14. P. Minkowski, $\mu \to e\gamma$ at a rate of one out of 10^9 Muon Decays? Phys. Lett. **B67**, 421–428 (1977)
15. T. Yanagida, Horizontal symmetry and masses of neutrinos. Conf. Proc. **C7902131**, 95–99 (1979). [Conf. Proc.C7902131,95(1979)]
16. M. Gell-Mann, P. Ramond, R. Slansky, Complex spinors and unified theories. Conf. Proc. **C790927**, 315–321 (1979). arXiv:1306.4669
17. S.L. Glashow, The future of elementary particle physics. NATO Sci. Ser. B **61**, 687 (1980)
18. R.N. Mohapatra, G. Senjanovic, Neutrino mass and spontaneous parity violation. Phys. Rev. Lett. **44**, 912 (1980)
19. J. Hisano, S. Matsumoto, M.M. Nojiri, O. Saito, Non-perturbative effect on dark matter annihilation and gamma ray signature from galactic center. Phys. Rev. **D71**, 063528 (2005). arXiv:hep-ph/0412403
20. M. Cirelli, N. Fornengo, A. Strumia, *Minimal dark matter*, Nucl. Phys. **B753**, 178–194 (2006). arXiv:hep-ph/0512090
21. M. Cirelli, A. Strumia, M. Tamburini, Cosmology and Astrophysics of Minimal Dark Matter. Nucl. Phys. **B787**, 152–175 (2007). arXiv:0706.4071
22. E. Del Nobile, M. Nardecchia, P. Panci, *Millicharge or Decay: A Critical Take on Minimal Dark Matter* (2015). arXiv:1512.05353
23. M. Cirelli, T. Hambye, P. Panci, F. Sala, M. Taoso, Gamma ray tests of Minimal Dark Matter. JCAP **1510**(10), 026 (2015). arXiv:1507.05519
24. C. Garcia-Cely, A. Ibarra, A.S. Lamperstorfer, M.H.G. Tytgat, Gamma-rays from Heavy Minimal Dark Matter. JCAP **1510**(10), 058 (2015). arXiv:1507.05536
25. J. Hisano, S. Matsumoto, M. Nagai, O. Saito, M. Senami, Non-perturbative effect on thermal relic abundance of dark matter. Phys. Lett. **B646**, 34–38 (2007). arXiv:hep-ph/0610249
26. L. Randall, R. Sundrum, Out of this world supersymmetry breaking. Nucl. Phys. **B557**, 79–118 (1999). arXiv:hep-th/9810155

27. G.F. Giudice, M.A. Luty, H. Murayama, R. Rattazzi, Gaugino mass without singlets, JHEP **12**, 027 (1998). arXiv:hep-ph/9810442

28. L. Di Luzio, R. Grober, J.F. Kamenik, M. Nardecchia, Accidental matter at the LHC, JHEP **07**, 074 (2015). arXiv:1504.00359

29. Y. Hamada, K. Kawana, K. Tsumura, Landau pole in the Standard Model with weakly interacting scalar fields. Phys. Lett. **B747**, 238–244 (2015). arXiv:1505.01721

30. CTA Consortium, M. Actis et al., Design concepts for the Cherenkov Telescope Array CTA: an advanced facility for ground-based high-energy gamma-ray astronomy. Exper. Astron. **32**, 193–316 (2011). arXiv:1008.3703

31. Y. Hamada, H. Kawai, K.-y. Oda, Predictions on mass of Higgs portal scalar dark matter from Higgs inflation and flat potential. JHEP **1407**, 026 (2014). arXiv:1404.6141

Chapter 6
Summary

In this thesis, we have considered Higgs potential and naturalness problem in light of the LHC result, the discovery of Higgs boson.

It is well known that the Higgs mass suffers from the quadratic divergence, that means that its mass highly depends on ultraviolet physics. This was primary motivation to look for the new physics beyond the SM, which is one of the target of the LHC. Because the largest contribution to the bare Higgs mass is given by the top quark loop, it is expected that a top partner exists and cancels the contribution from top quark. In order to obtain sufficiently cancelation, the mass of a top partner is the same order of magnitude as that of the top quark. However, contrary to this naive expectation, the LHC does not find any colored new particle up to 1 TeV. The above situation suggests that it is good time to be free from the conventional naturalness argument, and consider the scenario where the SM is valid up to very high scale such as the string/Planck scale.

Because the last parameter of the SM is determined, we can extrapolate the SM up to very high scale such as string/Planck scale. In Chap. 2, we have estimated bare parameters as functions of cutoff scale Λ. Especially, the quadratic divergent part of bare Higgs mass is calculated. We have shown that there is triple coincidence: Higgs self coupling, its beta function and bare Higgs mass all become zero around string/Planck scale. Probably, this fact indicates that the physics in the electroweak scale is directly connected to that in the Planck scale.

In Chap. 3, as an concrete example of this connection, we consider the Higgs inflation. First, we have explained why the Higgs inflation is impossible in the pure SM. Then, we have introduced the non-minimal coupling between the Higgs field and gravity. We have shown that, taking into account the running effect, the prediction of the conventional Higgs inflation can drastically change. We also have discussed the ambiguity of the renormalization scheme in the Higgs inflation.

In Chap. 4, we have investigated a solution to the naturalness problem without relying on TeV scale new physics. Starting from multi-local action, the coupling constant in the theory is no longer constant, but becomes dynamical variable. Using

this mechanism. We have explained the small cosmological constant, Higgs mass and CP violating θ parameter in QCD.

In Chap. 5, we have added the dark matter particle to the SM, and examined its impact on the Higgs potential. It has been found that, if we require thermally produced dark matter and the flat potential around the string/Planck scale as in multiple point criticality principle, the allowed $SU(2)_L$ charges of the dark matter are singlet and triplet for scalar, and triplet for fermion. These models can be detectable in the future direct and/or indirect experiment.

Appendix A—Convention

The metric in the flat space is taken as

$$\eta_{\mu\nu} = \begin{pmatrix} 1 & 0 & 0 & 0 \\ 0 & -1 & 0 & 0 \\ 0 & 0 & -1 & 0 \\ 0 & 0 & 0 & -1 \end{pmatrix},$$ (A.1)

In the thesis, we adopt the chiral representation

$$\gamma^{\mu} = \begin{pmatrix} 0 & \sigma^{\mu} \\ \bar{\sigma}^{\mu} & 0 \end{pmatrix}, \quad \sigma^{\mu} = (1, \sigma^{i}), \quad \bar{\sigma}^{\mu} = (1, -\sigma^{i}),$$

$$\sigma^{1} = \begin{pmatrix} 0 & 1 \\ 1 & 0 \end{pmatrix}, \quad \sigma^{2} = \begin{pmatrix} 0 & -i \\ i & 0 \end{pmatrix}, \quad \sigma^{3} = \begin{pmatrix} 1 & 0 \\ 0 & -1 \end{pmatrix},$$ (A.2)

as a concrete representation of the Clifford algebra,

$$\{\gamma_{\mu}, \gamma_{\nu}\} = 2g_{\mu\nu}.$$ (A.3)

This representation diagonalizes γ^5 which I will define below.

We focus on the four dimensional field theory, and, in the four dimension the irreducible representation of the spinor field is the Weyl spinor, which is the eigenvector of

$$\gamma^5 := i\gamma^0\gamma^1\gamma^2\gamma^3 = \begin{pmatrix} -1 & 0 \\ 0 & 1 \end{pmatrix}.$$ (A.4)

The left and right handed spinor have -1 and 1 eigenvalues, respectively.

The Lagrangian of the SM is given by

$$
\begin{aligned}
\mathcal{L}_{\text{SM}} = & -\frac{1}{4} G^{A\mu\nu} G^A_{\mu\nu} - \frac{1}{4} W^{a\mu\nu} W^a_{\mu\nu} - \frac{1}{4} B^{\mu\nu} B_{\mu\nu} \\
& + \left| D_\mu H \right|^2 + \mu^2 \left| H \right|^2 - \lambda \left(\left| H \right|^2 \right)^2 \\
& + \bar{q}^i i \slashed{D} q^i + \bar{u_R}^i i \slashed{D} u^i_R + \bar{d_R}^i i \slashed{D} d^i_R + \bar{l}^i i \slashed{D} l^i + \bar{e_R}^i i \slashed{D} e^i_R \\
& - (y_u^{ij} \bar{q}^i \tilde{H} u^j_R + \text{h.c.}) - (y_d^{ij} \bar{q}^i H d^j_R + \text{h.c.})) - (y_l^{ij} \bar{l}^i H e^j_R + \text{h.c.}). \quad \text{(A.5)}
\end{aligned}
$$

Here

$$
\begin{aligned}
G^A_{\mu\nu} &= \partial_\mu G^A_\nu - \partial_\nu G^A_\mu + g_3 f^{ABC} G^B_\mu G^C_\mu \\
W^a_{\mu\nu} &= \partial_\mu W^a_\nu - \partial_\nu W^a_\mu + g_2 \epsilon^{abc} G^b_\mu G^c_\mu \\
B_{\mu\nu} &= \partial_\mu B_\nu - \partial_\nu B_\mu
\end{aligned} \quad \text{(A.6)}
$$

are the field strength of $SU(3)_C$, $SU(2)_L$ and $U(1)_Y$, respectively. $A = 1, 2, \ldots 8$ and $a = 1, 2, 3$ are indexes of the adjoint representation of $SU(3)_C$ and $SU(2)_L$. f^{ABC} is the $SU(3)_C$ structure constant, and ϵ^{abc} is the $SU(2)_L$ structure constant. g_3, g_2, g_Y are the gauge couplings of each group. The covariant derivative D_μ acts on the field X whose $SU(3)_C \times SU(2)_L \times U(1)_Y$ representation is (r_3, r_2, r_1) is as follows:

$$
D_\mu X = (\partial_\mu - i g_3 G^A_\mu T^A_{r_3} - i g_2 W^a_\mu T^a_{r_2} - i g_Y B_\mu r_1) X. \quad \text{(A.7)}
$$

Here T_r is the generator corresponding to the representation r. For example, T_r is Gell-Mann matrix λ^A if X is fundamental representation of $SU(3)$, and T_r is Pauli matrix $\sigma^a / 2$ if X is fundamental representation of $SU(2)$. The definition of $\tilde{H}$ is

$$
\tilde{H} = i \sigma^2 H^\dagger = \begin{pmatrix} H^{0\dagger} \\ -H^- \end{pmatrix}. \quad \text{(A.8)}
$$

The field contents in the SM is summarized in Table A.1.

Table A.1 The field contents in the SM

Name	Field	$SU(3)_C$	$SU(2)_L$	$U(1)_Y$	spin
Left handed quark	$q_i = (u_L, d_L)_i$	3	2	$\frac{1}{6}$	$\frac{1}{2}$
Right handed quark	u_{Ri}	3	1	$\frac{2}{3}$	$\frac{1}{2}$
	d_{Ri}	3	1	$-\frac{1}{3}$	$\frac{1}{2}$
Left handed lepton	$l_i = (\nu_L, e_L)_i$	1	2	$-\frac{1}{2}$	$\frac{1}{2}$
Right handed lepton	e_{Ri}	1	1	-1	$\frac{1}{2}$
Higgs	$H = (H^+, H^0)$	1	2	$\frac{1}{2}$	0
Gluon	G_μ	8	1	0	1
$SU(2)_L$ gauge boson	W_μ	1	3	0	1
$U(1)_Y$ gauge boson	B_μ	1	1	0	1

Appendix B—Renormalization Group Equations

The beta functions of models that we consider in the thesis are listed. We have used the results of Refs. [1–4] to derive the equations below.

- SM

$$\frac{dg_Y}{dt} = \frac{1}{16\pi^2}\frac{41}{6}g_Y^3 + \frac{g_Y^3}{(16\pi^2)^2}\left(\frac{199}{18}g_Y^2 + \frac{9}{2}g_2^2 + \frac{44}{3}g_3^2 - \frac{17}{6}y_t^2\right),$$

$$\frac{dg_2}{dt} = -\frac{1}{16\pi^2}\frac{19}{6}g_2^3 + \frac{g_2^3}{(16\pi^2)^2}\left(\frac{3}{2}g_Y^2 + \frac{35}{6}g_2^2 + 12g_3^2 - \frac{3}{2}y_t^2\right),$$

$$\frac{dg_3}{dt} = -\frac{7}{16\pi^2}g_3^3 + \frac{g_3^3}{(16\pi^2)^2}\left(\frac{11}{6}g_Y^2 + \frac{9}{2}g_2^2 - 26g_3^2 - 2y_t^2\right),$$

$$\frac{dy_t}{dt} = \frac{y_t}{16\pi^2}\left(\frac{9}{2}y_t^2 - \frac{17}{12}g_Y^2 - \frac{9}{4}g_2^2 - 8g_3^2\right) + \frac{y_t}{(16\pi^2)^2}\left(-12y_t^4 + 6\lambda^2 - 12\lambda y_t^2\right.$$

$$+ \frac{131}{16}g_Y^2 y_t^2 + \frac{225}{16}g_2^2 y_t^2 + 36g_3^2 y_t^2$$

$$\left. + \frac{1187}{216}g_Y^4 - \frac{23}{4}g_2^4 - 108g_3^4 - \frac{3}{4}g_Y^2 g_2^2 + 9g_2^2 g_3^2 + \frac{19}{9}g_3^2 g_Y^2\right),$$

$$\frac{d\lambda}{dt} = \frac{1}{16\pi^2}\left(24\lambda^2 - 3g_Y^2\lambda - 9g_2^2\lambda + \frac{3}{8}g_Y^4 + \frac{3}{4}g_Y^2 g_2^2 + \frac{9}{8}g_2^4 + 12\lambda y_t^2 - 6y_t^4\right)$$

$$+ \frac{1}{(16\pi^2)^2}\left\{-312\lambda^3 + 36\lambda^2(g_Y^2 + 3g_2^2) - \lambda\left(-\frac{629}{24}g_Y^4 - \frac{39}{4}g_Y^2 g_2^2 + \frac{73}{8}g_2^4\right)\right.$$

$$+ \frac{305}{16}g_2^6 - \frac{289}{48}g_Y^2 g_2^4 - \frac{559}{48}g_Y^4 g_2^2 - \frac{379}{48}g_Y^6 - 32g_3^2 y_t^4 - \frac{8}{3}g_Y^2 y_t^4 - \frac{9}{4}g_2^4 y_t^2$$

$$+ \lambda y_t^2\left(\frac{85}{6}g_Y^2 + \frac{45}{2}g_2^2 + 80g_3^2\right) + g_Y^2 y_t^2\left(-\frac{19}{4}g_Y^2 + \frac{21}{2}g_2^2\right)$$

$$\left. - 144\lambda^2 y_t^2 - 3\lambda y_t^4 + 30y_t^6\right\}, \tag{B.1}$$

where $t = \log\mu$.

- SM with N singlet real scalar fields

$$\frac{dg_Y}{dt} = \frac{1}{16\pi^2}\frac{41}{6}g_Y^3 + \frac{g_Y^3}{(16\pi^2)^2}\left(\frac{199}{18}g_Y^2 + \frac{9}{2}g_2^2 + \frac{44}{3}g_3^2 - \frac{17}{6}y_t^2\right),$$

$$\frac{dg_2}{dt} = -\frac{1}{16\pi^2}\frac{19}{6}g_2^3 + \frac{g_2^3}{(16\pi^2)^2}\left(\frac{3}{2}g_Y^2 + \frac{35}{6}g_2^2 + 12g_3^2 - \frac{3}{2}y_t^2\right),$$

$$\frac{dg_3}{dt} = -\frac{7}{16\pi^2}g_3^3 + \frac{g_3^3}{(16\pi^2)^2}\left(\frac{11}{6}g_Y^2 + \frac{9}{2}g_2^2 - 26g_3^2 - 2y_t^2\right),$$

$$\frac{dy_t}{dt} = \frac{y_t}{16\pi^2}\left(\frac{9}{2}y_t^2 - \frac{17}{12}g_Y^2 - \frac{9}{4}g_2^2 - 8g_3^2\right) + \frac{y_t}{(16\pi^2)^2}\left(-12y_t^4 + 6\lambda^2 + \frac{1}{4}N\kappa^2 - 12\lambda y_t^2\right.$$
$$\left. + \frac{131}{16}g_Y^2 y_t^2 + \frac{225}{16}g_2^2 y_t^2 + 36g_3^2 y_t^2 + \frac{1187}{216}g_Y^4 - \frac{23}{4}g_2^4 - 108g_3^4 - \frac{3}{4}g_Y^2 g_2^2 + 9g_2^2 g_3^2 + \frac{19}{9}g_3^2 g_Y^2\right),$$

$$\frac{d\lambda}{dt} = \frac{1}{16\pi^2}\left(\frac{1}{2}N\kappa^2 + 24\lambda^2 - 3g_Y^2\lambda - 9g_2^2\lambda + \frac{3}{8}g_Y^4 + \frac{3}{4}g_Y^2 g_2^2 + \frac{9}{8}g_2^4 + 12\lambda y_t^2 - 6y_t^4\right)$$
$$+ \frac{1}{(16\pi^2)^2}\left\{-2N\kappa^3 - 5N\kappa^2\lambda - 312\lambda^3 + 36\lambda^2(g_Y^2 + 3g_2^2)\right.$$
$$- \lambda\left(-\frac{629}{24}g_Y^4 - \frac{39}{4}g_Y^2 g_2^2 + \frac{73}{8}g_2^4\right) + \frac{305}{16}g_2^6 - \frac{289}{48}g_Y^2 g_2^4 - \frac{559}{48}g_Y^4 g_2^2$$
$$- \frac{379}{48}g_Y^6 - 32g_3^2 y_t^4 - \frac{8}{3}g_Y^2 y_t^4 - \frac{9}{4}g_2^4 y_t^2$$
$$+ \lambda y_t^2\left(\frac{85}{6}g_Y^2 + \frac{45}{2}g_2^2 + 80g_3^2\right) + g_Y^2 y_t^2\left(-\frac{19}{4}g_Y^2 + \frac{21}{2}g_2^2\right)$$
$$\left. - 144\lambda^2 y_t^2 - 3\lambda y_t^4 + 30y_t^6\right\},$$

$$\frac{d\kappa}{dt} = \frac{\kappa}{16\pi^2}\left(12\lambda + \rho + \frac{N-1}{3}\rho + 4\kappa + 6y_t^2 - \frac{3}{2}g_Y^2 - \frac{9}{2}g_2^2\right)$$
$$+ \frac{\kappa}{(16\pi^2)^2}\left\{-\left(\frac{N}{2}+10\right)\kappa^2 - 72\kappa\lambda - 60\lambda^2 - (2N+4)\kappa\rho - \left(\frac{5N+10}{18}\right)\rho^2\right.$$
$$- y_t^2(12\kappa + 72\lambda) - \frac{27}{2}y_t^4 + g_Y^2(\kappa + 24\lambda) + g_2^2(3\kappa + 72\lambda) + y_t^2\left(\frac{85}{12}g_Y^2 + \frac{45}{4}g_2^2 + 40g_3^2\right)$$
$$\left. + \frac{557}{48}g_Y^4 - \frac{145}{16}g_2^4 + \frac{15}{8}g_Y^2 g_2^2\right\},$$

$$\frac{d\rho}{dt} = \frac{1}{16\pi^2}\left(3\rho^2 + \frac{N-1}{3}\rho^2 + 12\kappa^2\right) + \frac{1}{(16\pi^2)^2}\left\{-\frac{3N+14}{3}\rho^3 - 20\kappa^2\rho - 48\kappa^3\right.$$
$$\left. - 72\kappa^2 y_t^2 + 24\kappa^2 g_Y^2 + 72\kappa^2 g_2^2\right\}, \tag{B.2}$$

- SM with Majorana triplet scalar field

$$\frac{d\Gamma}{dt} = \frac{1}{(4\pi)^2}\left(\frac{9}{4}g_2^2 + \frac{3}{4}g_Y^2 - 3y_t^2\right), \tag{B.3}$$

$$\frac{dg_Y}{dt} = \frac{g_Y^3}{(4\pi)^2}\left(\frac{41}{6} + \eta\, n_\chi \frac{4}{3}Y_\chi^2\right)$$
$$+ \frac{g_Y^3}{(4\pi)^4}\left\{\left(\frac{199}{18} + 4\eta\, n_\chi Y_\chi^4\right)g_Y^2 + \left(\frac{9}{2} + 4\eta Y_\chi^2 C_n\right)g_2^2 + \frac{44}{3}g_3^2 - \frac{17}{6}y_t^2\right\},$$

$$\frac{dg_2}{dt} = \frac{g_2^3}{(4\pi)^2}\left(-\frac{19}{6} + \eta\frac{4}{3}S_n\right)$$

$$+ \frac{g_2^3}{(4\pi)^4}\left\{\left(\frac{3}{2} + \eta 4 Y_\chi^2 S_n\right)g_Y^2 + \left(\frac{35}{6} + \eta\frac{40}{3}S_n + \eta 4 C_n S_n\right)g_2^2 + 12g_3^2 - \frac{3}{2}y_t^2\right\},$$

$$\frac{dg_3}{dt} = -\frac{7}{(4\pi)^2}g_3^3 + \frac{g_3^3}{(4\pi)^4}\left(\frac{11}{6}g_Y^2 + \frac{9}{2}g_2^2 - 26g_3^2 - 2y_t^2\right),$$

$$\frac{dy_t}{dt} = \frac{y_t}{(4\pi)^2}\left(\frac{9}{2}y_t^2 + 3y_\nu^2 - 8g_3^2 - \frac{9}{4}g_2^2 - \frac{17}{12}g_Y^2\right)$$

$$+ \frac{y_t}{(4\pi)^4}\left\{\left(\frac{1187}{216} + \frac{29}{27}\eta\, n_\chi Y_\chi^2\right)g_Y^4 + \left(-\frac{23}{4} + \eta S_n\right)g_2^4 - \frac{3}{4}g_2^2 g_Y^2 + \frac{19}{9}g_3^2 g_Y^2 + 9g_3^2 g_2^2\right.$$

$$\left. - 108g_3^4 + \left(\frac{131}{16}g_Y^2 + \frac{225}{16}g_2^2 + 36g_3^2\right)y_t^2 + 6\lambda^2 - 12\lambda y_t^2 - 12y_t^4\right\},$$

$$\frac{d\lambda}{dt} = \frac{1}{16\pi^2}\left(\lambda\left(24\lambda - 9g_2^2 - 3g_Y^2 + 12y_t^2\right) + \frac{3}{4}g_Y^2 g_2^2 + \frac{9}{8}g_2^4 + \frac{3}{8}g_Y^4 - 6y_t^4\right)$$

$$+ \frac{1}{(4\pi)^4}\left\{-312\lambda^3 + 36\lambda^2\left(g_Y^2 + 3g_2^2\right)\right.$$

$$+ \lambda\left(\frac{629}{24}g_Y^4 + \frac{10}{3}Y_\chi^2 g_Y^4 - \frac{73}{8}g_2^4 + 10\eta S_n g_2^4 + \frac{39}{4}g_2^2 g_Y^2\right)$$

$$+ \left(\frac{305}{16} - 4\eta S_n\right)g_2^6 - \left(\frac{289}{48} + \frac{4}{3}\eta S_n\right)g_2^4 g_Y^2 - \left(\frac{559}{48} + \frac{4}{3}\eta\, n_\chi Y_\chi^2\right)g_2^2 g_Y^4$$

$$- \left(\frac{379}{48} + \frac{4}{3}n_\chi Y_\chi^2\right)g_Y^6$$

$$+ \left(\frac{85}{6}g_Y^2 + \frac{45}{2}g_2^2 + 80g_3^2\right)\lambda y_t^2 + g_Y^2 y_t^2\left(\frac{21}{2}g_2^2 - \frac{19}{4}g_Y^2\right) - \frac{9}{4}g_2^4 y_t^2 - \frac{8}{3}g_Y^2 y_t^4 - 32g_3^2 y_t^4$$

$$- 144\lambda^2 y_t^2 - 3\lambda y_t^4 + 30y_t^6\right\}. \tag{B.4}$$

$\eta = 1, \frac{1}{2}$ correspond to Dirac and Weyl spinor, respectively.

- SM with a real triplet scalar field

$$\frac{dg_2}{dt} = -\frac{g_2^3}{(4\pi)^2}\frac{17}{6}, \tag{B.5}$$

$$\frac{d\lambda}{dt} = \frac{1}{16\pi^2}\left(\lambda\left(24\lambda - 9g_2^2 - 3g_Y^2 + 12y_t^2\right) + \frac{3}{2}\kappa^2 + \frac{3}{4}g_Y^2 g_2^2 + \frac{9}{8}g_2^4 + \frac{3}{8}g_Y^4 - 6y_t^4\right), \tag{B.6}$$

$$\frac{d\lambda_{DM}}{dt} = \frac{1}{16\pi^2}\left(22\lambda_{DM}^2 + 2\kappa^2 - 24g_2^2\lambda_{DM} + 12g_2^4\right), \tag{B.7}$$

$$\frac{d\kappa}{dt} = \frac{1}{16\pi^2}\left(4\kappa^2 + 12\kappa\lambda + 10\kappa\lambda_{DM} + 6y_t^2\kappa - \frac{33}{2}g_2^2\kappa - \frac{3}{2}g_Y^2\kappa + 6g_2^4\right). \tag{B.8}$$

- SM with a real quintet scalar field

$$\frac{d\lambda}{dt} = \frac{1}{16\pi^2}\left(+24\lambda^2 - 6y_t^4 + \frac{3}{8}g_Y^4 + \frac{9}{8}g_2^4 + \frac{3}{4}g_Y^2 g_2^2 + \frac{5}{2}\kappa^2 + 12\lambda y_t^2 - 3\lambda g_Y^2 - 9\lambda g_2^2\right),$$

$$\frac{d\lambda_X}{dt} = \frac{1}{16\pi^2}\left(+26\lambda_X^2 + 108g_2^4 - 72\lambda_X g_2^2 + 2\kappa^2\right),$$

$$\frac{d\kappa}{dt} = \frac{1}{16\pi^2}\left(+18g_2^4 + 12\kappa\lambda + 14\kappa\lambda_X + 6y_t^2\kappa - \frac{3}{2}\kappa g_Y^2 - \frac{81}{2}\kappa g_2^2 + 4\kappa^2\right). \tag{B.9}$$

- SM with a real septet scalar field[1]

$$\frac{d\lambda}{dt} = \frac{1}{16\pi^2}\left(+24\lambda^2 - 6y_t^4 + \frac{9}{8}g_2^4 + \frac{3}{8}g_Y^4 + 12\lambda y_t^2 - 3\lambda g_Y^2 - 9\lambda g_2^2 + \frac{3}{4}g_Y^2 g_2^2 + \frac{7}{2}\kappa^2 \right),$$

$$\frac{d\lambda_X}{dt} = \frac{1}{16\pi^2}\left(+30\lambda_X^2 + 2448\lambda_X\lambda_X'' + 51840\lambda_X''^2 - 144\lambda_X g_2^2 + 2\kappa^2 \right),$$

$$\frac{d\lambda_X''}{dt} = \frac{1}{16\pi^2}\left(+6g_2^4 + 1530\lambda_X''^2 + 24\lambda_X\lambda_X'' - 144\lambda_X'' g_2^2 \right),$$

$$\frac{d\kappa}{dt} = \frac{1}{16\pi^2}\left(+36g_2^4 + 12\kappa\lambda + 18\kappa\lambda_X + 6y_t^2\kappa - \frac{3}{2}\kappa g_Y^2 - \frac{153}{2}\kappa g_2^2 + 4\kappa^2 + 1224\kappa\lambda_X'' \right). \quad \text{(B.10)}$$

References

1. M.E. Machacek, M.T. Vaughn, Two loop renormalization group equations in a general quantum field theory. 1. Wave function renormalization. Nucl. Phys. B **222**, 83 (1983)
2. M.E. Machacek, M.T. Vaughn, Two loop renormalization group equations in a general quantum field theory. 2. Yukawa couplings. Nucl. Phys. B **236**, 221 (1984)
3. M.E. Machacek, M.T. Vaughn, Two loop renormalization group equations in a general quantum field theory. 3. Scalar quartic couplings. Nucl. Phys. B **249**, 70 (1985)
4. M.-X. Luo, H.-W. Wang, Y. Xiao, Two loop renormalization group equations in general gauge field theories. Phys. Rev. D **67**, 065019 (2003). arXiv:hep-ph/0211440
5. C. Cai, Z.-M. Huang, Z. Kang, Z.-H. Yu, H.-H. Zhang, Perturbativity limits for scalar minimal dark matter with Yukawa interactions: septuplet. Phys. Rev. D **92**(11), 115004 (2015). arXiv:1510.01559
6. Y. Hamada, K. Kawana, K. Tsumura, Landau pole in the standard model with weakly interacting scalar fields. Phys. Lett. B **747**, 238–244 (2015). arXiv:1505.01721

---

[1]As pointed out in Ref. [5], the beta function of κ contains typo in Ref. [6]: The last term misses in the text, although this term is taken into account in the numerical calculation.

Appendix C—Brief Review of Inflation

When a scalar dominates the energy density of the universe, Friedmann equation becomes

$$\left(\frac{\dot{a}}{a}\right)^2 = \frac{V(\phi) + \frac{1}{2}\dot{\phi}^2}{3M_P^2}.$$ (C.1)

If the potential of ϕ is flat enough, $\dot{\phi}^2$ term can be neglected and $V(\phi)$ becomes constant, then it is found that

$$a \propto \exp\left(\sqrt{\frac{V}{3M_P}}\right),$$ (C.2)

which indicates the exponentially expansion of the universe.

The primordial quantum fluctuation of an inflation induces the observed temperature perturbation in the cosmic microwave background. The power spectrum of scalar and tensor perturbation is parametrized as

$$\mathcal{P}_{\mathcal{R}} = A_s \left(\frac{k}{k_*}\right)^{n_s - 1 + \frac{1}{2}\frac{dn_s}{d\ln k}\ln\frac{k}{k_*} + \frac{1}{3!}\frac{d^2 n_s}{d\ln k^2}\left(\ln\frac{k}{k_*}\right)^2 + \cdots}, \quad \mathcal{P}_t = A_t \left(\frac{k}{k_*}\right)^{n_t + \frac{1}{2}\frac{dn_t}{d\ln k}\ln\frac{k}{k_*} + \cdots}.$$ (C.3)

A_s and A_t are the overall amplitudes, n_s and n_t are the spectral index, $dn_s/d\ln k$ and $dn_t/d\ln k$ are the running of the spectral index, and so on. The expansion of the universe during the inflation is characterized by e-folding number N:

$$N_* = \int_{t_*}^{t_{\text{end}}} dt\, H = \int_{\varphi_*}^{\varphi_{\text{end}}} \frac{d\varphi}{\dot{\varphi}} H = \frac{1}{M_P^2}\int_{\varphi_{\text{end}}}^{\varphi_*} \frac{V}{V_\varphi} d\varphi = \frac{1}{M_P}\int_{\varphi_{\text{end}}}^{\varphi_*} \frac{d\varphi}{\sqrt{2\epsilon}}.$$ (C.4)

The N_* corresponding to the current cosmic microwave background fluctuation is

$$50 < N_* < 60. \tag{C.5}$$

In the slow roll approximation, the amplitude of scalar and tensor power spectrums are given by

$$A_s = \frac{V}{24\pi^2 M_P^4 \epsilon}, \qquad A_t = \frac{2V}{3\pi^2 M_P^4}, \qquad r = \frac{A_t}{A_s} = 16\epsilon, \tag{C.6}$$

$$n_s = 1 + 2\eta - 6\epsilon, \qquad\qquad\qquad n_t = -2\epsilon,$$

$$\frac{dn_s}{d\ln k} = 16\epsilon\eta - 24\epsilon^2 - 2\xi_V^2, \qquad\qquad \frac{dn_t}{d\ln k} = -4\epsilon\eta + 8\epsilon^2,$$

$$\frac{d^2 n_s}{d\ln k^2} = -192\epsilon^3 + 192\epsilon^2\eta - 32\epsilon\eta^2$$
$$- 24\epsilon\xi^2 + 2\eta\xi^2 + 2\varpi^3. \tag{C.7}$$

The current Planck 2015 data constrains the parameter space,

$$A_s \simeq 2.2 \times 10^{-9}, \qquad\qquad 0.954 < n_s < 0.980,$$

$$r < 0.168, \qquad\qquad -0.03 < \frac{dn_s}{d\ln k} < 0.007. \tag{C.8}$$

Here we adopt the Planck TT+low P data to obtain conservative bound.

Appendix D—Strong CP Problem

D.1 θ Term in Lagrangian

The following term,

$$\frac{\theta}{32\pi^2} \int d^4x\, F^a_{\mu\nu} \tilde{F}^{a\mu\nu}, \tag{D.1}$$

is consistent with gauge symmetry and Lorentz symmetry in the action. At first glance, this term is not important because this is the total derivative,

$$
\begin{aligned}
\mathrm{Tr}\left(F_{\mu\nu} \tilde{F}^{\mu\nu} \right) &= \mathrm{Tr}\left((2\partial_\mu A_\nu + ig[A_\mu, A_\nu]) \tilde{F}^{\mu\nu} \right) \\
&= \mathrm{Tr}\left((2\partial_\mu A_\nu + A_\nu \partial_\mu) \tilde{F}^{\mu\nu} \right) \\
&= \mathrm{Tr}\left((\partial_\mu A_\nu) \tilde{F}^{\mu\nu} + \partial_\mu (A_\nu \tilde{F}^{\mu\nu}) \right) \\
&= \mathrm{Tr}\left(\epsilon^{\mu\nu\rho\sigma} (\partial_\mu A_\nu)(\partial_\rho A_\sigma + ig A_\rho A_\sigma) + \partial_\mu (A_\nu \tilde{F}^{\mu\nu}) \right) \\
&= \mathrm{Tr}\left(\epsilon^{\mu\nu\rho\sigma} \partial_\mu (A_\nu \partial_\rho A_\sigma + \frac{1}{3} ig A_\nu A_\rho A_\sigma) + \partial_\mu (A_\nu \tilde{F}^{\mu\nu}) \right) \\
&= \mathrm{Tr}\left(\epsilon^{\mu\nu\rho\sigma} \partial_\mu (2 A_\nu \partial_\rho A_\sigma + \frac{4}{3} ig A_\nu A_\rho A_\sigma) \right),
\end{aligned} \tag{D.2}
$$

where have used Bianchi identity,

$$
\begin{aligned}
[D_\mu, \tilde{F}^{\mu\nu}] &= \epsilon^{\mu\nu\rho\sigma} [D_\mu, F_{\rho\sigma}] \\
&= \frac{2}{ig} \epsilon^{\mu\nu\rho\sigma} [D_\mu, D_\rho D_\sigma] \\
&= 0,
\end{aligned} \tag{D.3}
$$

in the second line. Nevertheless, θ term has physical meaning. It contributes the neutron electric dipole moment because θ term induces CP violating nucleon-pion coupling. The value of θ is constrained as [1]

$$\theta < 10^{-10}. \tag{D.4}$$

Here we note that the definition of the electric dipole moment of the neutron d_n is given by

$$\mathcal{L} \ni -\frac{i}{2} d_n \bar{n} \sigma^{\mu\nu} \gamma^5 F_{\mu\nu} n, \tag{D.5}$$

where n is the neutron field, and d_n is

$$d_n \simeq |\theta| e \frac{m_\pi^2}{m_n^3}. \tag{D.6}$$

D.2 $\theta = 0$ or π?

$\theta = \pi$ does not give complex phase, and does not violate CP. Therefore the measurement of the neutron electric dipole moment does not kill the possibility of $\theta = \pi$. The difference between $\theta = 0$ and π appears in the quark mass term. After rotating out θ by redefinition of the up quark field, we have

$$\begin{aligned} -m_u \bar{U} U - m_d \bar{D} D, &\quad \text{for} \quad \theta = 0, \\ m_u \bar{U} U - m_d \bar{D} D, &\quad \text{for} \quad \theta = \pi, \end{aligned} \tag{D.7}$$

as the quark mass term in the Lagrangian. Here both of m_u and m_d are real positive.

If $\theta = 0$, the current algebra tells us

$$\partial_\mu j^{5\mu a} = (m_u + m_d) \bar{q} \gamma^5 \tau^a q, \tag{D.8}$$

and the current associated with the broken symmetry couples with the Numbu-Goldstone boson,

$$\langle 0 | j^{5\mu a} | \pi^b \rangle = f_\pi p^\mu \delta^{ab}, \tag{D.9}$$

from which we have

$$\begin{aligned} m_\pi^2 &= (m_u + m_d) \frac{\langle 0 | \bar{q} \gamma^5 \tau^a q | \pi^a \rangle}{f_\pi} \\ &\sim (m_u + m_d) \Lambda_{\text{QCD}}. \end{aligned} \tag{D.10}$$

Similarly, the following formulas are derived.

$$
\begin{aligned}
m_{\pi^0}^2 &= B(m_u + m_d), \\
m_{\pi^\pm}^2 &= B(m_u + m_d) + \Delta_{em} \\
m_{K^0}^2 &= B(m_d + m_s), \\
m_{K^\pm}^2 &= B(m_u + m_s) + \Delta_{em},
\end{aligned}
\tag{D.11}
$$

where B is the order of Λ_{QCD}, and Δ_{em} represents the electromagnetic correction. We can obtain the ratio of the quark mass from Eq. (D.11) [2].

$$
\begin{aligned}
\frac{m_u}{m_d} &= \frac{2m_{\pi^0}^2 - m_{\pi^\pm}^2 + m_{K^\pm}^2 - m_{K^0}^2}{m_{K^0}^2 - m_{K^\pm}^2 + m_{\pi^\pm}^2} \\
&\simeq 0.56.
\end{aligned}
\tag{D.12}
$$

However, for $\theta = \pi$, we can derive the same formula with $m_u \to -m_u$, and therefore the prediction is

$$
\frac{2m_{\pi^0}^2 - m_{\pi^\pm}^2 + m_{K^\pm}^2 - m_{K^0}^2}{m_{K^0}^2 - m_{K^\pm}^2 + m_{\pi^\pm}^2} < 0,
\tag{D.13}
$$

which apparently contradicts an experiment.

D.3 Possibility of the Massless up Quark

Let us consider the Yukawa sector of the quarks in the SM Lagrangian:

$$
y_u^{ij} \bar{Q}_i \tilde{H} U_{Rj} + y_d^{ij} \bar{Q}_i \tilde{H} D_{Rj} + \text{h.c.} \quad .
\tag{D.14}
$$

What happens if the up quark mass is equal to zero? In this case, the up Yukawa matrix y_u^{ij} is the rank-2 matrix, and $y_u^{ij} U_{Rj}$ does not span the three dimensional family space. The orthogonal vector is nothing but the mass eigenstate of the up quark, that is, the up quark field does not appear in the Yukawa sector in the Lagrangian. Then, we can easily see that an extra symmetry appears, the rotation of up quark field. However, this symmetry is violated at the quantum level by an $SU(3)_C$ anomaly, and hence we can take $\theta = 0$ by the rotation of the fields.

By the particle data group [3], the recent studies which combines the lattice data and chiral perturbation in order to account for the isospin breaking report the following value of up and down quark masses:

$$
m_u = 2.15 \pm 0.15 \, \text{MeV}, \qquad m_d = 4.70 \pm 0.20 \, \text{MeV}.
\tag{D.15}
$$

Up to now, the lattice can only done in isospin conserving limit, $m_u = m_d$. In order to settle the situation, the improvement of the lattice simulation is desired.

However, even if this is a solution to the strong CP problem, it is unclear whether $y_u = 0$ itself is natural or not, and needs mechanism to explain $y_u = 0$ in my opinion.

D.4 Vacuum Energy Dependence of θ

In the discussion in Chap. 4, it is necessity to calculate the θ dependence of the vacuum energy in QCD. The estimation of the vacuum energy dependence of θ is similar to that of the axion [4–6]. The dependence comes from the quark mass term,

$$\mathcal{L}_m \ni - \cos \theta (m_u \bar{U} U + m_d \bar{D} D), \quad -(\bar{U} i \gamma^5 U + \bar{D} i \gamma^5 D), \tag{D.16}$$

in the basis where θ term is removed. We note that $\bar{U} i \gamma^5 U$, $\bar{D} i \gamma^5 D$ terms are P odd and CP odd. Due to the chiral symmetry breaking, the quark bilinear condensate appears:

$$\langle \bar{U} U \rangle = \langle \bar{D} D \rangle = \mathcal{O}(\Lambda_{QCD}^3). \tag{D.17}$$

On the other hand, P, CP odd terms are not have VEV,[2]

$$\langle \bar{U} i \gamma^5 U \rangle = \langle \bar{D} i \gamma^5 D \rangle = 0. \tag{D.18}$$

Then, the energy density coming from the quark mass term is

$$\epsilon \sim (m_u + m_d) \Lambda_{QCD}^3 \cos \theta, \tag{D.19}$$

and we can understand the θ dependence.

References

1. C.A. Baker et al., An Improved experimental limit on the electric dipole moment of the neutron. Phys. Rev. Lett. **97**, 131801 (2006). arXiv:hep-ex/0602020
2. S. Weinberg, The problem of Mass. Trans. New York Acad. Sci. **38**, 185–201 (1977)
3. Particle Data Group, K. Olive et al., Review of particle physics. Chin. Phys. C **38**, 090001 (2014)
4. R.D. Peccei, H.R. Quinn, CP conservation in the presence of instantons. Phys. Rev. Lett. **38**, 1440–1443 (1977)
5. J.E. Kim, Light pseudoscalars, particle physics and cosmology. Phys. Rept. **150**, 1–177 (1987)
6. M. Dine, *Supersymmetry and String Theory*.
7. C. Vafa, E. Witten, Parity conservation in QCD. Phys. Rev. Lett. **53**, 535 (1984)

---

[2]The proof is presented by Vafa and Witten [7].

Appendix E—Quantization of Majorana Field

The quantization of Majorana field is reviewed [1]. We first introduce the concept of the charge conjugation, which corresponds to exchange of the particle and antiparticle. Naively, one imagine that the field describing the antiparticle of ψ is written by ψ^*. However, this is conflict with the property of the Dirac field under Lorentz transformation which is

$$\psi \rightarrow e^{i S_{\mu\nu} \omega^{\mu\nu}} \psi \qquad\qquad S_{\mu\nu} = \frac{i}{4}[\gamma_\mu, \gamma_\nu] \qquad\qquad \text{(E.1)}$$

In order to reconcile this discrepancy, the definition of the charge conjugation should be

$$\psi^c = C\psi^* = i\gamma^2 \psi^*. \qquad\qquad \text{(E.2)}$$

The pre-factor is chosen so that $(\psi^c)^c = \psi$ is satisfied. If ψ is equal to its conjugate,

$$\psi^c = \psi, \qquad\qquad \text{(E.3)}$$

then ψ is called the Majorana fermion.

Then, let us consider the plain wave expansion of the field ψ. Starting from Dirac equation,

$$(i\slashed{\partial} - m)\psi = 0, \qquad\qquad \text{(E.4)}$$

we denote the positive energy solution and negative energy solution as $u^s(p)e^{-ip\cdot x}$ and $v^s(p)e^{-ip\cdot x}$, respectively. Here s denotes the spin degrees of freedom. On the other hand, the Hamltonian density of the spinor field is

$$\mathcal{H} = \psi^\dagger(-i\gamma^0\vec{\gamma} \cdot \vec{\nabla} + m\gamma^0)\psi, \qquad\qquad \text{(E.5)}$$

from which we can see that $H = -i\gamma^0\vec{\gamma}\cdot\vec{\nabla}+m\gamma^0$ gives the one particle Hamiltonian. The eigenfunctions of H are given by following solutions:

$$Hu^s(p)e^{-ip\cdot x} = (|\vec{p}|^2 + m^2)u^s(p)e^{-ip\cdot x},$$
$$Hv^s(p)e^{-ip\cdot x} = -(|\vec{p}|^2 + m^2)v^s(p)e^{-ip\cdot x}. \tag{E.6}$$

The complete set is formed by these eigenfunction, and ψ can be expanded as

$$\psi = \int \frac{d^3k}{(2\pi)^3} \frac{1}{2k_0} \sum_s \left(a_p^s u^s(p)e^{-ip\cdot x} + b_p^{s\dagger} v^s(p)e^{ip\cdot x} \right),$$

$$\psi^c = \int \frac{d^3k}{(2\pi)^3} \frac{1}{2k_0} \sum_s \left(a_p^{s\dagger}(Cu^{s*}(p))e^{ip\cdot x} + b_p^s(Cv^{s*}(p))e^{-ip\cdot x} \right). \tag{E.7}$$

The Majorana condition gives the relation $b_p^{s\dagger} v^s(p) = a_p^{s\dagger}(Cu^{s*}(p))$.

Let us quantize the field by imposing the equal time anticommutation relation,

$$\{\psi(\vec{x}), \psi^\dagger(\vec{y})\} = \delta^{(3)}(\vec{x} - \vec{y}), \tag{E.8}$$

or equivalently

$$\{a_p^s, a_q^{r\dagger}\} = (2\pi)^3 \delta^{(3)}(\vec{p} - \vec{q})\delta_{sr}. \tag{E.9}$$

In terms of creation and annihilation operators, the Hamiltonian is easily diagonalized,

$$\int d^3x \, \mathcal{H} = \int \frac{d^3p}{(2\pi)^3} \sum_s (|\vec{p}|^2 + m^2)a_p^{s\dagger} a_p^s, \tag{E.10}$$

and therefore Fock space can be constructed.

Next we derive the Feynman rule of the Majorana fermion, which we can infer from the action:

$$S = \int d^4x \left(\bar{\psi}(i\partial\!\!\!/ - m)\psi \right)$$
$$= \int d^4x \left(\psi^T i\gamma^2\gamma^0(i\partial\!\!\!/ - m)\psi \right) = \int d^4x \left(\bar{\psi}(i\partial\!\!\!/ - m)i\gamma^2\gamma^0\bar{\psi}^T. \right) \tag{E.11}$$

The propagator of the Majorana fermion is given by

$$\langle \bar{\psi}\psi \rangle = \int \frac{d^4p}{(2\pi)^4} \frac{i}{p\!\!\!/ - m} e^{-ip\cdot x}, \quad \langle \psi^T \psi \rangle = \int \frac{d^4p}{(2\pi)^4} \frac{i}{p\!\!\!/ - m}(-i\gamma^2\gamma^0)e^{-ip\cdot x},$$

$$\langle \bar{\psi}\bar{\psi}^T \rangle = \int \frac{d^4p}{(2\pi)^4}(-i\gamma^2\gamma^0)\frac{i}{p\!\!\!/ - m}e^{-ip\cdot x}. \tag{E.12}$$

We comment on a possible concrete example. In the case of Majorana neutrino, the Majorana field is

$$\nu_{M,L} = \frac{\nu_L + \nu_L^c}{\sqrt{2}} \qquad\qquad \nu_{M,R} = \frac{\nu_R + \nu_R^c}{\sqrt{2}}. \qquad (E.13)$$

In the case of the $SU(2)_L$ triplet and quintet Majorana fermion, we also need the quantization of Majorana field in order to calculate the annihilation cross section.

Reference

1. M.E. Peskin, D.V. Schroeder, *An introduction to Quantum Field Theory*

Appendix F—The Effect of the Principle Value

Here we evaluate the principle value integral:

$$PV \int_{-\infty}^{+\infty} \frac{dE}{E} \langle a|E; \Lambda\rangle \langle E; \Lambda|\epsilon\rangle. \tag{F.1}$$

This Appendix is taken from Ref. [1]. The WKB solution of $\langle a|E; \Lambda\rangle$ is given by

$$\langle a|E; \Lambda\rangle = M_P \sqrt{\frac{a}{p_{cl}}} \exp\left(i \int^a da' \, p_{cl}(a')\right), \tag{F.2}$$

where

$$p_{cl}(a) = M_P a^2 \sqrt{2\left(\frac{\rho(a)}{6} - \frac{E}{a^3}\right)} := M_P a^2 \sqrt{\frac{\tilde{\rho}(a)}{3}}. \tag{F.3}$$

Then, for a sufficiently large value of a, we have

$$\int_{a_M}^{a} da \, p_{cl}(a) = \frac{M_P}{3^{\frac{3}{2}}} \left(a^3 \sqrt{\tilde{\rho}(a)} - a_M^3 \sqrt{\tilde{\rho}(a_M)} + \frac{M-E}{\sqrt{\Lambda}} \log\left[\frac{a^{\frac{3}{2}}(\Lambda + \sqrt{\Lambda\tilde{\rho}(a)})}{a_M^{\frac{3}{2}}(\Lambda + \sqrt{\Lambda\tilde{\rho}(a_M)})}\right]\right)$$

$$:= \frac{M_P a^3}{3^{\frac{3}{2}}} g(\Lambda, E, a) \underset{a \gg a_M}{\simeq} \frac{M_P a^3}{3^{\frac{3}{2}}} \sqrt{\tilde{\rho}(a)}. \tag{F.4}$$

By substituting Eqs. (F.2) and (F.4) to Eq. (F.1), we obtain

$$PV \int_{-\infty}^{\infty} \frac{dE}{E} M_P \sqrt{\frac{a}{p_{cl}}} \exp\left(i \frac{M_P a^3}{3^{\frac{3}{2}}} \sqrt{\tilde{\rho}(a)}\right) \langle E; \Lambda|\epsilon\rangle. \tag{F.5}$$

By expanding the exponent around $E = 0$, we have

$$M_P \sqrt{\frac{a}{p_{cl}}} \exp\left(i\frac{M_P a^3}{3^{\frac{3}{2}}}\sqrt{\rho(a)} - i\frac{M_P E}{3^{\frac{3}{2}}\sqrt{\rho(a)}} + \mathcal{O}(E^2)\right) = \langle a|0; \Lambda \rangle \exp\left(-i\frac{M_P E}{3^{\frac{3}{2}}\sqrt{\rho(a)}} + \mathcal{O}(E^2)\right).$$

$$\text{(F.6)}$$

Therefore, only the region,

$$|E| \lesssim \frac{\sqrt{\rho(a)}}{M_P} \sim \frac{\sqrt{\Lambda}}{M_P}, \tag{F.7}$$

gives nonzero contribution to the integral. Hence, it is self-consistent to show $\Lambda = 0$ by using only the zero energy eigenstate $|0\rangle$.

Reference

1. Y. Hamada, H. Kawai, K. Kawana, Natural solution to the naturalness problem—universe does fine-tuning (2015). arXiv:1509.05955

Curriculum Vitae

Personal Data

Family name: Hamada   Given name: Yuta
Sex: Male   Marital status: Married
Date of birth: 23/1/1989   Age: 27
Nationality: Japan   Place of birth: Aichi, Japan
Reseach interst: Higgs boson, String theory, Cosmology
Affiliation: Department of Physics, University of Wisconsin-Madison
and Address: Chamberlin Hall
E-mail: yhamada@wisc.edu

Academic Degrees

	Degree	Subject	University	Place
24/3/2011	Bachelor of science	Physics	Kyoto University	Kyoto, Japan
23/3/2013	Master of science	Physics	Kyoto University	Kyoto, Japan
23/3/2016	Doctor of science	Physics	Kyoto University	Kyoto, Japan

Education

Period	Institution	Place
4/2007–3/2011	Faculty of science, Kyoto University	Kyoto, Japan
4/2011–3/2016	Department of physics, Kyoto University	Kyoto, Japan

Research Experience

Period	Position	Place
11/2013–1/2014	Kyoto University scholarship for short-term student dispatch program (at Oxford)	Oxford, U.K.
4/2013–3/2016	JSPS fellow (DC1)	Kyoto, Japan
4/2016–present	JSPS fellow (SPD)	Tsukuba, Japan
9/2016–present	Honorary fellow	Wisconsin, U.S

Teaching Experience

Period	Position	Place
4/2011–7/2011	Teaching assistant (Kyoto University)	Kyoto, Japan
10/2013–11/2013	Teaching assistant (Kyoto University)	Kyoto, Japan

Award

2016: Springer Theses award
2016: Particle Physics Medal, Young Scientist Award in Theoretical Particle Physics (Japan)
2016: Young Scientist Award of the Physical Society of Japan

Membership of Academic Society

The Physical Society of Japan
Japan Particle and Nuclear Theory Forum
International Journal of Modern Physics A reviewer
Nuclear Physics B reviewer
Progress of Theoretical and Experimental Physics reviewer